Polymer models in complex media

Nicolas Pétrélis

HABILITATION A DIRIGER LES RECHERCHES

Université de Nantes

présentée par

Nicolas PÉTRÉLIS

Discipline : Mathématiques Appliquées
Spécialité : Probabilités

Modèles de Polymères dans des milieux complexes

Date de soutenance : 14 Novembre 2014

Composition du Jury

Thierry Bodineau	Directeur de Recherche au CNRS
Jean Christophe Breton	Professeur, Université de Rennes I
Philippe Carmona	Professeur, Université de Nantes
Giambattista Giacomin,	Professeur, Université Paris VII
Frank den Hollander	Professeur, Université de Leiden
Wolfgang Koenig	Professeur, Institut Weierstrass Berlin

Après avis des rapporteurs

Kenneth Alexander	Professeur, Université de Californie du Sud
Wolfgang Koenig	Professeur, Institut Weierstrass Berlin
Fabio Toninelli	Directeur de Recherche au CNRS

Remerciements

Mes remerciements vont en premier lieu aux trois rapporteurs de cette habilitation: Ken Alexander, Wolfgang Koenig et Fabio Toninelli, ainsi qu'aux 6 membres du jury: Thierry Bodineau, Jean Christophe Breton, Philippe Carmona, Giambattista Giacomin, Frank den Hollander et Wolfgang Koenig. Je leur suis très reconnaissant pour le temps et l'attention qu'ils ont dédiés à mon manuscrit et à la soutenance.

Je remercie les 5 instituts de Mathématiques dont j'ai eu la chance d'être membre depuis le début de ma thèse

- le Laboratoire de Mathématiques Raphaël salem (Rouen),
- Eurandom (Eindhoven),
- l'Institut de Mathématiques de l'Université de Zurich,
- l'Institut de Mathématiques de la TU Berlin,
- le Laboratoire de Mathématiques Jean Leray (Nantes).

Dans le cadre de la bourse ERC Advanced Grant VARIS de Frank den Hollander, j'ai eu l'opportunité de séjourner pendant 8 mois au sein de l'Institut de Mathématiques de l'Université de Leiden. J'ai trouvé dans chacun de ces laboratoires un environnement très favorable à la recherche Mathématique.

Mes remerciements vont également à mes collaborateurs directs: Francesco Caravenna, Philippe Carmona, Frank den Hollander, Gia Bao Nguyen et François Pétrélis ainsi qu'aux mathématiciens avec qui j'ai l'occasion de travailler régulièrement: Mathias Birkner, Giambattista Giacomin, Mark Holmes, Grégory Maillard, Julien Poisat et Rongfeng Sun.

Je suis également très reconnaissant à mes deux directeurs de thèse Giambattista Giacomin et Roberto Fernandez ainsi qu'à Frank den Hollander, Erwin Bolthausen et Jean Dominique Deuschel qui m'ont recruté et accompagné en post-doctorat.

Je remercie l'Université de Nantes, le Laboratoire Jean Leray et le CNRS de m'avoir permis de travailler dans d'excellentes conditions dans le cadre de ma chaire Université CNRS pendant les 5 années qui viennent de s'écouler. Je sais gré a tous les membres du Laboratoire Jean Leray d'y entretenir une atmosphère si agréable et propice au travail.

Je remercie très chaleureusement mes proches Jean-Jacques, Françoise, François et Jean-Bertrand pour leur soutien sans faille.

Enfin, je remercie Katrin qui me supporte au quotidien et me rend très heureux.

Abstract.
Keywords: Polymers, collapse transition, large deviations, micro-emulsion, localization-delocalization transition, pinning, random walk, random media, coarse graining, wetting.

Résumé.
Mots clés: Polymères, transition d'effondrement, grandes déviations, microémulsion, transition de localisation-délocalisation, accrochage, marche aléatoire, milieu aléatoire, renormalisation, mouillage.

Contents

Chapter 1

Introduction

My work is mostly dedicated to a large class of models in Statistical Mechanics, i.e., the polymer models, that have attracted a lot of attention in mathematics within the last 20 years. Generally speaking, my research is articulated around two main directions. First, building and investigating new models for polymers interacting with some complex media, that had not been considered so far by mathematicians although they are physically relevant, e.g., microemulsions or multi-interface media. Second, using tools from Probability theory to go deeper into the investigation of some already existing models (e.g., the polymer collapse or the polymer in a slit) that had been studied almost exclusively with combinatoric technics.

The models that I have investigated up to now can be classified into 3 categories, corresponding to 3 different types of physical systems, and providing theoretical results that are both physically relevant and mathematically challenging. Each category is treated in one of the three main chapters of this monograph. The reader will find at the end of each chapter a section called "Perspectives" in which we present short-term and long-term objectives that justify, in our opinion, some further research. Note also that, each chapter contains an introduction and for this reason, we will keep this general introduction short.

In Section 1.1 below, we will give a short introduction about the physics of polymers and illustrate the importance of their modelization by describing an application in medicine of the so called "collapse transition" phenomenon that will be studied in detail in Chapter 3 of this manuscript. In Section 1.2, we will describe the Gibbs framework in which each model considered here is falling. Finally, in Section 1.3, we will give more details about the three main chapters constituting the core of the manuscript.

1.1 Polymers

To begin with, let us give some insight about the physical features of polymers. A long molecule made of elementary components (the monomers) that are tied up together by chemical bounds enters the class of polymers as soon as its length (in terms of monomers) passes above 10^3 units (for instance some proteins like the polysaccharide are approximately 10^3 units long). The largest known polymers can be up to 10^9 or 10^{10} units long (such as a DNA chain). The biopolymers are found in nature unlike the synthetic polymers that are obtained by chemical polymerization procedure in laboratories. One can also distinguish between homopolymers (e.g. polyethylene) whose monomers are all identical and copolymers that are constituted by at least two types of monomers. A copolymer can be either random if the distribution of the monomers along the chain is random (e.g. DNA) or periodic (such as agar).

The mathematical modeling of large physical systems involving polymers took an increasing importance in the field of Statistical Mechanics in the last 20 years. The reason for this raise of interest is, on the one hand, the large variety of physical phenomenon involving polymers that lead to industrial, medical or agronomic applications and, on the other hand, the fact that random walks, together with a Gibbsian formalism are particularly well adapted to build polymer models and to obtain theoretical results about them that are meaningful from a physical point of view.

To illustrate the former statement, we can give the example of the collapse transition of an homopolymer in a poor solvent. This phenomenon and its mathematical treatment will be further described and investigated in Chapter 3, but let us explain briefly the physical mechanism behind this transition and a medical application. When dipping an homopolymer in a repulsive solvent at low temperature, the monomers composing the solvent have the tendency to wrap themselves up in order to exclude the solvent so that the polymer adopts a configuration that looks very much like a compact ball. This collapsed regime is the result of an energy-entropy competition in which the energy gain induced by these compact configurations takes over their entropic cost. When heating up the system, in turn, the thermal agitation raises until some threshold above which the polymer expands itself, deflates and goes back to its classical diffusive behavior. For some polymer such as PINPAM (see [74] and [34]) this collapse transition occurs at a temperature that is close to the temperature of a human body. Such polymers are therefore used to trap some drugs inside their collapsed configuration before being inoculated into a human body where the drug will be released eventually.

1.2 Models of Statistical Mechanics for polymers

At the beginning of each three chapters of the manuscript, we will describe in details the model (or family of models) under consideration. However, let us recall briefly the Gibbs framework that allows for a theoretical investigation of large physical systems at thermodynamic equilibrium and in particular its application to polymer models.

When building a Statistical Mechanical model for a physical system, the first step consists in defining the allowed configurations of the system and to settle an a priori measure on them. For polymer models, these configurations correspond to trajectories of random walks. Thus, for a polymer consisting of N monomers, the set of configurations $\mathcal{W}_N$ is made of the N-step trajectories of a given random walk. We will mostly work with three types of random walk, i.e.,

a) random walks on $\mathbb{Z}^d$ that are neither directed nor self-avoiding, that is, $S = (S_i)_{i=0}^{\infty}$ where $(S_{i+1} - S_i)_{i=0}^{\infty}$ is an i.i.d sequence of random vectors in $\mathbb{Z}^d$, centered and with a finite second moment,

b) directed random walks of the form $S = (i, S_i)_{i=0}^{\infty}$ where $(S_{i+1} - S_i)_{i=0}^{\infty}$ is a random walk of type **a)**,

c) self-avoiding partially directed paths of the form $\pi = (\pi_i)_{i=0}^{N}$ where $\pi_{i+1} - \pi_i \in \{\downarrow, \rightarrow, \uparrow\}$ for all $i \in \{0, \dots, N-1\}$. In this case, the a priori measure $\mathbf{P}_N$ can for instance be uniform.

The random walk choice is made depending on both the type of physical system that we consider and the level of tractability that we want to maintain for the model. Self-avoiding walks are indeed often the most appropriate objects to model polymers since they fulfill the excluded volume effect, which simply tells us that two monomers can not occupy the exact same location. However, the computational complexity induced by self-avoiding walks may lead us to work with their directed counterparts. This simplification is often sufficient to shed light on an underlying renewal structure of the model, which turns out to be of key importance for many computations.

With the set of trajectories $(\mathcal{W}_N)$ in hand, one can build the polymer model by perturbing the a priori law $(\mathbf{P}_N)$ on $\mathcal{W}_N$ with the help of a Gibbs weight that is associated with each trajectory and takes into account the microscopic interactions between the monomers themselves and/or between the monomers and the medium around them. To be more specific, in size N, the polymer measure $\mathbf{P}_{N,\beta}$ is a probability law on $\mathcal{W}_N$ characterized by its Radon Nikodym derivative with respect to $\mathbf{P}_N$, i.e.

$$\frac{\mathrm{d}\mathbf{P}_{N,\beta}}{\mathrm{d}\mathbf{P}_N}(S) = \frac{e^{\beta H_N(S)}}{Z_{N,\beta}}, \quad S \in \mathcal{W}_N, \tag{1.2.1}$$

where $\beta \in (0, \infty)$ is the inverse temperature, where $H_N(S)$ is the Hamiltonian of a given trajectory obtained by summing the energetic contributions of each interactions, and where $Z_{N,\beta}$ is the normalizing constant referred to as the partition function of the system.

In each of the three main chapters we will describe the main issues that are raised by the model or type of models under investigation. However, let us mention here that these issues can roughly be classified into two categories, i.e.,

- the results concerning the thermodynamic limit of the model, that is the limit as the system size N diverges. The interest of considering such limits is that they rule out some finite size effects whose intensity decreases with the system size and thus disappear in the limit $N \to \infty$. In other words the thermodynamic limit acts like a filter that only preserves the dominant physical effects.

- the so called "path results" in finite size. To be more specific, for a given β, such results provide informations about the geometry of the path under $\mathbf{P}_{N,\beta}$ for N large but finite.

1.3 Content of the manuscript

In Chapter 2, we describe the results obtained with Frank den Hollander about a model for a copolymer in an emulsion. This model was introduced by den Hollander and Whittington in [54], and has subsequently being analyzed in details in [50], [51], [52]. In [53] it was extended to an even more realistic model which enters a new class consisting of those models for a polymer interacting with a random interface. Among the elements of this new class of models we can mention the random walk pinned at another random walk (see [8], [9] and [10]) or the famous directed polymer with bulk disorder (see [49] for a review). Most models for a copolymer at thermodynamic equilibrium had, up to the introduction of this new class of models, been built with a medium made of a single linear interface separating two solvents. The introduction of a random interface allows us to take into account some more complex media among which are the colloids (milk, ink, polluted water etc...) which are typically stabilized with polymers via the steric/depletion stabilization effect. The particularity of our model for a copolymer in an emulsion is that we managed to provide a variational characterization of its free energy. Such formulas are rarely available for disordered models in Statistical Mechanics and they turn out to be a powerful tool to analyze the phase diagram of the system.

Chapter 3 is dedicated to a completely different phenomenon, that is the collapse transition of a self-interacting partially directed self-avoiding walk. As mentioned above, this is a model for an homopolymer in a repulsive solvent. The model and its non directed counterpart have triggered a fair amount of activity within the physics community

(see [13], [14], [15] and [16]). We studied this model with Philippe Carmona and Gia-Bao Nguyen in [67], [27] and [28]. We analyzed the model with a new probabilistic technic that relies on a random walk representation of the partition function. Our method turns out to be much more explicit and simple than what had been obtained previously with combinatorics techniques. We derive a fine asymptotic for the free energy close to criticality and we provide, for both the collapsed phase and the interior of the extended phase, a complete description of the path under the polymer measure when the system size is large but finite.

In Chapter 4, we give a survey of the results obtained in [72], [73] and later in [24], [25] with Francesco Caravenna and in [18] with Francesco Caravenna and Philippe Carmona. The common point of the models studied in these papers is that they are elements of a wider class of models, i.e., the random walks in a random/deterministic potential. Many celebrated models enters this general framework such as the parabolic Anderson model via the Feynman Kac description of its solution, the pinning of a random walk by one or infinitely many horizontal interfaces, the polymer in a slit interacting with two walls but also the directed polymer in a random environment etc... Most of these models generate some phase transitions between very different regime corresponding to radically different conformations of the path. We focus on three models that are (1) the discrete parabolic Anderson model, (2) the homogeneous polymer pinned/depinned at infinitely many interfaces and (3) the copolymer randomly pinned at a selective layer between two solvents. We will provide some results concerning the limiting free energy and the critical point for (3), the free energy and the scaling limits of the path in (2) and some strong localization results on the path for (1).

Chapter 2

Copolymer in an emulsion

2.1 Introduction

The localization of a copolymer in the vicinity of an interface between two immiscible solvents has been intensively studied by mathematicians in the last twenty years (cf [38] Chapter 6 and [49] Chapter 9). However, apart from the two models that the present chapter is dedicated to, all models that have been investigated until now are dealing with a unique and flat linear interface between the two solvents. The localization of a copolymer along a non-flat interface, for instance a random interface or an interface with a slope, has, up to our knowledge, not been considered so far.

Emulsions are good examples of random media made of two immiscible solvents, which give raise to complex interfaces. Emulsions cover a wide range of chemical solutions, some of them being very common, for instance the milk (an emulsion of fat droplets floating in water), others being very sophisticated as the S(M)EDDS that are microemulsions used in medicines because their droplets are so tiny (10-100 nm) that they improve the absorption rate of some drugs in the intestine (cf. [59]). Ensuring the stability of an emulsion is an important technical issue and this can be achieved with the help of surfactant agents which prevent from an aggregation of droplets. Copolymers often play the role of surfactant agent. They can be present naturally in the emulsion as the casein of milk, or they can be added a posteriori in the medium to stabilize it, as an inulin based copolymer in an oil-water emulsion (see e.g. [79]). As a consequence, understanding the behavior of a copolymer in an emulsion, depending on parameters like chemical affinities, temperature, droplets density etc... turns out to be a mathematically challenging and physically relevant issue.

In this chapter, we present the results obtained with F. den Hollander in [50], [51], [52] and [53] about a model introduced by den Hollander and Whittington in [54]. This model deals with a random copolymer made of monomers of type A (say hydrophobic) and of type B (say hydrophilic) which is embedded in an emulsion of solvent A (say oil) in a pure

phase of solvent B (say water). The monomers are typically much smaller than the droplets and the droplets are typically much smaller than the polymer itself. Building and studying such a model required to take-up three main conceptual and technical challenges:

- build the model in such a way that: 1) the density $p \in (0,1)$ of A-droplets in the B-solvent can be tuned, 2) the three characteristic sizes of the system, namely, the monomers length, the droplets size and the polymer length, are living on different scales, 3) the model is still tractable enough to allow for a computation of its free energy.

- study the thermodynamic limit of such a model by proving that the quenched free energy exists, is self-averaging, and can be expressed under the form of a tractable variational formula.

- use the variational formula to study the phase diagram of the system and to investigate the different phase transitions that the model undergoes.

As we will see during the investigation of the model, the copolymer is still localized along flat linear interfaces in some regions of the phase diagram. However, this phenomenon is in competition with other physical effects like the targeting of A droplets when the AA chemical affinity becomes larger than the BB chemical affinity.

2.2 A first model with some geometric constraint

As mentionned in the introduction, the three basic objects constituting our model are living on three different scales, i.e.,

- a macroscopic scale, associated with the polymer length and denoted by $n \in \mathbb{N}$.

- a mesoscopic scale, associated with the droplets diameter and denoted by L_n.

- a microscopic scale, associated with the monomers themselves whose length is set unitary.

Some restriction on the growth speed of L_n as a function of n will be imposed in (2.2.6), in order to obtain a thermodynamic limit ($n \to \infty$).

2.2.1 The model

The microemulsion is modelled as follows. The parameter $p \in (0,1)$ represents the density of A-droplets in the medium, while $L_n \in \mathbb{N}$ gives the size of these droplets. Thus, we

partition $\mathbb{R}^2$ into square blocks of size L_n:

$$\mathbb{R}^2 = \bigcup_{x\in\mathbb{Z}^2} \Lambda_{L_n}(x), \qquad \Lambda_{L_n}(x) = xL_n + (0, L_n]^2. \tag{2.2.1}$$

Each block is randomly labelled A or B, with probability p, respectively, $1-p$, independently for different blocks. The resulting labelling is denoted by

$$\Omega = \{\Omega(x)\colon\ x \in \mathbb{Z}^2\} \in \{A, B\}^{\mathbb{Z}^2} \tag{2.2.2}$$

and represents the *randomness of the emulsion*, with A denoting oil and B denoting water.

The random repartition of monomers along the polymer chain is modelled by assigning to each positive integer a random label A or B, with probability $\frac{1}{2}$ each, independently for different integers, i.e.,

$$\omega = \{\omega_i\colon\ i \in \mathbb{N}\} \in \{A, B\}^{\mathbb{N}}. \tag{2.2.3}$$

Thus, ω encodes for the *randomness of the copolymer*, with A denoting a hydrophobic monomer and B a hydrophilic monomer.

It remains to define the set $\mathcal{W}_{n,L_n}$ of allowed path in size n,

- $\mathcal{W}_n$ = the set of n-step *directed self-avoiding paths* starting at the origin and being allowed to move *upwards, downwards and to the right.*
- $\mathcal{W}_{n,L_n}$ = the subset of $\mathcal{W}_n$ consisting of those paths that enter blocks at a corner, exit blocks at one of the two corners *diagonally opposite* the one where it entered, and in between *stay confined* to the two blocks that are seen upon entering (see Figure 2.1).

The corner restriction, which is unphysical, is set to make the model mathematically tractable. We will see that, despite this restriction, the model has physically relevant behaviour.

Given ω, Ω and n, with each path $\pi \in \mathcal{W}_{n,L_n}$ we associate an *energy* given by the Hamiltonian

$$H^{\omega,\Omega}_{n,L_n}(\pi) = \sum_{i=1}^{n} \Big(\alpha\, 1\left\{\omega_i = \Omega^{L_n}_{(\pi_{i-1},\pi_i)} = A\right\} + \beta\, 1\left\{\omega_i = \Omega^{L_n}_{(\pi_{i-1},\pi_i)} = B\right\}\Big), \tag{2.2.4}$$

where (π_{i-1}, π_i) denotes the i-th step of the path and $\Omega^{L_n}_{(\pi_{i-1},\pi_i)}$ denotes the label of the block this step lies in. What this Hamiltonian does is count the number of AA-matches and BB-matches and assign them energy $-\alpha$ and $-\beta$, respectively, where $\alpha, \beta \in \mathbb{R}$.

Given ω, Ω and n, we define the *quenched free energy per step* as

$$\begin{aligned} f^{\omega,\Omega}_{n,L_n} &= \frac{1}{n}\log Z^{\omega,\Omega}_{n,L_n}, \\ Z^{\omega,\Omega}_{n,L_n} &= \sum_{\pi\in\mathcal{W}_{n,L_n}} \exp\left[H^{\omega,\Omega}_{n,L_n}(\pi)\right]. \end{aligned} \tag{2.2.5}$$

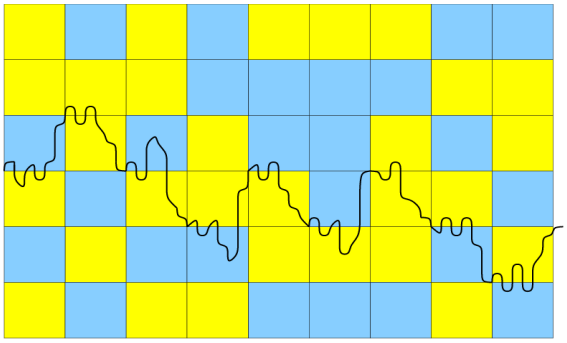

Figure 2.1: A directed self-avoiding path crossing blocks of oil and water diagonally. The light-shaded blocks are oil, the dark-shaded blocks are water. Each block is L_n lattice spacings wide in both directions. The path carries hydrophobic and hydrophilic monomers on the lattice scale, which are not indicated.

We are interested in the limit $n \to \infty$ subject to the restriction

$$L_n \to \infty \qquad \text{and} \qquad \frac{1}{n} L_n \to 0. \tag{2.2.6}$$

This is a *coarse-graining* limit where the path spends a long time in each single block yet visits many blocks. In this limit, there is a separation between a *copolymer scale* and an *emulsion scale*.

A variational formula for the free energy

In [54], den Hollander and Whittington proved that the free energy $f(\alpha, \beta; p)$ can be expressed under the form of a variational formula. Let us first explain briefly how this variational expression is built. First of all, because of the "corner constraint", when a trajectory $\pi \in \mathcal{W}_{n,L_n}$, crosses a given block column, it stays confined inside a pair of adjacent blocks, one of these blocks is crossed diagonally and the other one may or may not be visited by π. Thus, it is natural to consider the sequence of pairs of adjacent blocks that are crossed by π up to time n and subsequently, to decompose π into sub-trajectories, each of them corresponding to the crossing of one particular pair of blocks. This decomposition is the corner stone to obtain the variational expression of the free energy. The assumption $L_n \to \infty$ ensures, indeed, that the time spent in a pair of block tends to infinity with the copolymer length n so that we can define a free energy per step in each of the 4 types of block pairs. It remains to define the set $\mathcal{R}(p)$ of frequencies, with which each of the 4 types of pairs of blocks can be visited. These frequencies correspond to mesoscopic strategies of displacement in the medium. Finally, the variational formula will be obtained via an optimization over both $\mathcal{R}(p)$ and the time spent in each of the 4 block pairs.

To be more specific, let us give more details about the three main ingredients of the variational formula.

I. For $k, l \in \{A, B\}$, and $a \geq 2$ we let $\psi_{kl}(\alpha, \beta; a)$ be the free energy per step in a kl-block when the number of steps inside the block is a times the size of the block. The letter k labels the type of the block that is diagonally crossed, while l labels the type of the block that appears as its neighbour at the starting corner. It was proven in [54], Section 2.2, that the limit exists ω-a.s. and in mean, and is non-random. Both ψ_{AA} and ψ_{BB} take on a simple form, whereas ψ_{AB} and ψ_{BA} do not and can actually be expressed under the form of a variational formula.

II. For a given mesoscopic disorder Ω, we let $\mathcal{R}^{\Omega}$ be the set containing those 2×2 matrices of the form

$$\begin{pmatrix} \rho_{AA} & \rho_{AB} \\ \rho_{BA} & \rho_{BB} \end{pmatrix} \tag{2.2.7}$$

whose elements are non-negative, sum up to 1, and give a family of frequencies at which the four pairs of adjacent blocks can be visited by the copolymer. This subset is a priori Ω-dependent, but a straightforward application of Kolmogorov $0-1$ law ensures that Ω-a.s. $\mathcal{R}^{\Omega}$ equals a constant subset $\mathcal{R}(p)$. In other words, each $\rho \in \mathcal{R}(p)$ corresponds to an allowed strategy of displacement for the copolymer at the level of blocks (mesoscopic).

A rigorous definition of $\mathcal{R}(p)$ is provided in [54], section 1.3, and it is shown, in Proposition 3.2.1, that $p \mapsto \mathcal{R}(p)$ is continuous in the Hausdorff metric and that, for $p \geq p_c$, $\mathcal{R}(p)$ contains matrices of the form

$$M_\gamma = \begin{pmatrix} 1-\gamma & \gamma \\ 0 & 0 \end{pmatrix} \quad \text{for } \gamma \in C \subset (0,1) \text{ closed.} \tag{2.2.8}$$

III. Let $\mathcal{A}$ be the set of 2×2 matrices whose elements are ≥ 2. The elements of these matrices are used to record the average number of steps made by the path inside the four block pairs divided by the block size.

With these three objects in hand, we can state the result from [54] that settle the issues of the convergence, of the self-averaging property and of the variational expression of the quenched free energy.

Theorem 2.2.1. ([54], Theorem 1.3.1)
(i) For all $(\alpha, \beta) \in \mathbb{R}^2$ and $p \in (0,1)$,

$$\lim_{n \to \infty} f_{n, L_n}^{\omega, \Omega} = f = f(\alpha, \beta; p) \tag{2.2.9}$$

exists ω, Ω-a.s. and in mean, is finite and non-random, and is given by

$$f = \sup_{(\rho_{kl}) \in \mathcal{R}(p)} \sup_{(a_{kl}) \in \mathcal{A}} \frac{\sum_{kl} \rho_{kl} a_{kl} \psi_{kl}(a_{kl})}{\sum_{kl} \rho_{kl} a_{kl}}. \tag{2.2.10}$$

(ii) For all $(\alpha, \beta) \in \mathbb{R}^2$ *and* $p \in (0,1)$,

$$\begin{aligned} f(\alpha,\beta;p) &= f(\beta,\alpha;1-p), \\ f(\alpha,\beta;p) &= \tfrac{1}{2}(\alpha+\beta) + f(-\beta,-\alpha;p). \end{aligned} \tag{2.2.11}$$

Part (ii) is the reason why without loss of generality we may restrict the parameters to the cone

$$\text{CONE} = \{(\alpha,\beta) \in \mathbb{R}^2 \colon\ \alpha \geq |\beta|\}. \tag{2.2.12}$$

The behaviour of f as a function of (α, β) is different for $p \geq p_c$ and $p < p_c$ (where p_c is the critical percolation density for directed bond percolation on the square lattice). The reason is that, due to the geometric constraint that they must satisfy, the trajectories from $\mathcal{W}_{n,L_n}$ sample the mesoscopic disorder Ω just like paths in directed bond percolation on the square lattice rotated by 45 degrees sample the percolation configuration (see Figure 2.1).

2.2.2 The supercritical regime $p \geq p_c$

In the supercritical regime the *oil blocks percolate*, and so the copolymer can choose between moving deep inside the infinite oil cluster forever or spending some time along the oil-water interface (see Figure 2.2). Thus, a transition occurs between a phase that is fully delocalized in the A solvent and another phase associated with a partial localization of the copolymer at the interface between the infinite oil-cluster and the water around it.

In [54], den Hollander and Whittington proved that the phase transition occurs along a critical curve $\alpha \in [0,\infty) \mapsto \beta_c(\alpha) \in [0,\infty)$ that is concave, non-decreasing, admits an horizontal asymptote β^*, and follows the first diagonal for awhile before exiting it at some α^* in such a way that the slope of $\beta_c(\cdot)$ at $(\alpha^*)^+$ is strictly smaller than 1.

In [50], we pushed forward the analysis of the phase diagram by, 1) identifying the critical exponent of the phase transition off the diagonal, 2) proving that the critical curve is strictly increasing which yields that $\alpha^* < \beta^*$ and that the critical curve is not trivially equal to β^* when $\alpha > \alpha^*$, 3) proving that, subject to a mild assumption on $\mathcal{R}(p)$, the free energy is infinitely differentiable inside the localized phase which rules out the possibility that another phase transition occurs in the CONE.

Background

We begin by recalling two important theorems from den Hollander and Whittington [54]. They allow for a first quantitative picture of the phase diagram when $p \geq p_c$ (see Figure 2.3).

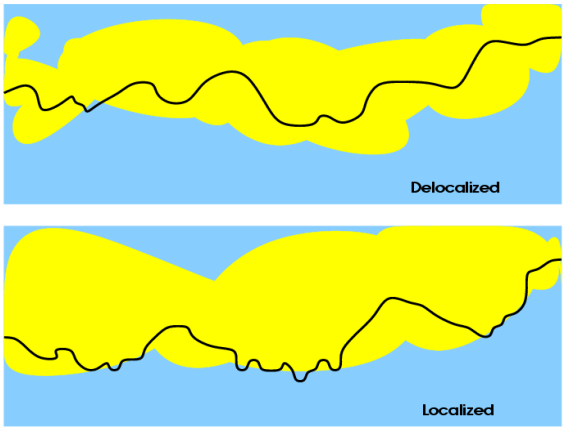

Figure 2.2: Two possible strategies when the oil percolates.

Theorem 2.2.2. ([54], Theorems 1.4.1 and 1.4.3) *Let $p \geq p_c$.*
(i) $(\alpha, \beta) \mapsto f(\alpha, \beta; p)$ is non-analytic along the curve in CONE *separating the two regions*

$$\begin{aligned} \mathcal{D} = \ & \textit{delocalized phase} \ = \left\{(\alpha,\beta) \in \text{CONE}\colon f(\alpha,\beta;p) = \tfrac{1}{2}\alpha + \varpi\right\}, \\ \mathcal{L} = \ & \textit{localized phase} \ = \left\{(\alpha,\beta) \in \text{CONE}\colon f(\alpha,\beta;p) > \tfrac{1}{2}\alpha + \varpi\right\}. \end{aligned} \tag{2.2.13}$$

Here, $\varpi = \lim_{n\to\infty} \frac{1}{n} \log |\mathcal{W}_{n,L_n}| = \frac{1}{2} \log 5$ is the entropy per step of the walk subject to (2.2.6).
(ii) For every $\alpha \geq 0$ there exists a $\beta_c(\alpha) \in [0, \alpha]$ such that the copolymer is

$$\textit{delocalized} \quad \textit{if} \quad -\alpha \leq \beta \leq \beta_c(\alpha), \tag{2.2.14}$$

$$\textit{localized} \quad \textit{if} \quad \beta_c(\alpha) < \beta \leq \alpha. \tag{2.2.15}$$

(iii) $\alpha \mapsto \beta_c(\alpha)$ is independent of p, continuous, non-decreasing and concave on $[0, \infty)$. There exist $\alpha^* \in (0, \infty)$ and $\beta^* \in [\alpha^*, \infty)$ such that

$$\beta_c(\alpha) = \alpha \quad \textit{if} \quad \alpha \leq \alpha^*, \tag{2.2.16}$$

$$\beta_c(\alpha) < \alpha \quad \textit{if} \quad \alpha > \alpha^*, \tag{2.2.17}$$

and

$$\lim_{\alpha \downarrow \alpha^*} \frac{\beta_c(\alpha) - \alpha^*}{\alpha - \alpha^*} \in [0, 1), \qquad \lim_{\alpha\to\infty} \beta_c(\alpha) = \beta^*. \tag{2.2.18}$$

Theorem 2.2.2 (i-ii) shows that traveling inside the infinite cluster of type A *has no entropic cost*. Thus, the free energy in the saturated phase $\mathcal{D}$ takes a simple form $\frac{\alpha}{2} + \varpi$ since half of the monomers (those of type A) are placed in their favorite solvent. The phase transition between $\mathcal{D}$ and $\mathcal{L}$ occurs when α is not too small and when there is a larger energetic advantage for the copolymer to move some of its monomers from the A-blocks

to the B-blocks by *crossing the interface inside the AB-block pairs*. There is some entropic loss associated with doing so, but if β is large enough, then the energetic advantage will dominate, so that AB-localization sets in. The value at which this happens depends on α and is strictly positive.

The proof of (iii) relies on a representation of $\mathcal{D}$ and $\mathcal{L}$ in terms of a single interface free energy which requires a proper definition. For $\mu \geq 1$ and $L \in \mathbb{N}$, we let $\mathcal{W}_{\mu,L}$ denote the set of μL-step directed self-avoiding paths starting at $(0,0)$ and ending at $(L,0)$. Define

$$\phi^{\mathcal{I}}(\mu;\alpha,\beta) = \lim_{L\to\infty} \frac{1}{\mu L} \log \sum_{\pi\in\mathcal{W}_{\mu,L}} \exp\left[-H_{cL}^{\omega,\mathcal{I}}(\pi)\right] \tag{2.2.19}$$

$$\hat{\kappa}(\mu) = \lim_{L\to\infty} \frac{1}{\mu L} \log |\mathcal{W}_{\mu,L}| \tag{2.2.20}$$

with

$$H_{\mu L}^{\omega,\mathcal{I}}(\pi) = -\sum_{i=1}^{\mu L} \Big(\alpha\, 1\{\omega_i = A, (\pi_{i-1},\pi_i) > 0\} + \beta\, 1\{\omega_i = B, (\pi_{i-1},\pi_i) \leq 0\}\Big), \tag{2.2.21}$$

where $(\pi_{i-1},\pi_i) > 0$ means that the i-th step lies in the upper halfplane and $(\pi_{i-1},\pi_i) \leq 0$ means that the i-th step lies in the lower halfplane or in the interface. The convergence of $\phi^{\mathcal{I}}$ in (2.2.19) and its self-averaging property in ω were proven in [54] Section 2.2.2, whereas explicit formulas for $\hat{\kappa}(\mu)$ were displayed in Section 2.1.2. The strict concavity of $\mu \to \mu\phi^{\mathcal{I}}(\mu)$ on $[1,\infty)$, which was stated as an assumption in [50] and [51] has been proven in [53] Lemma 3.3.

Note that, for $\mu > 1$ and $\alpha > 0$ fixed, the single linear interface model undergoes a localization transition between a delocalized phase in which $\phi^{\mathcal{I}}(\mu) = \frac{\alpha}{2} + \hat{\kappa}(\mu)$ and a localized phase characterized by $\phi^{\mathcal{I}}(\mu) > \frac{\alpha}{2} + \hat{\kappa}(\mu)$. In the delocalized phase the copolymer remains above the interface, whereas in the localized phase, it puts a positive fraction of its monomers of type B in the B solvent. The monotonicity of $\beta \to \phi^{\mathcal{I}}(\mu;\alpha,\beta)$ yields that the phase transition occurs at some $\beta_c^{\mathcal{I}}(\mu,\alpha) \in (0,\infty)$.

With the latter definition in hand, we can give the single interface representation of the phase transition.

Proposition 2.2.3. ([54], Proposition 2.3.1)
Let $p \geq p_c$. Then $(\alpha,\beta) \in \mathcal{L}$ if and only if

$$\sup_{\mu\geq 1} \mu\left[\phi^{\mathcal{I}}(\alpha,\beta;\mu) - \tfrac{1}{2}\alpha - \tfrac{1}{2}\log 5\right] > \tfrac{1}{2}\log\tfrac{9}{5}. \tag{2.2.22}$$

A straightforward consequence of Proposition 2.2.3 is that the critical curve is independent of $p \geq p_c$ since the single interface representation itself is independent of $p \geq p_c$. Moreover, this representation expresses the fact that localization occurs for the emulsion

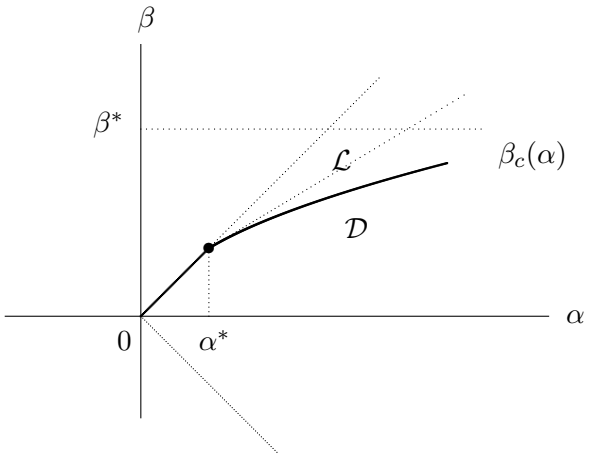

Figure 2.3: Qualitative picture of $\alpha \mapsto \beta_c(\alpha)$ for $p \geq p_c$.

free energy only when the single interface free energy is *sufficiently deep inside* its localized phase. By picking $\alpha > \alpha^*$ it can be shown that the inequality in (2.2.22) becomes an equality at $(\alpha, \beta_c(\alpha))$. Moreover, the strict concavity of $\mu \to \mu\phi^{\mathcal{I}}(\mu)$ implies that the supremum in (2.2.22) with $\beta = \beta_c(\alpha)$ is attained at a unique $\mu_\alpha > 1$. Then, we use Lemma 2.1.2 in [54] (iii) which states that

$$\sup_{\mu \geq 1} \mu[\hat{\kappa}(\mu) - \tfrac{1}{2}\log 5] < \tfrac{1}{2}\log\tfrac{9}{5},$$

so that $\phi^{\mathcal{I}}(\mu_\alpha; \alpha, \beta) > \hat{\kappa}(\mu_\alpha) + \frac{\alpha}{2}$ and therefore $\beta_c(\alpha) > \beta_c^{\mathcal{I}}(\mu, \alpha)$. Heuristically, this gap is needed to compensate for the loss of entropy associated with running along the AB interface and crossing the A block at a steeper angle.

A deeper analysis of the phase diagram

In [50], we managed to obtain a complete picture of the phase diagram with the 3 Theorems below. Note that Theorems 2.2.5 and 2.2.6 have an analogue for the single flat infinite interface that have been derived in Giacomin and Toninelli [43], [44]. For that model the phase transition is shown to be *at least of second order*, i.e., only the quadratic upper bound is proved. Numerical simulation indicates that the transition may well be of higher order.

Theorem 2.2.4. *Let $p \geq p_c$. Then $\alpha \mapsto \beta_c(\alpha)$ is strictly increasing on $[0, \infty)$.*

Theorem 2.2.4 implies that the critical curve never reaches the horizontal asymptote, which in turn implies that $\alpha^* < \beta^*$ and that the slope in (2.2.18) is > 0. The proof of Theorem 2.2.4 relies on the single interface representation of the phase transition. To be more specific, we recall that at $(\alpha, \beta_c(\alpha))$ with $\alpha > \alpha^*$, the inequality in (2.2.22) is an equality and the supremum in the l.h.s. of (2.2.22) is attained at a unique $\mu_\alpha > 0$.

Therefore, the strict monotonicity of $\alpha \to \beta_c(\alpha)$ is obtained by picking $\alpha' \in (\alpha^*, \alpha)$ and by proving that $\phi^{\mathcal{I}}(\mu_\alpha; \alpha', \beta_c(\alpha)) > \phi^{\mathcal{I}}(\mu_\alpha; \alpha, \beta_c(\alpha))$. To prove the latter inequality, it suffices to show that, for the single linear interface model at $(\mu_\alpha, \alpha, \beta_c(\alpha))$, the copolymer puts a strictly positive fraction of its monomers of type A in their favorite solvent. We show this last point by using that the single linear interface model at $(\mu_\alpha, \alpha, \beta_c(\alpha))$ is already localized and therefore that its excursions away from the interface are exponentially tight.

Theorem 2.2.5. *Let $p \geq p_c$. Then for every $\alpha \in (\alpha^*, \infty)$ there exist $0 < C_1 < C_2 < \infty$ and $\delta_0 > 0$ (depending on p and α) such that*

$$C_1\,\delta^2 \leq f\,(\alpha, \beta_c(\alpha) + \delta; p) - f\,(\alpha, \beta_c(\alpha); p) \leq C_2\,\delta^2 \qquad \forall\,\delta \in (0, \delta_0]. \tag{2.2.23}$$

The mechanisms behind the phase transitions in our emulsion model and in the single interface model are different. While for the single interface model the copolymer makes long excursions away from the interface and dips below the interface during a fraction of time that is at most of order δ^2, in our emulsion model the copolymer runs along the interface during a fraction of time that is of order δ, and in doing so stays close to the interface. Moreover, since the single interface model is already inside its localized phase at $(\alpha, \beta_c(\alpha))$, the variation of the single interface free energy is of order δ. Thus, the δ^2 in the emulsion model is the product of two factors δ, one coming from the time spent running along the interface and one coming from the variation of the constituent single interface free energy away from its critical curve. See [50] Section 4.1 for more details.

Theorem 2.2.6. *Let $p \geq p_c$. Then, under Assumption* 2.2.7 *below, $(\alpha, \beta) \mapsto f(\alpha, \beta; p)$ is infinitely differentiable throughout $\mathcal{L}$.*

In the proof of Theorem 2.2.6 we use some of the ingredients of the proof in Giacomin and Toninelli [44] of the analogous result for the single interface model. However, in the emulsion model there is an extra complication, namely, the speed per step to move one unit of space forward may vary (because steps are up, down and to the right), while in the single interface model this is fixed at one (because steps are up-right and down-right). We need to control the infinite differentiability with respect to this speed variable. This is done by considering the Fenchel-Legendre transform of the free energy, in which the dual of the speed variable enters into the Hamiltonian rather than in the set of paths. Moreover, since the block pair free energies and the total free energy are both given by variational problems, we need to show *uniqueness of maximisers* and prove *non-degeneracy of the Jacobian matrix at these maximisers* in order to be able to apply implicit function theorems. See [50] Section 5 for more details.
Note that in [50], Theorem 2.2.6 was proven subject to the assumption that $\mu \to \phi^{\mathcal{I}}(\mu; \alpha, \beta)$ is strictly concave for $(\alpha, \beta) \in$ CONE. The strict concavity has, later on, been proven in [53] but we figured out afterwards that another subtle assumption, which is stated below, has to be made to prove the Theorem.

Assumption 2.2.7. *For all $p \geq p_c$,*

$$\max\{\rho_{AB} \colon \rho \in \mathcal{R}(p)\} = \max\left\{\gamma \colon \begin{pmatrix} 1-\gamma & \gamma \\ 0 & 0 \end{pmatrix} \in \mathcal{R}(p)\right\}.$$

What assumption (2.2.7) says is that the mesoscopic strategies of displacement that maximize the fraction of AB blocks crossed by the copolymer are those moving inside the infinite cluster of type A and close to its boundary with the B solvent. In other words, one can not cross more AB blocks by spending time deep inside the B solvent.

2.2.3 The subcritical regime

When $p < p_c$, the A blocks do not percolate anymore and therefore a strictly positive fraction of the blocks that are diagonally crossed by the copolymer are of type B (water), even though the copolymer prefers oil (recall $\alpha \geq \beta$). As a consequence, the phase diagram is more complicated than its super-critical counterpart. So far, we can distinguish between 4 different phases, separated by 4 critical curves, meeting up at 2 tricritical points. Let us give some physical interpretations of each phase:

- $\mathcal{D}_1$: the copolymer is fully delocalized into A blocks and B blocks and never visits the neighboring block when it crosses an AB or a BA block. Physically, this corresponds to the copolymer traveling inside big clusters of solvents A and B alternatively, without paying attention to AB interfaces. The latter typically happens at small values of α and β.

- $\mathcal{D}_2$: the copolymer is fully delocalized into A blocks and B blocks but makes a long excursion inside the neighboring A block when crossing a BA block. Physically, this corresponds to the copolymer targeting small A droplets when it travels in solvent B in order to make excursions inside these droplets and away from their interface. This typically happens for large α and small β.

- $\mathcal{L}_1$: the copolymer localizes along the interface when crossing a BA block. Physically, this corresponds to the copolymer targeting small A droplets when it travels in solvent B and localizing at the interface of these droplets. This typically happens for large α and moderate β.

- $\mathcal{L}_2$: the copolymer localizes along the interface when crossing both a BA or an AB block. Physically, this corresponds to the copolymer targeting small A (respectively B) droplets when it travels in solvent B (resp. A) and localizing at the interface of these droplets. This typically happens for large α and large β.

In [54], den Hollander and Whittington identified $\mathcal{D}_1$ and showed that the free energy is infinitely differentiable inside $\mathcal{D}_1$. They also provided a criterium to decide whether

$(\alpha, \beta) \in \mathcal{D}_1$ or not (see [54] Theorem 1.5.2) and gave some qualitative properties of the boundary of $\mathcal{D}_1$ (see [54] Theorem 1.5.3). Finally, they also conjectured the existence of $\mathcal{L}_2$.

In [51] we brought the investigation of the subcritical regime much further. We identified the phases $\mathcal{D}_2$ and $\mathcal{L}_1$, and proved under a mild assumption that the free energy is infinitely differentiable inside $\mathcal{D}_2$. We gave criterions to decide whether $(\alpha, \beta) \in \mathcal{D}_2$ or not and whether $(\alpha, \beta) \in \mathcal{L}_1$ or not. We identified a critical curve separating $\mathcal{D}_2$ and $\mathcal{L}_1$ and gave qualitative properties about it. Finally, we gave bounds on the order of the phase transitions between $\mathcal{D}_1$ and $\mathcal{D}_2$, $\mathcal{D}_1$ and $\mathcal{L}_1$ and also between $\mathcal{D}_2$ and $\mathcal{L}_1$.

In Section 2.2.4 we characterize the four phases.

2.2.4 Characterization of the four phases and analysis of the phase diagram

The characterization of the 4 phases will involve four free energies

$$f_{\mathcal{D}_1} \leq f_{\mathcal{D}_2} \leq f_{\mathcal{L}_1} \leq f_{\mathcal{L}_2} = f, \tag{2.2.24}$$

with the inequalities becoming strict successively. We will see that the phase diagram looks like Fig. 2.4. Furthermore, we will see that the typical path behavior in the four phases looks like Fig. 2.5.

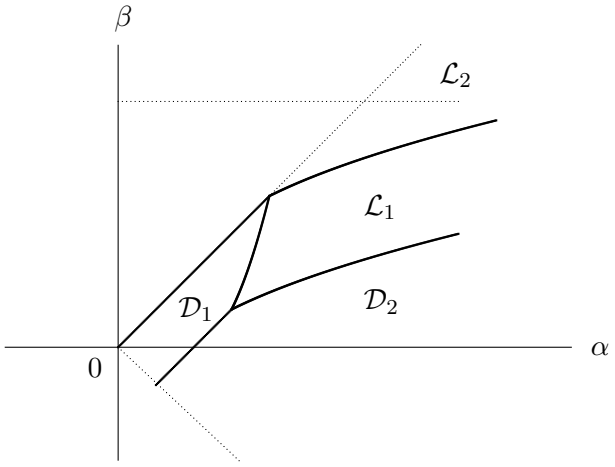

Figure 2.4: Sketch of the phase diagram for $p < p_c$. There are 4 phases, separated by 4 critical curves, meeting a two tricritical points.

At this stage, we lighten the notations by introducing a shift of $-\alpha/2$ in the definition of the free energy (2.2.5). By the law of large number, this shift amounts to subtract the

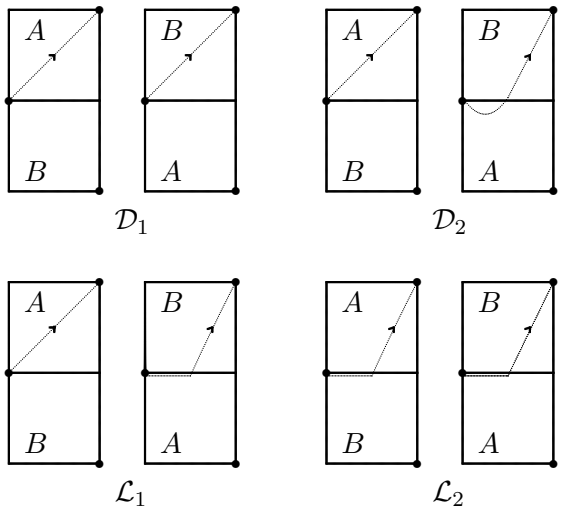

Figure 2.5: Behavior of the copolymer inside the four block pairs containing oil and water for each of the four phases.

term $\alpha \sum_{i=1}^{n} 1\{\omega_i = A\}$ from the Hamiltonian in (2.2.4), which becomes

$$H_{n,L_n}^{\omega,\Omega}(\pi) = \sum_{i=1}^{n} \Big(-\alpha\, 1\{\omega_i = A\} + \beta\, 1\{\omega_i = B\} \Big) 1\Big\{\Omega_{(\pi_{i-1},\pi_i)}^{L_n} = B\Big\}. \tag{2.2.25}$$

This shift is of course harmless when studying the phase diagram and it eases the exposition.

The $\mathcal{D}_1$-phase: A-delocalization and B-delocalization

As mentioned in the introduction, $\mathcal{D}_1$ corresponds to a full delocalization of the copolymer into the A-blocks and B-blocks, i.e., when the copolymer crosses an AB-block or a BA-block it does not spend appreciable time near the AB-interface (see Fig. 2.5). Consequently, in $\mathcal{D}_1$ the free energy is given by a reduced version of the variational expression in (2.2.10), namely, ψ_{AB} (resp. ψ_{BA}) is replaced by ψ_{AA} (resp. ψ_{BB}) and the supremum over $\mathcal{R}(p)$ is reached at ρ^* which maximizes $\rho_{AA} + \rho_{AB}$. Thus, the free energy depends on $\alpha - \beta$ and p only.

Definition 2.2.8. *For $p < p_c$,*

$$\mathcal{D}_1 = \big\{(\alpha,\beta) \in \text{CONE}\colon\ f(\alpha,\beta;p) = f_{\mathcal{D}_1}(\alpha-\beta;p)\big\} \tag{2.2.26}$$

with

$$f_{\mathcal{D}_1}(\alpha-\beta;p) = \sup_{x\geq 2,\, y\geq 2} \frac{\rho^*(p)\, x\, \psi_{AA}(x) + [1-\rho^*(p)]\, y\, \psi_{BB}(y)}{\rho^*(p)\, x + [1-\rho^*(p)]\, y}, \tag{2.2.27}$$

where $\rho^*(p)$ is the maximal frequency at which the A-blocks can be crossed, defined by (see Fig. 2.6)

$$\rho^*(p) = \max_{(\rho_{kl})\in\mathcal{R}(p)} [\,\rho_{AA} + \rho_{AB}\,]. \tag{2.2.28}$$

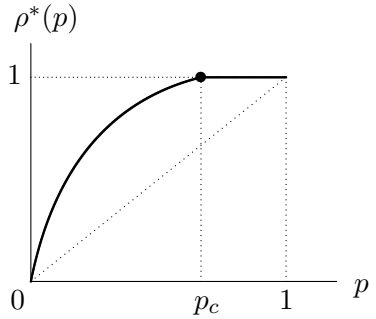

Figure 2.6: Sketch of $p \mapsto \rho^*(p)$.

The $\mathcal{D}_2$-phase: A-delocalization, BA-delocalization

Starting from $(\alpha, \beta) \in \mathcal{D}_1$ with $\beta \leq 0$, we increase α until it becomes energetically advantageous for the copolymer to spend some time in the A-solvent when crossing a BA-block. It turns out that the copolymer does not localize along the BA-interface, but rather crosses the interface to make a long excursion inside the A-block before returning to the B-block to cross it diagonally (see Fig. 2.5). The free energy is then given by another restricted version of (2.2.10), namely, ψ_{AB} is replaced by ψ_{AA} while ψ_{BA} is replaced by $\psi_{BA}^{\hat{\kappa}}$ which is the contribution to ψ_{BA} of those trajectories making exactly one excursion in the A block before diagonally crossing the B block.

Definition 2.2.9. *For $p < p_c$,*

$$\mathcal{D}_2 = \big\{(\alpha, \beta) \in \text{CONE}\colon\ f_{\mathcal{D}_1}(\alpha - \beta; p) < f(\alpha, \beta; p) = f_{\mathcal{D}_2}(\alpha - \beta; p)\big\} \tag{2.2.29}$$

with

$$f_{\mathcal{D}_2}(\alpha - \beta; p) = \sup_{x \geq 2,\, y \geq 2,\, z \geq 2} \sup_{\rho \in \mathcal{R}(p)} \frac{\rho_A\, x\, \psi_{AA}(x) + \rho_{BA}\, y\, \psi_{BA}^{\hat{\kappa}}(y) + \rho_{BB}\, z\, \psi_{BB}(z)}{\rho_A\, x\, + \rho_{BA}\, y\, + \rho_{BB}\, z}, \tag{2.2.30}$$

where $\rho_A = \rho_{AB} + \rho_{AA}$.

By using some explicit expressions for ψ_{AA}, ψ_{BB} and $\psi_{BA}^{\hat{\kappa}}$ (see [51] Lemma 1.1), we can state that $f_{\mathcal{D}_2}$ depends on $\alpha - \beta$ and p only and we can provide two characterizations of $\mathcal{D}_2$: one in terms of the block pair free energies and another one in terms of the single interface free energy (see [51], Proposition 1.9 and Corollary 1.10). As a consequence, $\mathcal{D}_1$ and $\mathcal{D}_2$ touch each other along a diagonal segment (cf. Fig. 2.4) and the order of the phase transition between $\mathcal{D}_1$ and $\mathcal{D}_2$ is smaller than or equal to 2 (see [51] Theorem 1.19).

Finally, we prove in [51] Theorem 1.17, that the free energy is infinitely differentiable inside $\mathcal{D}_2$ subject to the following assumption. We indeed assume that on the whole $\mathcal{D}_2$, the second supremum in (2.2.30) is uniquely taken at $(\rho_{kl}) = (\rho_{kl}^*(p))$ with $\rho_{AA}^*(p) + \rho_{AB}^*(p) = \rho^*(p)$ given by (2.2.28) and with $\rho_{BA}^*(p)$ maximal subject to the latter equality. In view of

Fig. 2.5, this is a resonnable assumption indeed, because in $\mathcal{D}_2$ the copolymer will first try to maximize the fraction of time it spends crossing A-blocks, and then try to maximize the fraction of time it spends crossing B-blocks that have an A-block as neighbor.

The $\mathcal{L}_1$-phase: A-delocalization, BA-localization

In the $\mathcal{L}_1$ phase, when the copolymer crosses a BA block, it sticks first to the interface for awhile before crossing diagonally the B-block. Thus, the free energy in $\mathcal{L}_1$ is given by the same expression as in (2.2.30) except that $\psi_{BA}^{\hat{\kappa}}$ is replaced by ψ_{BA}.

Definition 2.2.10. *For $p < p_c$,*

$$\mathcal{L}_1 = \big\{(\alpha,\beta) \in \text{CONE}\colon\ f_{\mathcal{D}_2}(\alpha-\beta;p) < f(\alpha,\beta;p) = f_{\mathcal{L}_1}(\alpha,\beta;p)\big\} \tag{2.2.31}$$

with

$$f_{\mathcal{L}_1}(\alpha,\beta;p) = \sup_{x\geq 2,\, y\geq 2,\, z\geq 2}\ \sup_{(\rho_{kl})\in\mathcal{R}(p)} \frac{\rho_A\, x\, \psi_{AA}(x) + \rho_{BA}\, y\, \psi_{BA}(y) + \rho_{BB}\, z\, \psi_{BB}(z)}{\rho_A\, z\ + \rho_{BA}\, y\ + \rho_{BB}\, z}. \tag{2.2.32}$$

If we let (α,β) run in $\mathcal{D}_2$ along a linear segment parallel to the first diagonal, then the free energy $f(\alpha,\beta;p)$ remains constant until (α,β) enters $\mathcal{L}_1$. In other words, if we pick $(\alpha_0,\beta_0) \in \mathcal{D}_2$ and consider for $u \geq 0$ the point $s_u = (\alpha_0+u, \beta_0+u)$, then the free energy $f(s_u;p)$ remains equal to $f(\alpha_0,\beta_0;p)$ until u reaches a critical value at which s_u exits $\mathcal{D}_2$ and enters $\mathcal{L}_1$. This transition is closely related to the localization transition of the single linear interface model because the copolymer transforms the excursion it was making in the A solvent when crossing a BA block into a path that is localized along the AB interface. This passage from $\mathcal{D}_2$ to $\mathcal{L}_1$ comes with a non-analyticity of the free energy and is represented on the phase diagram by a critical curve (see Fig. 2.4). In [51] Theorem 1.16, we prove the existence of the latter critical curve and give some of its analytic properties. In [51] Theorem 1.20, we show that the order of the phase transition is smaller than or equal to the order of the phase transition for the single linear interface model.

Similarly to what we described above for the $\mathcal{D}_2$ to $\mathcal{L}_1$ transition, we can pick $(\alpha_0,\beta_0) \in \mathcal{D}_1$ and consider for $u \geq 0$ the point $s_u = (\alpha_0+u, \beta_0+u)$, so that the free energy $f(s_u;p)$ remains equal to $f(\alpha_0,\beta_0;p)$ until u reaches a critical value at which s_u exits $\mathcal{D}_1$ and enters $\mathcal{L}_1$. In [51] Theorem 1.15, we analyze the critical curve separating $\mathcal{D}_1$ and $\mathcal{L}_1$ and prove, among other things, that it is continuous and strictly contained in the upper-half plane. We note that this transition is of the same type as the phase transition we studied in the super-critical regime. In the latter regime indeed, the change of strategy in the copolymer displacement happens in AB blocks between full A delocalization and partial AB localization. In the present case, the transformation happens in BA blocks but again between full B delocalization and partial AB localization. In [51] Theorem 1.19, we show

that the order of the phase transition is smaller than or equal to 2 and strictly larger than 1, but the analogy with the super-critical regime tells us that the true value should be exactly 2.

The $\mathcal{L}_2$-phase: AB-localization, BA-localization

The remaining phase is:

Definition 2.2.11. *For $p < p_c$,*

$$\mathcal{L}_2 = \big\{(\alpha,\beta) \in \text{CONE}\colon\ f_{\mathcal{L}_1}(\alpha,\beta;p) < f(\alpha,\beta;p)\big\}. \tag{2.2.33}$$

Starting from $(\alpha,\beta) \in \mathcal{L}_1$, we increase β until it becomes energetically advantageous for the copolymer to localize at the interface in the AB-blocks as well. This new phase has both AB- and BA-localization (see Fig. 2.5). Unfortunately, we are not able to show non-analyticity at the crossover from $\mathcal{L}_1$ to $\mathcal{L}_2$ because, unlike in $\mathcal{D}_2$, in $\mathcal{L}_1$ the free energy is not constant in one particular direction (and the argument we gave for the non-analyticity at the crossover from $\mathcal{D}_2$ to $\mathcal{L}_1$ is not valid here). Consequently, the phase transition between $\mathcal{L}_1$ and $\mathcal{L}_2$ is still a *conjecture* at this stage, but we strongly believe that a third critical curve indeed exists.

2.3 A more realistic model: removal of the corner restriction

Despite the *non-physical* corner restriction that we imposed on the former model, we have seen in Section 2.2 that the model displays in both the super-critical and sub-critical regimes a rich and physically relevant phase diagram. However, the corner restricted model has two main limitations that we are willing to overstep. First, the fact that the copolymer can not follow an AB interface on a distance larger than L_n is a limitation. We indeed conjecture that for α and β large, the copolymer localizes whenever it encounters an AB interface and then, follows this interface on its whole length. Another limitation comes from the fact that, in the corner restricted model, there is no loss of entropy associated with the mesoscopic strategy of displacement chosen by the copolymer. In other words, the copolymer may choose to travel with a positive vertical speed (by exiting every block pair it crosses via the north-eastern corner) without being entropically more penalized than if it had traveled with a null vertical speed.

In order to overstep these limitations we decided to relax as much as possible the geometric constraint on the set of allowed trajectories, while keeping a variational expression for the free energy that is tractable enough to allow for an investigation of the phase diagram. We achieved this goal in [53] and the present section is dedicated to this work.

2.3.1 The free model

In size $n \in \mathbb{N}$, the lattice $\mathbb{Z}^2$ is partitioned into square blocks of size $L_n \in \mathbb{N}$. The microscopic and mesoscopic disorders (ω, Ω) are defined as in (2.2.2) and (2.2.3) for the corner restricted model. The new set of allowed trajectories is defined as follows. We pick $M \in \mathbb{N}$ that is *arbitrary but fixed* and we bound the vertical displacement on the block scale in each column of blocks by M. In other words, instead of considering the full set of trajectories $\mathcal{W}_n$, we consider only trajectories that exit a column through a block at most M above or M below the block where the column was entered (see Fig. 2.7). Note that the corner restriction has been completely relaxed. We denote by $\mathcal{W}_{n,M}$ the new set of allowed paths.

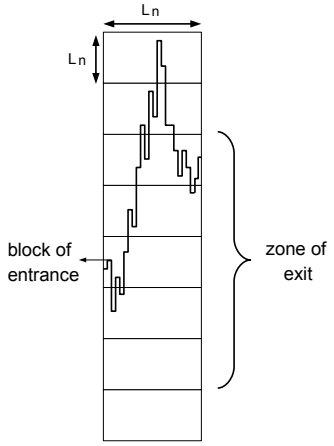

Figure 2.7: Example of a trajectory $\pi \in \mathcal{W}_{n,M}$ with $M = 2$.

Given ω, Ω, M and n, with each path $\pi \in \mathcal{W}_{n,M}$ we associate the same Hamiltonian as in (2.2.25), i.e.

$$H^{\omega,\Omega}_{n,L_n}(\pi;\alpha,\beta) = \sum_{i=1}^{n} \Big(\beta\, 1\{\omega_i = B\} - \alpha\, 1\{\omega_i = A\}\Big)\, 1\Big\{\Omega^{L_n}_{(\pi_{i-1},\pi_i)} = B\Big\}. \tag{2.3.1}$$

Similarly to what was done for the corner restricted model, we may, without loss of generality, restrict the interaction parameters to the CONE defined in (2.2.12). For $n \in \mathbb{N}$ and $M \in \mathbb{N}$, the free energy per monomer is defined as

$$f^{\omega,\Omega}_n(\alpha,\beta;M) = \tfrac{1}{n}\log Z^{\omega,\Omega}_{n,L_n}(\alpha,\beta;M) \quad \text{with} \quad Z^{\omega,\Omega}_{n,L_n}(\alpha,\beta;M) = \sum_{\pi\in\mathcal{W}_{n,M}} e^{H^{\omega,\Omega}_{n,L_n}(\pi;\alpha,\beta)}, \tag{2.3.2}$$

and we consider the limit of $f^{\omega,\Omega}_n(\alpha,\beta;M)$ as $n \to \infty$ with $L_n \to \infty$ and $\frac{L_n}{n} \to 0$.

2.3.2 The slope-based variational formula for the quenched free energy per step

The variational expressions of the free energy for the corner restricted model and for the free model are quite different. Indeed, instead of partitioning each trajectory into sub-pieces that correspond to the crossing of successive block columns, we rather decompose the trajectories into long sub-pieces during which the copolymer travels in a given solvent and at a given slope or along a linear AB interface. As a consequence, the constituting elements of the variational formula will be:

- for $u \geq 1 + l$ and $l \geq 0$, an entropy per step $\widetilde{\kappa}(u, l)$ for the trajectories traveling with a slope $l \in [0, \infty)$ and with a number of steps per horizontal step of u.
- For $u \geq 1$, the free energy $\phi^{\mathcal{I}}(u; \alpha, \beta)$ (defined earlier in (2.2.19)) for the trajectories traveling along an AB interface with a number of steps per horizontal step of u.
- Three functions $v = (v_A, v_B, v_{\mathcal{I}})$ in $\bar{\mathcal{B}}$ with

$$\bar{\mathcal{B}} = \{v = (v_A, v_B, v_{\mathcal{I}}) \in \mathcal{C} \times \mathcal{C} \times [1, \infty)\} \tag{2.3.3}$$

  with

$$\mathcal{C} = \big\{l \mapsto u_l \text{ on } \mathbb{R}_+ \colon \text{ continuous with } u_l \geq 1 + l \ \ \forall\, l \in \mathbb{R}_+\big\}. \tag{2.3.4}$$

  For each $l \in [0, \infty)$, the numbers $v_{A,l}, v_{B,l} \in [1 + l, \infty)$ indicate how many steps per horizontal step the copolymer takes when traveling at slope l in solvents A and B, respectively. Similarly, $v_{\mathcal{I}} \in [1, \infty)$ denotes the number of steps per horizontal step the copolymer takes when traveling along AB-interfaces.
- A subset $\bar{\mathcal{R}}_{p,M}$ of $\mathcal{M}_1\big(\mathbb{R}_+ \cup \mathbb{R}_+ \cup \{\mathcal{I}\}\big)$ such that each $\bar{\rho} \in \bar{\mathcal{R}}_{p,M}$ corresponds to a particular strategy of displacement in the medium. To be more specific, $\bar{\rho} \in \bar{\mathcal{R}}_{p,M}$ tells us that the copolymer may travel in the medium in such a way that, for each $l \in [1, \infty)$, $\bar{\rho}_A(dl)$ and $\bar{\rho}_B(dl)$ denote the fractions of horizontal steps at which the copolymer travels through solvents A and B at a slope that lies between l and $l + dl$, and $\rho_{\mathcal{I}}$ denotes the fraction of horizontal steps at which the copolymer travels along AB-interfaces. Note that $\bar{\mathcal{R}}_{p,M}$ should a priori depend on the mesoscopic disorder Ω as well. However, Kolmogorov 0-1 Law ensures that the subset is constant Ω-a.s. We refer to [53] Section 3.4.3 for a detailed definition of $\bar{\mathcal{R}}_{p,M}$.

With these ingredients we can now state our *slope-based variational formula*.

Theorem 2.3.1. **[slope-based variational formula]** *For every* $(\alpha, \beta) \in$ CONE*,* $M \in \mathbb{N}$ *and* $p \in (0, 1)$

$$\lim_{n \to \infty} f_n^{\omega,\Omega}(\alpha, \beta; M) = f(\alpha, \beta; M, p) \tag{2.3.5}$$

exists ω, Ω-a.s. and in mean, is finite and non-random, and is given by

$$f(\alpha,\beta;M,p) = \sup_{\bar\rho\in\bar{\mathcal{R}}_{p,M}} \sup_{v\,\in\,\bar{\mathcal{B}}} \frac{\bar N(\bar\rho,v)}{\bar D(\bar\rho,v)}, \tag{2.3.6}$$

where

$$\begin{aligned}
\bar N(\bar\rho,v) &= \int_0^\infty v_{A,l}\,\widetilde\kappa(v_{A,l},l)\,\bar\rho_A(dl) + \int_0^\infty v_{B,l}\left[\widetilde\kappa(v_{B,l},l) + \tfrac{\beta-\alpha}{2}\right]\bar\rho_B(dl) + v_{\mathcal I}\,\phi_{\mathcal I}(v_{\mathcal I};\alpha,\beta)\,\bar\rho_{\mathcal I},\\
\bar D(\bar\rho,v) &= \int_0^\infty v_{A,l}\,\bar\rho_A(dl) + \int_0^\infty v_{B,l}\,\bar\rho_B(dl) + v_{\mathcal I}\,\bar\rho_{\mathcal I},
\end{aligned} \tag{2.3.7}$$

with the convention that $\bar N(\bar\rho,v)/\bar D(\bar\rho,v) = -\infty$ when $\bar D(\bar\rho,v) = \infty$.

Discussion

Proving the variational formula in Theorem 2.3.1 is very difficult and most of our work in [53] is dedicated to that. We begin by proving a first auxiliary variational formula, similar to its corner restricted analogue in (2.2.10), but where the 4 types of block pairs are replaced by multiple types of block columns. Then, we prove a second auxiliary variational formula to express the free energy per step in each type of block column with the help of $\widetilde\kappa$ and $\phi^{\mathcal I}$. Finally, we combine these two auxiliary formulas to complete the proof of Theorem 2.3.1.

The variational formula in (2.3.6-2.3.7) is tractable, to the extent that the $\widetilde\kappa$-function is known explicitly, the $\phi_{\mathcal I}$-function has been studied in depth in the literature (and much is known about it), while the set $\bar{\mathcal B}$ is simple. *The key difficulty of* (2.3.6–2.3.7) *resides in the set $\bar{\mathcal R}_{p,M}$, whose structure is not easy to control.* However, it turns out that much can be said about the phase diagram without knowing too much on this set.

Finally, note that we are unable at the moment to prove the existence of the quenched free energy per step $f(\alpha,\beta;p)$ of the *free model*, i.e., the model with no restriction on the mesoscopic vertical displacement. By monotonicity,

$$f(\alpha,\beta;\infty,p) = \lim_{M\to\infty} f(\alpha,\beta;M,p) = \sup_{M\in\mathbb N} f(\alpha,\beta;M,p) \tag{2.3.8}$$

exists for all α,β and p. Taking the supremum over $M\in\mathbb N$ on both sides of (2.3.6), we obtain a variational formula for $f(\alpha,\beta;\infty,p)$, namely,

$$f(\alpha,\beta;\infty,p) = \sup_{\bar\rho\in\bar{\mathcal R}_{p,\infty}} \sup_{v\,\in\,\bar{\mathcal B}} \frac{\bar N(\bar\rho,v)}{\bar D(\bar\rho,v)} \tag{2.3.9}$$

with $\bar{\mathcal R}_{p,\infty} = \cup_{M\in\mathbb N}\bar{\mathcal R}_{p,M}$. Clearly, we have $f(\alpha,\beta;p) \geq f(\alpha,\beta;\infty,p)$, and we expect that equality holds. Indeed, if the inequality would be strict, then the partition function of the free model would be dominated by trajectories whose mesoscopic vertical displacements are unbounded. Such a domination is very unlikely because long and steep vertical displacements come with heavy entropic penalties. Therefore we do not expect such trajectories to be optimal.

Comparison with the directed polymer with bulk disorder

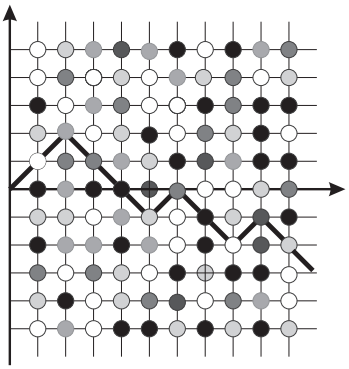

Figure 2.8: Picture of a directed polymer with bulk disorder. The different shades of black, grey and white represent different values of the disorder.

A model of a polymer with disorder that has been studied intensively in the literature is the *directed polymer with bulk disorder*. Here, the set of paths is

$$\mathcal{W}_n = \big\{\pi = (i,\pi_i)_{i=0}^n \in (\mathbb{N}_0 \times \mathbb{Z}^d)^{n+1} \colon\ \pi_0 = 0,\ \|\pi_{i+1} - \pi_i\| = 1\ \forall\, 0 \le i < n\big\}, \tag{2.3.10}$$

where $\|\cdot\|$ is the Euclidean norm on $\mathbb{Z}^d$, and the Hamiltonian is

$$H_n^\omega(\pi) = \lambda \sum_{i=1}^n \omega(i,\pi_i), \tag{2.3.11}$$

where $\lambda > 0$ is a parameter and $\omega = \{\omega(i,x) \colon\ i \in \mathbb{N},\ x \in \mathbb{Z}^d\}$ is a field of i.i.d. $\mathbb{R}$-valued random variables with zero mean, unit variance and finite moment generating function, where $\mathbb{N}$ is time and $\mathbb{Z}^d$ is space (see Fig. 2.8). This model can be viewed as a version of a copolymer in a micro-emulsion where the droplets are of the *same* size as the monomers. For this model *no variational formula is known for the free energy*, and the analysis relies on the application of martingale techniques (for details, see e.g. den Hollander [49], Chapter 12).

In our model (which is restricted to $d = 1$ and has self-avoiding paths that may move north, south and east instead of north-east and south-east), the droplets are much larger than the monomers. This causes a *self-averaging of the microscopic disorder*, both when the copolymer moves inside one of the solvents and when it moves near an interface. Moreover, since the copolymer is much larger than the droplets, also *self-averaging of the mesoscopic disorder* occurs. This is why the free energy can be expressed in terms of a variational formula, as in Theorem 2.3.1. This variational formula acts as a *jumpboard* for a detailed analysis of the phase diagram. Such a detailed analysis is missing for the directed polymer with bulk disorder.

The directed polymer in random environment has two phases: a *weak disorder phase* (where the quenched and the annealed free energy are asymptotically comparable) and a *strong disorder phase* (where the quenched free energy is asymptotically smaller than the annealed free energy). The strong disorder phase occurs in dimension $d = 1, 2$ for all $\lambda > 0$ and in dimension $d \geq 3$ for $\lambda > \lambda_c$, with $\lambda_c \in [0, \infty]$ a critical value that depends on d and on the law of the disorder. It is predicted that in the strong disorder phase the copolymer moves within a narrow corridor that carries sites with high energy (recall our convention of not putting a minus sign in front of the Hamiltonian), resulting in *superdiffusive* behavior in the spatial direction. We expect a similar behavior to occur in the localized phases of our model, where the polymer targets the AB-interfaces. It would be interesting to find out how far the coarsed-grained path in our model travels vertically as a function of n.

2.4 Phase diagram

In [53], we use the variational formula from Theorem 2.3.1 to investigate the phase diagram of the model. Note that, in this new model, the mesoscopic displacement of the copolymer can be viewed as the trajectory of a self-avoiding random walk taking unitary steps up, down and to the right. Therefore, if we denote by p_c the critical value of p above which the A blocks percolate, it turns out that p_c is also the critical threshold for directed bond percolation in the positive quadrant of $\mathbb{Z}^2$. Of course, we should add a dependence in M in the definition of p_c but for notational convenience we will not.

In the first part of our investigation in [53] we provide a general structure for the phase diagram that is valid for both the supercritical and the subcritical regimes. To be more specific, we identify a localized phase $\mathcal{L}$ in which AB-localization occurs and a delocalized phase $\mathcal{D}$ in which no AB-localization occurs. We give a rigorous definition of theses two phases in section 2.4.1 below.

When going deeper in the analysis of the phase diagram, we figure out that, in both regimes, the delocalized phase $\mathcal{D}$ can be partitioned into two subphases $\mathcal{D}_1$ and $\mathcal{D}_2$, where $\mathcal{D}_2$ corresponds to an A saturation whereas $\mathcal{D}_1$ does not. In other words, for β small, we can increase α until it reaches a threshold above which the copolymer maximizes the fraction of monomers it places in solvent A. Of course the latter maximal fraction is equal to 1 in the supercritical regime and is strictly smaller than 1 in the subcritical regime. Similarly, the localized phase can be partitioned into two subphases $\mathcal{L}_1$ and $\mathcal{L}_2$ so that $\mathcal{L}_2$ corresponds to an A saturation combined with an AB localization whereas the A saturation does not hold in $\mathcal{L}_2$.

We will give more details about the fine structure of the phase diagram in Section 2.4.2 for the supercritical regime. For the subcritical regime, we refer the reader to [53] Section 2.2.2, where we give some conjectures about the splitting of the $\mathcal{D}$ and $\mathcal{L}$ phases.

2.4.1 General structure

All the results stated in this section are valid for $M \in \mathbb{N} \cup \{\infty\}$, but we suppress the M-dependence from the notation for simplicity. To state the general structure of the phase diagram, we need to define a reduced version of the free energy, called the *delocalized free energy* $f_{\mathcal{D}}$, obtained by taking into account those trajectories that, when moving along an AB-interface, are delocalized in the A-solvent. The latter amounts to replacing the linear interface free energy $\phi_{\mathcal{I}}(v_{\mathcal{I}};\alpha,\beta)$ in (2.3.6) by the entropic constant lower bound $\widetilde{\kappa}(v_{\mathcal{I}},0)$. Thus, we define

$$f_{\mathcal{D}}(\alpha,\beta;p) = \sup_{\bar{\rho}\in\bar{\mathcal{R}}_p} \sup_{v\in\bar{\mathcal{B}}} \frac{\bar{N}_{\mathcal{D}}(\bar{\rho},v)}{\bar{D}_{\mathcal{D}}(\bar{\rho},v)} \tag{2.4.1}$$

with

$$\bar{N}_{\mathcal{D}}(\bar{\rho},v) = \int_0^\infty v_{A,l}\,\widetilde{\kappa}(v_{A,l},l)\,[\bar{\rho}_A + \bar{\rho}_{\mathcal{I}}\,\delta_0](dl) + \int_0^\infty v_{B,l}\left[\widetilde{\kappa}(v_{B,l},l) + \tfrac{\beta-\alpha}{2}\right]\bar{\rho}_B(dl), \tag{2.4.2}$$

$$\bar{D}_{\mathcal{D}}(\bar{\rho},v) = \int_0^\infty v_{A,l}\,[\bar{\rho}_A + \bar{\rho}_{\mathcal{I}}\,\delta_0](dl) + \int_0^\infty v_{B,l}\,\bar{\rho}_B(dl), \tag{2.4.3}$$

provided $\bar{D}_{\mathcal{D}}(\bar{\rho},v) < \infty$. Note that $f_{\mathcal{D}}(\alpha,\beta;p)$ depends on (α,β) through $\alpha-\beta$ only.

We partition the CONE into the two phases $\mathcal{D}$ and $\mathcal{L}$ defined by

$$\begin{aligned}\mathcal{L} &= \{(\alpha,\beta)\in \text{CONE}\colon\, f(\alpha,\beta;\,p) > f_{\mathcal{D}}(\alpha,\beta;p)\},\\ \mathcal{D} &= \{(\alpha,\beta)\in \text{CONE}\colon\, f(\alpha,\beta;\,p) = f_{\mathcal{D}}(\alpha,\beta;p)\}.\end{aligned} \tag{2.4.4}$$

The localized phase $\mathcal{L}$ corresponds to large values of β, for which the energetic reward to spend some time travelling along AB-interfaces exceeds the entropic penalty to do so. The delocalized phase $\mathcal{D}$, on the other hand, corresponds to small values of β, for which the energetic reward does not exceed the entropic penalty.

For $\alpha \geq 0$, let J_α be the halfline in CONE defined by

$$J_\alpha = \{(\alpha+\beta,\beta)\colon\, \beta\in[-\tfrac{\alpha}{2},\infty)\}. \tag{2.4.5}$$

Theorem 2.4.1. *(a) For every $\alpha\in(0,\infty)$ there exists a $\beta_c(\alpha)\in(0,\infty)$ such that*

$$\begin{aligned}\mathcal{L}\cap J_\alpha &= \{(\alpha+\beta,\beta)\colon\, \beta\in(\beta_c(\alpha),\infty)\},\\ \mathcal{D}\cap J_\alpha &= \big\{(\alpha+\beta,\beta)\colon\, \beta\in[-\tfrac{\alpha}{2},\beta_c(\alpha)]\big\}.\end{aligned} \tag{2.4.6}$$

(b) Inside phase $\mathcal{D}$ the free energy f is a function of $\alpha-\beta$ only, i.e., f is constant on $J_\alpha\cap\mathcal{D}$ for all $\alpha\in(0,\infty)$.

2.4.2 Fine structure of the supercritical phase diagram

Throughout this section $M\in\mathbb{N}$, but once again we suppress the M-dependence from the notation. We will first provide a rigorous definition of the non saturated subphase $\mathcal{D}_1$ and

of the saturated subphase $\mathcal{D}_2$ that partition $\mathcal{D}$. We will do the same for $\mathcal{L}_1$ and $\mathcal{L}_2$ such that $\mathcal{L} = \mathcal{L}_1 \cup \mathcal{L}_2$. We will see that, subject to two hypotheses, both $\mathcal{D}_1$ and $\mathcal{D}_2$ are non-empty. We will give a characterization of the critical curve $\alpha \mapsto \beta_c(\alpha)$ (recall (2.4.6)) in terms of the single linear free energy and state some properties of this curve. Subsequently, we will formulate a conjecture stating that both $\mathcal{L}_1$ and $\mathcal{L}_2$ are non-empty as well.

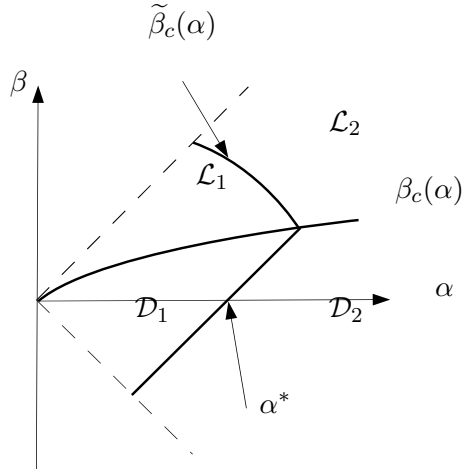

Figure 2.9: Qualitative picture of the phase diagram in the supercritical regime $p > p_c$.

Splitting of the $\mathcal{D}$-phase. We introduce the *delocalized A-saturated free energy*, denoted by $f_{\mathcal{D}_2}(p)$, which is obtained by restricting the supremum in (2.4.1) to those $\bar{\rho} \in \bar{\mathcal{R}}_p$ that do not charge B. Such $\bar{\rho}$, which we call A-saturated, exist because $p > p_c$, allowing for trajectories that do not visit B-blocks. Thus, $f_{\mathcal{D}_2}(p)$ is defined as

$$f_{\mathcal{D}_2}(p) = \sup_{\substack{\bar{\rho}\in\bar{\mathcal{R}}_p \\ \bar{\rho}_B([0,\infty))=0}} \sup_{v\in\bar{\mathcal{B}}} \frac{\bar{N}_{\mathcal{D}_2}(\bar{\rho}, v)}{\bar{D}_{\mathcal{D}}(\bar{\rho}, v)} \tag{2.4.7}$$

with

$$\bar{N}_{\mathcal{D}_2}(\bar{\rho}, v) = \int_0^\infty v_{A,l}\, \widetilde{\kappa}(v_{A,l}, l)\, [\bar{\rho}_A + \bar{\rho}_{\mathcal{I}}\, \delta_0](dl), \tag{2.4.8}$$

provided $\bar{D}_{\mathcal{D}}(\bar{\rho}, v) < \infty$. Note that $f_{\mathcal{D}_2}(p)$ is a constant that does not depend on (α, β).

With the help of this definition, we can split the $\mathcal{D}$-phase defined in (2.4.4) into two parts:

- The $\mathcal{D}_1$-phase corresponds to small values of β and small to moderate values of α. In this phase there is no AB-localization and no A-saturation. For the variational

formula in (2.3.6) this corresponds to the restriction where the AB-localization term disappears while the A-block term and the B-block term contribute, i.e.,

$$\mathcal{D}_1 = \big\{(\alpha,\beta) \in \text{CONE}\colon\ f(\alpha,\beta;\, p) = f_{\mathcal{D}}(\alpha,\beta;\, p) > f_{\mathcal{D}_2}(p)\big\}. \tag{2.4.9}$$

- The $\mathcal{D}_2$-phase corresponds to small values of β and large values of α. In this phase there is no AB-localization but A-saturation occurs. For the variational formula in (2.3.6) this corresponds to the restriction where the AB-localization term disappears and the B-block term as well, i.e.,

$$\mathcal{D}_2 = \big\{(\alpha,\beta) \in \text{CONE}\colon\ f(\alpha,\beta;\, p) = f_{\mathcal{D}_2}(p)\big\}. \tag{2.4.10}$$

Theorem 2.4.4 below is proven in [53] subject to hypotheses 2.4.2 and 2.4.3. For the second hypothesis, we will not give a rigorous formulation here because it requires more notations and we do not want to go into too many details. We will rather state heuristic explanations for both of them and refer the reader to [53] Section 2.2.1 for the details.

Hypothesis 2.4.2. *For all $p > p_c$ and all $\alpha \in (0,\infty)$ the first supremum in* (2.3.6) *is attained at some $\bar\rho \in \mathcal{R}(p)$ satisfying $\bar\rho_{\mathcal{I}} > 0$.*

Recall that $(\alpha, 0) \in \mathcal{D}$ (cf Theorem 2.4.1 (a)), which implies that for such coupling parameters the copolymer does not localize along AB interfaces. Thus, the copolymer switches directions (by changing the sign of the slope at which it travels in the medium) only to avoid clusters of type B and therefore spend more time in solvent A. However, for entropic reasons the optimal strategy when passing over (or below) a cluster of type B consists in following the AB-interface (consisting of the highest B-blocks on top of the cluster and of the A-solvent above them) without being localized, i.e., the copolymer performs a long excursion into the A-solvent but the two ends of this excursion are located on the AB-interface. This long excursion is counted in $\bar\rho_{\mathcal{I}}$. Consequently, Hypothesis 2.4.2 ($\bar\rho_{\mathcal{I}} > 0$) will be satisfied if we can show that the copolymer necessarily spends a strictly positive fraction of its time performing such changes of vertical direction. But, by the ergodicity of ω and Ω, this has to be the case.

The second hypothesis is more technical and therefore harder to state. Let us try to explain it in a few words.

Hypothesis 2.4.3. For all $p > p_c$, by spending an arbitrarily small fraction of time in the B-solvent, the trajectories can not travel flatter when it is in the A-solvent during a fraction of the time that is arbitrarily larger than the fraction of the time it spends in the B-solvent. In other words, if this hypothesis failed, it would mean that, instead of going around some large cluster of the B-solvent, the copolymer simply crosses it straight to travel flatter. However, the fact that large subcritical clusters scale as round balls contradicts this

scenario, because it means that the time needed to go around the cluster is of the same order as the time required to cross the cluster.

Hypothesis 2.4.2 will allow us to derive an expression for $\beta_c(\alpha)$ in (2.4.6). Hypothesis 2.4.3 will allow us to show that $\mathcal{D}_1$ and $\mathcal{D}_2$ are non-empty.

Let

$$\alpha^* = \sup\{\alpha \geq 0\colon\ f_{\mathcal{D}}(\alpha, 0; p) > f_{\mathcal{D}_2}(p)\}. \tag{2.4.11}$$

Theorem 2.4.4. *(a) If Hypothesis* 2.4.3 *holds, then* $\alpha^* \in (0, \infty)$.
(b) For every $\alpha \in [0, \alpha^*)$,

$$J_\alpha \cap \mathcal{D}_1 = J_\alpha \cap \mathcal{D} = \{(\alpha + \beta, \beta)\colon\ \beta \in [-\tfrac{\alpha}{2},\, \beta_c(\alpha)]. \tag{2.4.12}$$

(c) For every $\alpha \in [\alpha^*, \infty)$,

$$J_\alpha \cap \mathcal{D}_2 = J_\alpha \cap \mathcal{D} = \{(\alpha + \beta, \beta)\colon\ \beta \in [-\tfrac{\alpha}{2}, \beta_c(\alpha)]\}. \tag{2.4.13}$$

(d) If Hypothesis 2.4.2 *holds, then for every* $\alpha \in [0, \infty)$

$$\beta_c(\alpha) = \inf\big\{\beta > 0\colon\ \phi_{\mathcal{I}}(\bar{v}_{A,0}; \alpha + \beta, \beta) > \widetilde{\kappa}(\bar{v}_{A,0}, 0)\big\} \quad \textit{with} \quad \bar{v} = v(f_{\mathcal{D}}(\alpha, 0; p)). \tag{2.4.14}$$

(e) $\alpha \mapsto \beta_c(\alpha)$ *is concave, continuous, non-decreasing and bounded from above on* $[\alpha^*, \infty)$.
(f) Inside phase $\mathcal{D}_1$ *the free energy* f *is a function of* $\alpha - \beta$ *only, i.e.,* f *is constant on* $J_\alpha \cap \mathcal{D}_1$ *for all* $\alpha \in [0, \alpha^*]$.
(g) Inside phase $\mathcal{D}_2$ *the free energy* f *is constant.*

Splitting of the $\mathcal{L}$-phase. We introduce the *localized A-saturated free energy*, denoted by $f_{\mathcal{L}_2}$, which is obtained by restricting the supremum in (2.3.6) to those $\bar{\rho} \in \bar{\mathcal{R}}_p$ that do not charge B, i.e.,

$$f_{\mathcal{L}_2}(\alpha, \beta; p) = \sup_{\substack{\bar{\rho} \in \bar{\mathcal{R}}_p \\ \bar{\rho}_B([0,\infty))=0}} \sup_{v \in \vec{\mathcal{B}}} \frac{\bar{N}(\bar{\rho}, v)}{\bar{D}(\bar{\rho}, v)}, \tag{2.4.15}$$

provided $\bar{D}(\bar{\rho}, v) < \infty$.

With the help of this definition, we can split the $\mathcal{L}$-phase defined in (2.4.4) into two parts:

- The $\mathcal{L}_1$-phase corresponds to small to moderate values of α and large values of β. In this phase AB-localization occurs, but A-saturation does not, so that the free energy is given by the variational formula in (2.3.6) without restrictions, i.e.,

$$\mathcal{L}_1 = \big\{(\alpha, \beta) \in \text{CONE}\colon\ f(\alpha, \beta; p) > \max\{f_{\mathcal{D}}(\alpha, \beta; p),\, f_{\mathcal{L}_2}(\alpha, \beta; p)\}\big\}. \tag{2.4.16}$$

- The $\mathcal{L}_2$-phase corresponds to large values of α and β. In this phase both AB-localization and A-saturation occur. For the variational formula in (2.3.6) this corresponds to the restriction where the contribution of B-blocks disappears, i.e.,

$$\mathcal{L}_2 = \big\{(\alpha, \beta) \in \text{CONE}\colon\ f(\alpha, \beta; p) = f_{\mathcal{L}_2}(\alpha, \beta; p) > f_{\mathcal{D}}(\alpha, \beta; p)\big\}. \tag{2.4.17}$$

Conjecture

(a) For every $\alpha \in (0, \alpha^*]$ there exists a $\widetilde{\beta}_c(\alpha) \in (\beta_c(\alpha), \infty)$ such that

$$\begin{aligned} \mathcal{L}_1 \cap J_\alpha &= \{(\alpha+\beta, \beta) \colon \beta \in (\beta_c(\alpha), \widetilde{\beta}_c(\alpha)]\}, \\ \mathcal{L}_2 \cap J_\alpha &= \big\{(\alpha+\beta, \beta) \colon \beta \in [\widetilde{\beta}_c(\alpha), \infty)\big\}. \end{aligned} \tag{2.4.18}$$

(b) For every $\alpha \in (\alpha^*, \infty)$, the set $\mathcal{L}_1 \cap J_\alpha = \emptyset$.

2.5 Perspectives

A short-term goal, concerning the copolymer in a micro-emulsion would of course consist in improving our knowledge of the phase diagram for the model without corner restriction. It would, in particular, be interesting to look closely at the super-critical regime and to provide rigorous proofs of Hypothesis 2.4.2 and 2.4.3. Generally speaking, obtaining more informations about the set $\mathcal{R}(p)$ would be of crucial importance to get finer details on the phase diagram. Note that, questions around $\mathcal{R}(p)$ are mostly related to percolation theory, and are very challenging in themselves.

Several long-term objectives could be identified but let us focus on one of them. After the removal of the corner restriction, the next natural improvement of the model, in order to make it physically more realistic, would be to give the droplets of solvant A a deterministic non-squared shape at first and later on a random shape. For the deterministic shape, one option would be to choose first a regular enough closed curve $\gamma : [0, 1] \to \mathbb{R}^2$ e.g. a circle of radius 1 or the Wulff shape of a rescaled large droplet of $+$ in the phase transition regime of the 2D Ising model with $-$ boundary conditions (see [56], [57] or [58]). Then, for $n \in \mathbb{N}$, we enlarge these droplets into $\gamma_n = L_n\gamma$ and place them randomly in $\mathbb{R}^2$, for instance by sampling their center as a Poisson point process on $\mathbb{R}^2$ conditioned on the event that any two droplets do not intersect each other. Finally, we fill the interior of each droplet with solvent A. Note that obtaining a random shape for the droplets boundary could be achieved with the very same mechanism by sampling a random walk loop around each droplet γ_n conditioned on not entering the droplet. The mathematical issues addressed by this new model would be:

1) first, study an auxiliary model for a copolymer interacting with one such large droplet, in the limit where the copolymer size and the droplet size diverge at the same speed. In particular, give a variational formula for the free energy of such system. As a preparation, this requires to study the existence and the main properties of the free energy of a copolymer in the vicinity of a random AB interface with a given slope.

2) Once the questions raised in **1)** are solved, prove that the free energy admits a variational formulation similar to what is obtained in Theorem 2.3.1, except that an

additional ingredient is required, i.e., the limiting free energy for a copolymer at an AB interface with a given slope (cf. **1)**) .

3) Analyze the phase diagram of this new model with the variational formula from **2)** and identify its phase transitions and critical curves.

As a side remark, the auxiliary model suggested in **1**) is in itself challenging. Consider indeed a copolymer of size cL ($c \geq 2$) interacting with a single big droplet $\gamma_L = \gamma L$ centered on $(0, 0)$. One could for instance let the random walk start at $(-L, 0)$ and end at $(L, 0)$ so that the copolymer crosses the droplet by passing either above/below it or through it. For a given $\alpha > 0$ and a small β, the polymer will clearly ignore the AB interface and simply cross the droplet horizontally. When increasing β, in turn, we will reach a threshold $\beta_c(\alpha)$ above which the copolymer will follow the interface for awhile. However, even the type of localization that one should expect is not clear at all. Following an AB interface with a steep slope is clearly much harder than following a flat interface. For this reason, determining the location of the point around γ_n at which localization should start would already be very interesting.

Chapter 3

Modèle d'effondrement d'un polymère

La transition d'effondrement d'un homopolymère placé dans un solvent "pauvre" (répulsif) a reçu beaucoup d'attention de la part des physiciens. Parmis les modèles mathématiques qui permettent d'étudier cette transition de phase, le plus populaire est sans doute la marche aléatoire partiellement dirigée en auto-interaction à laquelle on se réferera par son acronyme anglais IPDSAW. D'un point de vue mathématique, ce modèle a jusqu'à très recemment été étudié presque exclusivement à l'aide de méthodes combinatoires. Si ces méthodes permettent d'accéder à certains résultats concernant la limite hydrodynamique du modèle, elles ne permettent pas en général de donner les caractéristiques géométriques du polymère à une température fixée.

Dans ce chapitre, nous présenterons une approche probabiliste, développée récemment dans [27], [28], [66] et [67], qui consiste à relier le modèle IPDSAW à une marche aléatoire auxiliaire à accroissement géométrique. Ceci permet, entre autres, d'utiliser les résultats très nombreux de la théorie des marches aléatoires pour, d'une part, simplifier les preuves et la compréhension des résultats existants et, d'autre part, caractériser géométriquement les configurations adoptées par le polymère dans les différentes phases.

Dans la Section 3.1, nous présentons le phénomène physique d'éffrondrement d'un polymère dans un solvant répulsif et nous définissons le modèle IPDSAW. La Section 3.2 est dédiée à l'introduction de notre approche probabiliste et à la discussion de sa pertinence. Dans la Section 3.3, nous décrivons les résultats principaux que nous avons obtenus. La limite hydrodynamique du système est donc traitée en Section 3.3.1, tandis que les sections (3.3.2–3.3.3) sont entièrement dédiées aux résultats trajectoriels.

3.1 Phénomène physique et modèle mathématique

3.1.1 Un homopolymère dans un solvant pauvre

La structure géométrique qu'adopte un homopolymère lorsqu'on le plonge dans un solvant pauvre est déterminée par deux types d'interactions, parfois antagonistes:

- monomère-solvant: en fonction de leur affinité chimique mutuelle, les monomères et les molécules du solvant vont soit s'attirer soit se repousser.

- monomère-monomère: ces interactions peuvent être attractives (forces de van der Walls) ou bien répulsives (par exemple entre deux monomère dont les charges électriques respectives sont de même signe)

Pour bâtir une théorie générale et prendre en compte la grande variété d'homopolymères et de solvants qui peuvent mener à des phénomène d'effondrement, les physiciens considèrent qu'un solvant est "pauvre" pour un homopolymère donné s'il est énergétiquement plus favorable pour les monomères d'être en contact les uns avec les autres plutôt que d'être en contact avec les molécules du solvant qui les entoure.

Lorsqu'on plonge un homopolymère dans un solvant suffisament pauvre, le polymère s'enroule sur lui même pour exclure le solvant et adopte donc une configuration qui ressemble à une boule compacte. Ensuite, si on chauffe suffisament le solvant, l'affinité chimique entre les monomères et le solvant va augmenter jusqu'à ce qu'elle atteigne un seuil au-delà duquel le polymère se détend de façon à ce qu'une fraction strictement positive de ses monomères soient en contact avec le solvant. Ce changement très brutal de configuration géométrique est appelé transition d'effondrement et intervient en une température critique Θ_c, appelée également point-ϑ.

Un exemple classique de couple homopolymère-solvant associé à une transition d'effondrement est donné par le polystyrène plongé dans une phase pure de cyclohexane. La transition d'effondrement se produit alors entre 30^o et 35^o degrés celsius (cf. [75]). On peut également considérer un polymère branchant comme le Poly(N-isopropilacrylamide) (PNIPAM) dans l'eau pour lequel la transition d'effondrement intervient à 32 degrés celsius. Lorsque la température dépasse ce seuil critique, le PINPAM se dégonfle et perd 90 pour cent de son volume total. La proximité entre cette température d'effondrement et la température du corps humain est utilisée dans la recherche médicale comme nouveau vecteur de transport de médicament (cf [74] et [34]). Dans ce cas, le polymère transporte, dans sa phase effondrée, des molécules qui se trouvent prisonnières de sa configuration très compacte. Une fois dans le corps humain, la température augmente, et le polymère se détend, libérant ainsi les molécules du principe actif qui peuvent commencer à agir dans les cellules.

3.1.2 Le modèle IPDSAW

Le modèle IPDSAW (interacting partially-directed self-avoiding walk) fut introduit par Zwanzig et Lauritzen dans [84] comme un modèle d'homopolymère dans un solvant pauvre. Les configurations spatiales d'un polymère de taille L (comportant L monomères) sont modélisées par les trajectoires d'une marche aléatoire *auto-évitante* sur $\mathbb{Z}^2$ qui fait des pas unitaires vers *le nord, le sud ou l'est*. Ainsi, en taille L, l'ensemble des trajectoires autorisées est

$$\begin{aligned}\mathcal{W}_L = \{w = (w_i)_{i=0}^{L} \in (\mathbb{N}_0 \times \mathbb{Z})^{L+1} : & w_0 = 0,\, w_L - w_{L-1} = \rightarrow, \\ & w_{i+1} - w_i \in \{\uparrow, \downarrow, \rightarrow\}\ \forall 0 \le i < L-1, \\ & w_i \neq w_j\ \forall i < j\}.\end{aligned}$$

On remarque que le choix de terminer chaque trajectoire w par un pas vers la droite est purement technique pour faciliter l'exposition. Dorénavant, nous considérerons deux lois de probabilité a priori sur $\mathcal{W}_L$, l'une uniforme et l'autre non-uniforme, notées $\mathbf{P}_L^{\mathsf{m}}$ avec $\mathsf{m} \in \{\mathsf{u}, \mathsf{nu}\}$.

(1) Le modèle uniforme: chaque trajectoire de taille L a la même probabilité, i.e.,

$$\mathbf{P}_L^{\mathsf{u}}(w) = \frac{1}{|\mathcal{W}_L|}, \quad w \in \mathcal{W}_L. \tag{3.1.1}$$

(2) Le modèle non-uniforme: les trajectoires de taille L ont la loi suivante

- À l'origine ou après un pas horizontal, la marche peut faire un pas vers le haut, la droite ou le bas avec probabilité 1/3.
- Après un pas vers le haut (resp. vers le bas): la marche peut faire un pas soit vers le haut (resp. vers le bas) soit vers la droite avec probabilité 1/2.

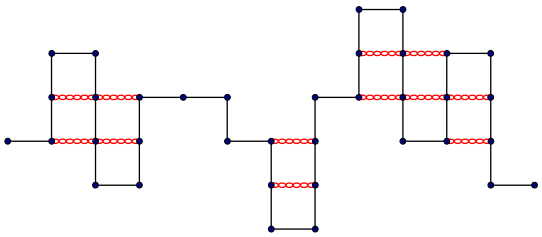

Figure 3.1: Exemple d'une trajectoire avec 12 self-touching représentés en gris.

L'interaction monomère-solvant n'est pas directement prise en compte dans le modèle IPDSAW. On considère plutôt que, une fois plongés dans un solvant pauvre, les monomères tentent de repousser le solvant et en conséquence s'attirent mutuellement. Pour modéliser

cette attraction entre monomères on appelle *self-touching* tout couple de sites non-consécutifs le long de la trajectoire mais adjacents dans $\mathbb{Z}^2$ (cf. Fig. 3.1) et on attribue un prix énergétique $\beta \geq 0$ à une trajectoire pour chacun de ses self-touching (en conséquence de quoi, une affinité chimique plus faible correspond à un β plus grand). Ainsi, on associe à chaque trajectoire de la marche aléatoire $w = (w_i)_{i=0}^{L} \in \mathcal{W}_L$ un Hamiltonien

$$H_{L,\beta}(w) := \beta \sum_{\substack{i,j=0 \\ i<j-1}}^{L} \mathbf{1}_{\{\|w_i - w_j\|=1\}}, \tag{3.1.2}$$

qui permet de définir la loi $P^{\mathsf{m}}_{L,\beta}$ du polymère en taille L comme,

$$P^{\mathsf{m}}_{L,\beta}(w) = \frac{e^{H_{L,\beta}(w)}}{Z^{\mathsf{m}}_{L,\beta}} \mathbf{P}^{\mathsf{m}}_{L}(w), \quad \mathsf{m} \in \{\mathsf{u}, \mathsf{nu}\}. \tag{3.1.3}$$

où $Z^{\mathsf{m}}_{L,\beta}$ est la constante de renormalisation connue sous le nom de fonction de partition du système. Dorénavant, pour le modèle unifome $\mathsf{m} = \mathsf{u}$, on omettra le terme $1/|\mathcal{W}_L|$ de la définition de $\mathbf{P}^{\mathsf{u}}_{L}$ (cf. (3.1.1)) et du calcul de la fonction de partition $Z^{\mathsf{u}}_{L,\beta}$. Bien que $\mathbf{P}^{\mathsf{u}}_{L}$ ne soit plus une loi de probabilité, cette simplification est transparente, puisqu'elle ne modifie pas la loi du polymère $P^{\mathsf{u}}_{L,\beta}$ et pusiqu'elle ajoute seulement un terme constant à l'énergie libre $f^{\mathsf{u}}(\beta)$ que l'on introduira en Section 3.1.4.

3.1.3 Un modèle non dirigé (ISAW)

Le modèle ISAW en dimension 2 (acronyme anglais de Interacting self-avoiding walk) est l'homologue non-dirigé du modèle IPDSAW. Il est obtenu en appliquant l'Hamiltonien (3.1.2) à l'ensemble de toutes les trajectoires auto-évitantes à pas unitaire. Très peu de résultats rigoureux sur le plan mathématique ont été prouvés pour le modèle ISAW. Il est conjecturé (cf. [14] et [49]) qu'une transition d'effondrement se produit en un paramètre critique β_c. Si l'existence de l'énergie libre $f^{\mathrm{ISAW}}(\beta)$ est obtenue facilement par sous-additivité et que la valeur de l'énergie libre effondrée semble être la même que pour le modèle IPDSAW, la preuve de l'existence de la transition d'effondrement semble plus difficile à obtenir, tant par des méthodes combinatoires que par une éventuelle représentation probabiliste.

Notons également que le modèle ISAW, correspond au cas limite d'un modèle non dirigé étudié dans [46] et décrit dans [49]. Dans ce modèle la marche aléatoire auto-évitante est remplacée par une marche aléatoire faiblement répulsive. Les configurations autorisées sont les trajectoires d'une marche aléatoire à pas unitaires (non nécessairement auto-évitante). En taille L, une énergie est associée à chaque trajectoire w, i.e.,

$$H_{L,\beta,\gamma}(w) := -\gamma \sum_{\substack{i,j=0 \\ i<j-1}}^{L} \mathbf{1}_{\{\|w_i - w_j\|=0\}} + \beta \sum_{\substack{i,j=0 \\ i<j-1}}^{L} \mathbf{1}_{\{\|w_i - w_j\|=1\}}, \tag{3.1.4}$$

où $\beta, \gamma \in [0, \infty)$ sont les paramètres de couplage du système. Il est prouvé dans [46] que la demi-droite $\beta = \gamma$ est une courbe critique qui sépare une phase localisée ($\beta > \gamma$) dans laquelle le nombre de sites visités par la marche aléatoire est borné uniformément en L, d'une phase effondrée dans laquelle l'extension typique d'une trajectoire de taille L est d'ordre $L^{1/2}$. Sur la courbe critique ($\beta = \gamma$) il est conjecturé que l'extension typique d'une trajectoire soit $L^{1/3}$ (cf [46]). L'existence d'une seconde courbe critique $\gamma \to \beta_c(\gamma)$ séparant la phase effondrée d'une phase étendue est également conjecturée (cf [14] et [49]). La phase étendue correspond à une extension typique du même ordre que celle d'une marche aléatoire auto-évitante en dimension 2. Sur la courbe critique, la conjecture donne une extension d'ordre $L^{4/7}$. Finalement, La courbe critique $\gamma \to \beta_c(\gamma)$ admet une asymptote horizontale β_c^* en $+\infty$. La quantité β_c^* devrait correspondre au paramètre critique d'effondrement du modèle ISAW.

3.1.4 Transition entre phase étendue et phase effondrée pour le modèle IPDSAW

Pour chacun des deux modèles, i.e., $\mathsf{m} \in \{\mathsf{u}, \mathsf{nu}\}$, l'existence de l'énergie libre en volume infini est assurée par le caractère sous-additif de la suite $\{\log Z_{L,\beta}^{\mathsf{m}}\}_L$ et par le fait que l'hamiltonien dans (3.1.2) soit borné supérieurement par βL. En conséquence, on peut définir l'énergie libre par pas $f^{\mathsf{m}} : (0, \infty) \to \mathbb{R}$ comme

$$f^{\mathsf{m}}(\beta) = \lim_{L \to \infty} \frac{1}{L} \log Z_{L,\beta}^{\mathsf{m}} = \sup_{L \in \mathbb{N}} \frac{1}{L} \log Z_{L,\beta}^{\mathsf{m}} \leq \beta. \tag{3.1.5}$$

La transition d'effondrement du système correspond à une perte d'analyticité de la fonction $\beta \mapsto f^{\mathsf{m}}(\beta)$ en une valeur critique particulière du paramètre de couplage $\beta_c^{\mathsf{m}} \in (0, \infty)$ au dessus de laquelle une saturation intervient correspondant à une fraction des monomères impliqués dans un self-touching égale à 1. Dans cette phase effondrée l'expression de l'énergie libre devient simple, i.e., $\beta + \kappa_{\mathsf{m}}$, où κ_{m} est la constante entropique associée aux trajectoires de $\mathcal{W}_L$ ayant une densité de self-touching de $1 + o(1)$. Pour atteindre une telle saturation des self-touching, le polymère doit adopter une configuration qui respecte deux contraintes géométriques majeures:

- le nombre de pas horizontaux est $o(L)$ (négligeable devant la taille totale du polymère)
- la plupart des segments verticaux ont une direction opposée à celle du segment qui les précède.

Une seule trajectoire bien choisie et satisfaisant les deux contraintes géométriques précédentes est suffisante pour obtenir l'énergie libre effondrée. Ainsi, pour $L \in \mathbb{N}$: $\sqrt{L} \in \mathbb{N}$ on considère la trajectoire $l^* \in \mathcal{L}_{\sqrt{L},L}$ définie par $l_i^* = (-1)^{i-1}(\sqrt{L} - 1)$ pour $i \in \{1, \ldots, \sqrt{L}\}$. En calculant la contribution de l^* à $Z_{L,\beta}^{\mathsf{m}}$, on obtient immédiatement que, pour $\beta > 0$ et

$\mathsf{m} \in \{\mathsf{u}, \mathsf{nu}\}$,

$$f^{\mathsf{m}}(\beta) \geq \varphi_{\beta}^{\mathsf{m}}, \tag{3.1.6}$$

où $\varphi_{\beta}^{\mathsf{u}} = \beta$ et $\varphi_{\beta}^{\mathsf{nu}} = \beta - \log 2$. A ce stade, on peut définir *l'énergie libre en excès* $\widetilde{f}^{\mathsf{m}}(\beta) := f^{\mathsf{m}}(\beta) - \varphi_{\beta}^{\mathsf{m}}$, qui est positive par (3.1.6). On définit alors le paramètre critique

$$\beta_c^{\mathsf{m}} := \inf\{\beta \geq 0 : \widetilde{f}^{\mathsf{m}}(\beta) = 0\}, \tag{3.1.7}$$

et la convexité de $\beta \mapsto \widetilde{f}^{\mathsf{m}}(\beta)$ nous permet de partager $[0, \infty)$ en une phase effondrée notée $\mathcal{C}$ et une phase étendue notée $\mathcal{E}$, i.e,

$$\mathcal{C} := \{\beta : \widetilde{f}^{\mathsf{m}}(\beta) = 0\} = \{\beta : \beta \geq \beta_c^{\mathsf{m}}\} \tag{3.1.8}$$

et

$$\mathcal{E} := \{\beta : \widetilde{f}^{\mathsf{m}}(\beta) > 0\} = \{\beta : \beta < \beta_c^{\mathsf{m}}\}. \tag{3.1.9}$$

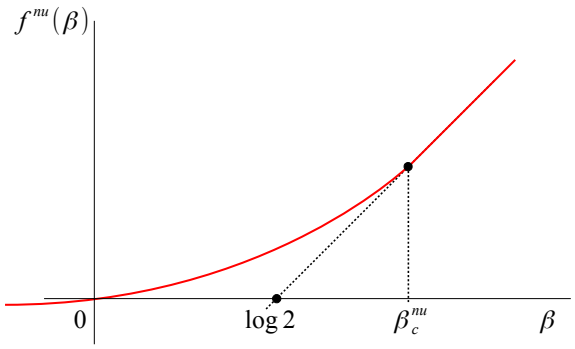

Figure 3.2: Phase diagram in the the non-uniform case.

Nous remarquons à ce stade que la transition d'effondrement du modèle IPDSAW est d'une nature très différente de celle de la transition de phase du modèle d'accrochage (pinning) d'un processus de renouvellement récurrent à valeurs dans $\mathbb{N}$ par un potentiel constant (cf. [38] Chapitre 2). Pour le modèle d'accrochage en effet, la phase saturée, dans laquelle l'énergie libre prend la valeur 0, correspond à un paramètre de couplage trop faible pour que l'énergie l'emporte dans la compétition énergie-entropie qui régit le comportement du polymère. C'est l'inverse que l'on observe dans le cas du polymère effondré. La phase saturée correspond à un paramètre de couplage suffisamment fort pour que le terme energétique l'emporte sur l'entropie.

3.2 Une nouvelle approche

3.2.1 Résultats antérieurs

Le modèle IPDSAW et ses versions continues ont été l'objet de travaux multiples menés par des physiciens jusqu'à très récemment encore (cf. par exemple [13] et [77]). Dans ces

travaux, le traitement mathématique du modèle s'est appuyé exclusivement sur des techniques combinatoires (cf. [15], [70] ou plus récemment [69]). Pour être plus précis, cette méthode consiste à exhiber une expression analytique de la fonction de partition grand canonique du système, i.e., $G(z) = \sum_{L=1}^{\infty} Z_{L,\beta}^{\mathsf{m}} z^L$ dont le rayon de convergence R satisfait $f^{\mathsf{m}} = -\log R$. Ce calcul est mené à bien en reexprimant $G(z)$ sous la forme $\sum_{r=0}^{\infty} g_r(z)$ où $g_r(z)$ est la contribution à $G(z)$ des trajectoires dont les r premiers pas sont verticaux, indépendamment de la longueur totale de la trajectoire. Par des techniques de concaténation adhoc de trajectoires, une relation de récurrence est établie entre g_{r-1}, g_r et g_{r+1} de sorte que, en cherchant à exprimer g_r comme la somme d'une série numérique, la relation de recurrence nous permet de calculer tous les termes de la série donnant g_r. Une version détaillée de ces calculs est disponible dans [23, p. 371–375].

Le calcul de la fonction de partition grand canonique G permet de déterminer la valeur exacte de β_c et de prédire le comportement de l'énergie libre au voisinage du point critique. Cependant, l'expression analytique de G est très compliquée et donne un accés seulement très indirect à la fonction de partition. De plus, cette méthode combinatoire est inopérante pour étudier des quantités non ballistiques comme par exemple l'extension horizontale du polymère dans sa phase effondrée qui se révèle être de l'ordre de $\sqrt{L}$, ce qui ne peut pas être prouvé par une telle méthode.

3.2.2 Une représentation probabiliste de la fonction de partition

Il est facile de constater que que chaque trajectoire de $\mathcal{W}_L$ peut être décomposée en un succession de segments verticaux orientés et séparés par un pas horizontal. Ainsi, on introduit $\Omega_L := \bigcup_{N=1}^{L} \mathcal{L}_{N,L}$, où $\mathcal{L}_{N,L}$ est l'ensemble des familles de N segments verticaux ayant une longueur totale de $L - N$, c'est à dire

$$\mathcal{L}_{N,L} = \Big\{ l \in \mathbb{Z}^N : \textstyle\sum_{n=1}^{N} |l_n| + N = L \Big\}. \tag{3.2.1}$$

On construit une bijection naturelle de Ω_L dans $\mathcal{W}_L$ en associant à chaque $l \in \Omega_L$ la trajectoire de $\mathcal{W}_L$ qui part de 0, fait $|l_1|$ pas verticaux vers le nord si $l_1 > 0$ et vers le sud si $l_1 < 0$, puis fait un pas horizontal, puis fait $|l_2|$ pas verticaux vers le nord si $l_2 > 0$ où vers le sud si $l_2 < 0$ puis fait un pas horizontal et ainsi de suite... (cf. Fig. 3.3). On rappelle (3.1.1) et on remarque que pour un $N \in \{1, \dots, L\}$ donné, la fonction $l \mapsto \mathbf{P}_L^{\mathsf{m}}(l)$ est constante sur $\mathcal{L}_{N,L}$ et égale à 1 si $\mathsf{m} = \mathsf{u}$ et $(2/3)^N (1/2)^{L-N}$ si $\mathsf{m} = \mathsf{nu}$. L'Hamiltonien associé à une trajectoire donnée de $\mathcal{W}_L$ peut être réécrit à l'aide de sa famille de segments verticaux associée $l \in \Omega_L$ sous la forme

$$H_{L,\beta}(l_1, \dots, l_N) = \beta \textstyle\sum_{n=1}^{N-1} (l_n \mathbin{\widetilde{\wedge}} l_{n+1}) \tag{3.2.2}$$

où

$$x \mathbin{\widetilde{\wedge}} y = \begin{cases} |x| \wedge |y| & \text{si } xy < 0, \\ 0 & \text{sinon.} \end{cases} \tag{3.2.3}$$

Ainsi la fonction de partition du système peut être écrite sous la forme

$$Z^{\mathsf{m}}_{L,\beta} = \sum_{N=1}^{L} \sum_{l \in \mathcal{L}_{N,L}} \mathbf{P}^{\mathsf{m}}_{L}(l)\ e^{\beta \sum_{i=1}^{N-1} (l_i \,\widetilde{\wedge}\, l_{i+1})}. \tag{3.2.4}$$

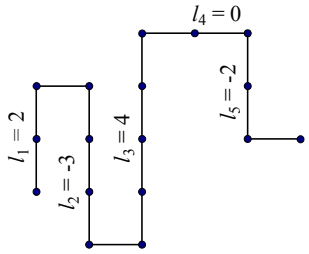

Figure 3.3: un exemple de trajectoire avec 5 segments verticaux et une longueur totale $L = 16$.

Marche aléatoire auxiliaire

Nous introduisons une marche aléatoire symétrique auxiliaire $V := (V_n)_{n\in\mathbb{N}}$ à incréments géométriques, i.e., $V_0 = 0$, $V_n = \sum_{i=1}^{n} v_i$ pour $n \in \mathbb{N}$ et $v := (v_i)_{i\in\mathbb{N}}$ est une suite i.i.d de variables aléatoires de loi $\mathbf{P}_\beta$ donnée par

$$\mathbf{P}_\beta(v_1 = k) = \tfrac{e^{-\frac{\beta}{2}|k|}}{c_\beta} \quad \forall k \in \mathbb{Z} \quad \text{et} \quad c_\beta := \tfrac{1+e^{-\beta/2}}{1-e^{-\beta/2}}. \tag{3.2.5}$$

On définit aussi $A_N(V) := \sum_{i=1}^{N} |V_i|$ l'aire géométrique entre la trajectoire $V \in \mathbb{Z}^{\mathbb{N}}$ et l'axe des abscisses après N pas. Finallement, pour $n, k \in \mathbb{N}$ on définit $\mathcal{V}_{n,k}$ l'ensemble des trajectoires à n pas dont l'aire géometrique vaut k, i.e.,

$$\mathcal{V}_{n,k} := \big\{V\colon\ A_n(V) = k,\, V_n = 0\big\},$$

et on définit $\varphi^{\mathsf{m}}_{L,\beta}$ comme

$$\begin{cases} \varphi^{\mathsf{u}}_{L,\beta} = e^{\beta L}, \\ \varphi^{\mathsf{nu}}_{L,\beta} = (e^{\beta}/2)^{L}. \end{cases} \tag{3.2.6}$$

On partitionne l'ensemble $\mathcal{W}_L$ en L sous-ensembles, chacun d'eux contenant les trajectoires ayant le même nombre de pas horizontaux. A l'aide d'une transformation algébrique de l'Hamiltonien, nous allons pouver que la contribution à la fonction de partition des trrajectoires faisant exactement N pas horizontaux peut être reexprimée sous la forme du produit d'un terme "énergétic" β-dépendant élevé à la puissance N par la probabilité pour que la marche aléatoire auxiliaire V satisfasse des contraintes géométriques particulières.

Proposition 3.2.1. *Pour tout $\beta > 0$, $L \in \mathbb{N}$, $\mathsf{m} \in \{\mathsf{u}, \mathsf{nu}\}$, on a*

$$Z^{\mathsf{m}}_{L,\beta} = c_\beta \, \varphi^{\mathsf{m}}_{L,\beta} \sum_{N=1}^{L} \left(\Gamma^{\mathsf{m}}(\beta)\right)^N \mathbf{P}_\beta(\mathcal{V}_{N+1,L-N}). \tag{3.2.7}$$

Proof. Nous présentons la preuve de la Proposition 3.2.1 dans le cas non-uniforme uniquement (le cas uniforme étant tout a fait similaire). On rappelle (3.2.1–3.2.4), et on reécrit la fonction de partition sous la forme

$$Z^{\mathsf{nu}}_{L,\beta} = \sum_{N=1}^{L} \sum_{l \in \mathcal{L}_{N,L}} \left(\tfrac{1}{3}\right)^N \left(\tfrac{1}{2}\right)^{L-N} e^{\beta \sum_{n=1}^{N-1} (l_n \,\widetilde{\wedge}\, l_{n+1})}. \tag{3.2.8}$$

À ce stade, il est utile de remarquer que l'opérateur $\widetilde{\wedge}$ peut s'écrire sous la forme

$$x \,\widetilde{\wedge}\, y = \left(|x| + |y| - |x+y|\right)/2, \quad \forall x, y \in \mathbb{Z}. \tag{3.2.9}$$

Ainsi, pour $\beta > 0$ et $L \in \mathbb{N}$, la fonction de partition (3.2.8) devient

$$\begin{aligned} Z^{\mathsf{nu}}_{L,\beta} &= \sum_{N=1}^{L} \left(\tfrac{1}{3}\right)^N \left(\tfrac{1}{2}\right)^{L-N} \sum_{\substack{l \in \mathcal{L}_{N,L} \\ l_0 = l_{N+1} = 0}} \exp\Big(\beta \sum_{n=1}^{N} |l_n| - \tfrac{\beta}{2} \sum_{n=0}^{N} |l_n + l_{n+1}|\Big) \\ &= \left(\tfrac{e^\beta}{2}\right)^L \sum_{N=1}^{L} c_\beta \left(\tfrac{2c_\beta}{3e^\beta}\right)^N \sum_{\substack{l \in \mathcal{L}_{N,L} \\ l_0 = l_{N+1} = 0}} \prod_{n=0}^{N} \frac{\exp\Big(-\frac{\beta}{2}|l_n + l_{n+1}|\Big)}{c_\beta}, \end{aligned} \tag{3.2.10}$$

avec c_β defini en (3.2.5). Pour tout $N \in \{1, \dots, L\}$ on définit la bijection $T_N : \mathcal{V}_{N+1,L-N} \mapsto \mathcal{L}_{N,L}$ par $T_N(V)_i = (-1)^{i-1} V_i$ pour tout $i \in \{1, \dots N\}$. Pour tout $l \in \mathcal{L}_{N,L}$, on considère $V = (T_N)^{-1}(l)$ (cf. Fig. 3.5) et on remarque que les incréments $(v_i)_{i=1}^{N+1}$ de V satisfont nécessairement $v_i := (-1)^{i-1}(l_{i-1} + l_i)$. Ainsi,

$$Z^{\mathsf{nu}}_{L,\beta} = c_\beta \left(\tfrac{e^\beta}{2}\right)^L \sum_{N=1}^{L} \left(\tfrac{2c_\beta}{3e^\beta}\right)^N \sum_{V \in \mathcal{V}_{N+1,L-N}} \mathbf{P}_\beta(V), \tag{3.2.11}$$

ce qui implique (3.2.7). □

Avantages de la représentation probabiliste

Une première conséquence de la formule (3.2.7) est que, dans la mesure ou le taux de croissance exponentiel de $\varphi^{\mathsf{m}}_{L,\beta}$ est égale à $\varphi^{\mathsf{m}}_{\beta}$, l'énergie libre en excès $\widetilde{f}^{\mathsf{m}}(\beta)$ correspond exactement au taux de croissance exponentiel de la somme dans (3.2.7). Dans le même esprit, le diagramme de phase peut être lu directement sur cette formule. En effet, en fonction de la valeur prise par $\Gamma^{\mathsf{m}}(\beta)$, on peut identifier le régime dans laquelle se trouve le modèle:

- $\Gamma^{\mathsf{m}}(\beta) > 1$: *le régime étendu.* Soit $c \in (0,1)$, les quantités $\mathbf{P}_\beta\big(\mathcal{V}_{cL,L(1-c)}\big)$ décroissent exponentiellement vite lorsque $L \to \infty$, à un taux qui croît avec c. Ainsi, les termes dominants dans (3.2.7) sont ceux indexés par $N \sim \widetilde{c}L$, où $\widetilde{c} \in (0,1)$ est le résultat d'une optimisation. Cette phase est dite étendue puisque les trajectoires qui dominent la fonction de partition ont une extension horizontale N du même ordre que leur taille totale L (cf. Fig. 3.4).

- $\Gamma^{\mathsf{m}}(\beta) = 1$: *le régime critique.* Les termes dominants dans (3.2.7) sont indexés par N d'ordre $L^{2/3}$, puisque la quantité $\mathbf{P}_\beta\big(\mathcal{V}_{N+1,L-N}\big)$ atteint son maximum pour ces valeurs de N.

- $\Gamma^{\mathsf{m}}(\beta) < 1$: *le régime effondré.* Soit $c \in (0,\infty)$, les quantités $\mathbf{P}_\beta\big(\mathcal{V}_{c\sqrt{L},L}\big)$ décroissent sous-exponentiellement vite comme $e^{-t_c\sqrt{L}}$ où $t_c > 0$ lui aussi est décroissant en c. Ainsi, les termes dominants dans la fonction de partition (3.2.7) sont indexés par $N \sim \hat{c}\sqrt{L}$, où $\hat{c} \in (0,\infty)$ est, là encore, le résultat d'une optimisation. Cette phase est effondrée parce que les trajectoires dont les contributions dominent la fonction de partition ont une extension horizontale N négligeable devant leur taille totale L (cf. Fig. 3.4).

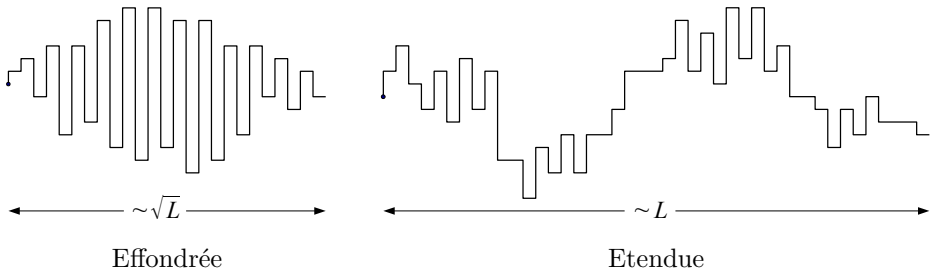

Figure 3.4: Une trajectoire typique de chacune des deux phases.

La seconde propriété de notre représentation probabiliste (3.2.11) qui va s'avérer déterminante pour la suite de notre étude, vient du fait que, une fois conditionnée à faire un nombre donné de pas horizontaux N, la mesure de l'IPDSAW est exactement la mesure image par la bijection T_N de la marche aléatoire auxiliaire V, elle même conditionnée à revenir à l'origine au temps $N+1$ et à faire une aire géométrique de $L-N$, i.e.,

$$P^{\mathsf{m}}_{L,\beta}\big(l \in \cdot \mid N_L(l) = N\big) = \mathbf{P}_\beta\big(T_N(V) \in \cdot \mid V_N = 0, A_N = L-N\big). \tag{3.2.12}$$

Pour illustrer l'efficacité de cette propriété, nous remarquons que chaque trajectoire d'IPDSAW peut être partitionnée en une famille de perles, de sorte que l'énergie totale de la trajectoire soit la somme des énergies de ses perles (cf. Fig. 3.6 et Section 3.3.2 pour une définition rigoureuse). À $\beta > 0$ donné, il est essentiel d'étudier la répartition de ces perles pour

décrire géométriquement les trajectoires typiques d'IPDSAW. Il faut par exemple, comprendre combien de perles apparaissent typiquement le long d'une trajectoire, estimer la taille des plus grandes perles etc... Il se trouve que la transformation T_N établit une correspondance entre les perles d'une trajectoire $l \in \mathcal{L}_{N,L}$ et les excursions de la marche aléatoire associée $V = (T_N)^{-1}(l)$ (cf. Fig. 3.5). On peut donc espèrer que certains résultats issus de la théorie des excursions des marches aléatoires pourront être utilisés pour étudier la distribution de ces perles.

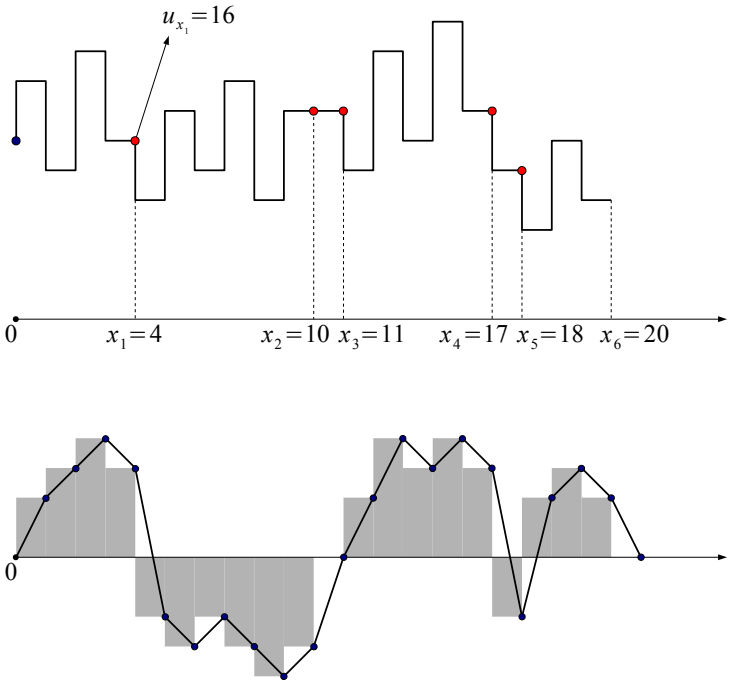

Figure 3.5: Un exemple de trajectoire $l = (l_i)_{i=1}^{20}$ contenant 6 perles est dessiné sur la figure du dessus. La marche aléatoire auxiliaire V associée à l, i.e., $(V_i)_{i=0}^{21} = (T_{20})^{-1}(l)$ est dessinée sur la figure du dessous.

3.3 Résultats principaux

La première partie de notre étude concerne la limite hydrodynamique du modèle IPDSAW. L'objet auquel nous nous intéressons en particulier est donc l'énergie libre en excès du modèle (définie en (3.1.4)), que nous exprimerons tout d'abord sous la forme d'une formule variationnelle dans le Théorème 3.3.1 et dont nous déduirons aisément le paramètre critique β_c^{m} ainsi que l'ordre de la transition de phase. Nous donnerons ensuite, une seconde expression de $\widetilde{f}^{\mathsf{m}}(\beta)$ dans le Théorème 3.3.2, liée à la première par un principe de grande déviation, et nous utiliserons cette représentation pour déterminer l'asymptotique exacte

de $\widetilde{f}^{\mathsf{m}}(\beta)$ au point critique (Théorème (3.3.3)). Si certains des résultats que nous énonçons ici étaient déjà connus, comme par exemple la valeur de β_c^{m} et l'ordre de la transition de phase, nous en donnons des preuves beaucoup plus directes et explicites. De plus, la représentation probabiliste nous permet d'aller au delà des résultats existants dans certains cas. La formule variationnelle n'était en effet pas connue ainsi que le lien entre le préfacteur dans l'asymptotique de $\widetilde{f}^{\mathsf{m}}(\beta)$ et l'énergie libre d'un modèle continu associé.

3.3.1 Transition de phase: analyse de l'énergie libre au point critique

L'obtention du comportement de l'énergie libre près du point critique est un point clé de la compréhension du phénomène qui mène le polymère d'une configuration étendue à une configuration effondrée lors du passage de $\beta < \beta_c^{\mathsf{m}}$ à $\beta > \beta_c^{\mathsf{m}}$. En effet:

- l'exposant critique $\alpha > 0$ qui vérifie $\widetilde{f}(\beta_c - \delta) \sim \delta^\alpha$ nous donne la régularité du paramètre d'ordre du système au voisinage de la température critique. Ainsi, un exposant critique $\alpha \leq 1$ marque une discontinuité du paramètre d'ordre et donc une transition plus "brutale" au sens où le comportement du polymère change d'une façon très radicale lorsque T atteint T_c. C'est le cas pour différents modèles homogènes résolubles de la Mécanique Statistique, comme par exemple le modèle d'Ising en dimension 2 avec $T < T_c$ et un champ extérieur qui varie autour de 0, ou pour les modèles d'accrochage homogènes avec des renouvellements en $L(n)/n^{1+\eta}$ et $\eta \geq 1$ (cf. [38]). Lorsque $\alpha > 1$ en revanche, le paramètre d'ordre varie continûment, c'est le cas de notre modèle IPDSAW ainsi que du modèle d'accrochage avec renouvellements en $L(n)/n^{1+\eta}$ et $\eta < 1$.

- L'exposant critique est lié à la vitesse avec laquelle la longueur de corrélation du système diverge lorsque $\beta \to \beta_c^-$. Cette longueur, notée ici $l_c(\beta)$ satisfait $l_c(\beta) \sim (\beta - \beta_c)^{-\alpha}$, ce qui sous tend que le système peut être décomposé en une suite de blocs indépendants de taille $(\beta - \beta_c)^{-\alpha}$.

- L'ordre de la transition de phase nous permet également, via le critère de Harris, de faire certaines conjectures concernant la version désordonnée de notre modèle. L'ajout d'un désordre se fait au niveau de l'intensité de l'interaction qui devient dépendante de caractéristiques propres (nature, charge électrique) aux deux monomères réalisant un self-touching. L'une des questions importantes concernant les modèles homogènes résolubles de Mécanique Statistique est de savoir si la version quenched (à désordre gelé) de leur homologue désordonné diffère de sa version annealed (avec intégration sur le désordre) au moins pour de petits désordres. Cette question a été traitée avec succès dans le cas des modèles d'accrochage dans une série de travaux récents (cf. [30], [40] et [39] pour une revue) où il est établi que le désordre est non pertinent lorsque

l'exposant critique du modèle homogène est strictement supérieur à 2 et pertinent pour un exposant critique strictement inférieur à 2. Le cas marginal d'un exposant égal à 2 y est également traité en détail.

Nous donnons tout d'abord une caractérisation variationnelle de l'énergie libre en excès $\widetilde{f}^{\mathsf{m}}(\beta)$ qui sera utilisée par la suite pour déterminer β_c^{m} et étudier $\widetilde{f}^{\mathsf{m}}(\beta)$ au voisinage de β_c. Nous rappelons (3.2.5) et, nous introduisons la fonction $g_\beta(\alpha)$ (pour $\alpha > 0$) correspondant au taux de décroissance exponentiel de la probabilité qu'une trajectoire de marche aléatoire V de loi $\mathbf{P}_\beta$ décrive, après N pas, une aire géométrique $A_N := \sum_{i=1}^N |V_i|$ plus petite que αN, i.e.,

$$g_\beta(\alpha) := \lim_{N\to\infty} \tfrac{1}{N} \log \mathbf{P}_\beta\big(A_N(V) \le \alpha N,\, V_N = 0\big), \quad \alpha \in [0,\infty). \tag{3.3.1}$$

Theorem 3.3.1 ([67], Theorem 1.2)**.** *Pour* $\mathsf{m} \in \{\mathsf{u}, \mathsf{nu}\}$*, l'énergie libre en excès* $\widetilde{f}^{\mathsf{m}}(\beta)$ *est donnée par*

$$\widetilde{f}^{\mathsf{m}}(\beta) = \sup_{\alpha\in[0,1]} \left[\alpha \log\left(\Gamma^{\mathsf{m}}(\beta)\right) + \alpha\, g_\beta\left(\tfrac{1-\alpha}{\alpha}\right)\right], \tag{3.3.2}$$

où

$$\begin{cases} \Gamma^{\mathsf{u}}(\beta) = \frac{c_\beta}{e^\beta}, \\ \Gamma^{\mathsf{nu}}(\beta) = \frac{2c_\beta}{3e^\beta}. \end{cases} \tag{3.3.3}$$

Remarquons tout d'abord que le terme $\alpha \log\left(\Gamma^{\mathsf{m}}(\beta)\right) + \alpha\, g_\beta\left(\frac{1-\alpha}{\alpha}\right)$ correspond à l'énergie libre en excès restreinte aux configurations dont l'extension horizontale est de la forme $\alpha L + o(L)$. Ainsi, dans la phase étendue ($\widetilde{f}^{\mathsf{m}}(\beta) > 0$), prouver que le supremum de (3.3.2) est atteint en un point unique donnerait automatiquement une loi des grands nombres sur l'extension horizontale d'une trajectoire typique d'IPDSAW. Cependant, la stricte concavité de $\alpha \mapsto g_\beta(\alpha)$ est difficile à obtenir et pour cette raison nous énoncerons cette loi des grands nombres en Section 3.3.4, Théorème 3.3.38, où elle sera obtenue par une autre méthode.

Une conséquence immédiate du théorème 3.3.1 est que le point critique β_c^{m} est l'unique solution de l'équation $\Gamma^{\mathsf{m}}(\beta) = 1$. Il est facile, en effet, de prouver (cf. [67] Lemme 3.1) que $\alpha \mapsto g_\beta(\alpha)$ est concave et strictement croissante sur $[0,\infty)$ et que $\lim_{\alpha\to\infty} g_\beta(\alpha) = 0$. Ainsi, $\Gamma^{\mathsf{m}}(\beta) > 1$ implique, en choisissant α assez petit dans (3.3.2), que $\widetilde{f}^{\mathsf{m}}(\beta) > 0$. Si $\Gamma^{\mathsf{m}}(\beta) \le 1$, en revanche, (3.3.2) implique que $\widetilde{f}^{\mathsf{m}}(\beta) = 0$. Une seconde conséquence assez directe du théorème 3.3.1 est que la transition de phase est du deuxième ordre avec un exposant critique de 3/2. Nous prouvons en effet, dans [67] (Proposition 3.3) qu'il existe $c_1 > c_2 > 0$ tels que pour α assez grand

$$-\frac{c_1}{\alpha^2} \le g_\beta(\alpha) \le -\frac{c_2}{\alpha^2}. \tag{3.3.4}$$

Une explication heuristique de (3.3.4) peut se formuler de la manière suivante. Sous l'évènement $\{A_N(V) \le \alpha N\}$ et en choisissant $c > 0$ assez grand, la marche aléatoire V place une fraction

arbitrairement proche de 1 de ses N premiers pas à une distance inférieure à $c\alpha$ de l'origine. De plus, la probabilité qu'une marche aléatoire symétrique, dont les incréments sont non constants et ont un premier moment fini, reste jusqu'au temps N dans une bande de taille $2T$ autour de l'origine, décroit comme $e^{-\kappa N/T^2}$ avec $\kappa > 0$. En conséquence, en substituant $c\alpha$ à T dans l'estimé précédente, on peut affirmer que $\mathbf{P}_\beta(A_N(V) \leq \alpha N)$ décroit comme $e^{-\kappa N/\alpha^2}$ ce qui implique (3.3.4). À ce stade, il suffit de vérifier que $\log \Gamma^{\mathsf{m}}(\beta_c^{\mathsf{m}} - \varepsilon) \sim \varepsilon$ et d'insérer (3.3.4) dans (3.3.2) pour affirmer qu'il existe $c_3, c_4 > 0$ telles que pour ε assez petit

$$c_3\, \varepsilon^{3/2} \leq \widetilde{f}^{\mathsf{m}}(\beta_c^{\mathsf{m}} - \varepsilon) \leq c_4\, \varepsilon^{3/2}. \tag{3.3.5}$$

Grâce au Théorème 3.3.2 ci-dessous, nous exprimons l'énergie libre en excès $\widetilde{f}^{\mathsf{m}}(\beta)$ comme l'unique solution d'une équation. Cette nouvelle caractérisation de $\widetilde{f}^{\mathsf{m}}(\beta)$ sera utilisée par la suite pour prouver le théorème 3.3.3, qui améliore le développement asymptotique de l'énergie libre au point critique. Nous introduisons le taux de décroissance exponentiel $h_\beta(\delta)$ (for $\delta > 0$) de la transformée de Laplace de $A_N(V)$, où V est toujours une marche aléatoire de $\mathbf{P}_\beta$, i.e.,

$$h_\beta(\delta) := \lim_{N\to\infty} \frac{1}{N} \log \mathbf{E}_\beta\big(e^{-\delta\, A_N(V)}\big). \tag{3.3.6}$$

Theorem 3.3.2 ([27], Theorem 1.3)**.** *Pour* $\mathsf{m} \in \{\mathsf{u}, \mathsf{nu}\}$*, l'énergie libre en excès* $\widetilde{f}^{\mathsf{m}}(\beta)$ *est l'unique solution de l'équation* $\log(\Gamma^{\mathsf{m}}(\beta)) - \delta + h_\beta(\delta) = 0$ *si une telle solution existe et* $\widetilde{f}^{\mathsf{m}}(\beta) = 0$ *sinon.*

Le lien entre les théorèmes 3.3.1 et 3.3.2 s'explique par le fait que g_β est en réalité la transformée de Legendre de of h_β, i.e.,

$$g_\beta(\alpha) = \sup_{\delta>0} (\delta\alpha + h_\beta(\delta)). \tag{3.3.7}$$

Theorem 3.3.3 (Développement asymptotique de l'énergie libre au point critique)**.** *Pour* $\mathsf{m} \in \{\mathsf{u}, \mathsf{nu}\}$*, la transition de phase est du second ordre avec un exposant critique égal à* $3/2$*. De plus, le premier ordre du développement de Taylor de l'énergie libre en excès au point* $(\beta_c^{\mathsf{m}})^-$ *est donné par*

$$\lim_{\varepsilon\to 0^+} \frac{\widetilde{f}^{\mathsf{m}}(\beta_c^{\mathsf{m}} - \varepsilon)}{\varepsilon^{3/2}} = \Big(\frac{c_{\mathsf{m}}}{d_{\mathsf{m}}}\Big)^{3/2}, \tag{3.3.8}$$

où $\sigma_\beta^2 = \mathbf{E}_\beta(v_1^2)$ *et*

$$\begin{cases} c_{\mathsf{u}} = 1 + \frac{e^{-\beta_c^{\mathsf{u}}/2}}{1-e^{-\beta_c^{\mathsf{u}}}}, \\ c_{\mathsf{nu}} = \frac{2}{3}\Big[1 + \frac{e^{-\beta_c^{\mathsf{nu}}/2}}{1-e^{-\beta_c^{\mathsf{nu}}}}\Big], \end{cases} \tag{3.3.9}$$

et où

$$d_{\mathsf{m}} = -\lim_{T\to\infty} \frac{1}{T} \log \mathbf{E}\big(e^{-\sigma_{\beta_c^{\mathsf{m}}} \int_0^T |B(t)|dt}\big) = 2^{-1/3} |a_1'| \sigma_{\beta_c^{\mathsf{m}}}^{2/3}, \tag{3.3.10}$$

avec a_1' le plus petit zéro (en valeur absolue) de la première dérivée de la fonction d'Airy.

Remark 3.3.4. *La transformée de Laplace $\mathbf{E}(e^{-s\int_0^1 |B_s|ds})$ pour $s > 0$ a été calculé pour la première fois par Kac dans [61] (cf. par exemple la revue de Janson [60]).*

Nous expliquons à présent en quelques mots comment le Théorème 3.3.3 est obtenu. Grâce au Théorème 3.3.2, il est facile de comprendre que le développement asymptotique de $\widetilde{f}^{\mathsf{m}}(\beta)$ en $(\beta_c^{\mathsf{m}})^-$ est intimement lié au fait qu'il existe $c > 0$ tel que

$$h_\beta(\delta) = -c\,\delta^{2/3} + o(\delta^{2/3}), \quad \text{quand } \delta \to 0^+. \tag{3.3.11}$$

Ce dernier développement asymptotique est obtenu en appliquant une méthode de coarse graining, dans le même esprit que celle appliquée dans [48]. Cette méthode consiste à décomposer la trajectoire de la marche aléatoire V en des blocs indépendants, de taille $T\delta^{-2/3}$ pour un $T \in \mathbb{N}$ choisi arbitrairement et un δ assez petit. Nous avons environ $N/(T\delta^{-2/3})$ blocs de ce type que nous utilisons pour prouver que, quand $\delta \searrow 0$, on a

$$\lim_{N\to\infty} \frac{1}{N} \log \mathbf{E}_\beta(e^{-\delta A_N}) \sim \lim_{T\to\infty} \frac{\delta^{2/3}}{T} \log \mathbf{E}_\beta(e^{-\delta A_{T\delta^{-2/3}}}). \tag{3.3.12}$$

Le principe d'invariance de Donsker nous assure alors (en supposant que $\mathbf{E}_\beta(v_1^2) = 1$) (cf [32, p. 405]) que

$$k^{-3/2} \sum_{i=1}^{Tk} |V_i| \xrightarrow{\mathcal{L}} \int_0^T |B(t)|dt \quad \text{quand } k \to \infty, \tag{3.3.13}$$

où B est un mouvement Brownien standard. Ainsi, on choisit $k = \delta^{-2/3}$ dans (3.3.13) et puisque $|e^{-\delta A_{T\delta^{-2/3}}}| \le 1$, on conclut que

$$\mathbf{E}_\beta(e^{-\delta A_{T\delta^{-2/3}}}) \to \mathbf{E}(e^{-\sigma_{\beta_c^{\mathsf{m}}} \int_0^T |B(t)|dt}) \quad \text{quand } \delta \to 0. \tag{3.3.14}$$

Cette dernière convergence et (3.3.12) impliquent que $h_\beta(\delta) \sim -c\,\delta^{2/3}$ où c peut être exprimé à l'aide de la loi de l'*aire Brownienne*, i.e.,

$$c = -\lim_{T\to\infty} \frac{1}{T} \log \mathbf{E}(e^{-\sigma_{\beta_c^{\mathsf{m}}} \int_0^T |B(t)|dt}) > 0. \tag{3.3.15}$$

Discussion

L'assymptotique $h_\beta(\gamma) \sim -c\,\gamma^{2/3}$ est très liée à l'étude de phénomène de pre-mouillage (cf [55], pour lequel l'exposant de scaling est obtenu par une méthode de renormalisation similaire à celle que nous employons ici). Ce phénomène est observé lorsqu'un gaz dans

un état thermodynamique stable est en contact avec un substrat (mur) qui lui-même a une preférence pour la phase liquide de ce gaz. Dans une telle situation, une fine couche de liquide peut se créer qui sépare le gaz du substrat. Lorsque la température T se rapproche de la température d'ébulition du gaz T_b, la couche fine de liquide s'épaissit. L'interface liquide-gaz peut en conséquence être modélisée par une trajectoire de marche aléatoire contrainte de rester positive et dont l'aire géométrique est pénalisée par un facteur Gibbsien $\delta A_N(V)$ où δ disparaît lorsque $T \to T_b$. A proximité du point critique ($\delta = 0$), la longueur de corrélation du système varie comme $\delta^{-2/3}$, ce qui explique l'exposant $2/3$ dans le développement de h_β en 0^+.

3.3.2 Résultats trajectoriels et limite d'échelle dans chaque phase

Le premier type de résultat que nous souhaitons obtenir concerne la décomposition en perles d'une trajectoire typique d'IPDSAW. Heuristiquement, on s'attend à ce qu'un accroissement du paramètre de couplage β se traduise, pour une trajectoire typique, par une augmentation de la taille moyenne de ses segments verticaux et par une augmentation de la fraction de ses paires de segments consécutifs qui sont alternés (de signe opposés). Dès lors, augmenter β devrait provoquer une diminution du nombre total de perles et une augmentation de leur taille totale (ou volume) respective. Dans le même esprit, l'extension horizontale d'une trajectoire typique d'IPDSAW devrait diminuer avec β puisque chaque pas horizontal diminue d'une unité le nombre de self-touching maximal réalisable par la trajectoire.

Définition rigoureuse des perles.

Une perle est constituée de segments verticaux de longueur strictement positive et disposés de façon à ce que deux segments consécutifs soient de signes opposés (cf. Fig. 3.6). Une perle se termine lorsque deux segments consécutifs sont de même signe (pas alternés) ou bien lorsqu'un segment est de longueur 0 (ce qui correspond à deux pas horizontaux consécutifs).

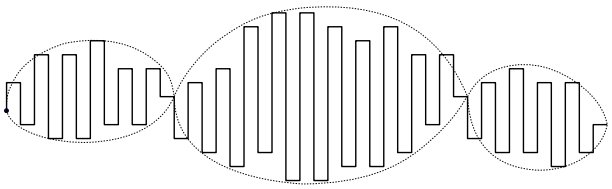

Figure 3.6: Un example de trajectoire avec 3 perles.

Pour tout $l \in \mathcal{L}_{N,L}$ on pose $(u_j)_{j=1}^N$ la suite des nombres cumulés de monomères après chaque segment vertical, i.e., $u_j = |l_1| + \ldots |l_j| + j$ pour $j \in \{1, \ldots, N\}$. Pour faciliter la présentation, on pose $l_{N+1} = 0$. On définit aussi $x_0 = 0$ et pour $j \in \mathbb{N}$ tel que $x_{j-1} < N$, on

pose $x_j = \inf\{i \geq x_{j-1}+1 \colon\ l_i \barwedge l_{i+1} = 0\}$ (cf. Fig. 3.5). Finalement, on note $n_L(l)$ l'indice du dernier x_j qui est bien défini, i.e., $x_{n_L(l)} = N$. Ainsi, nous pouvons décomposer chaque trajectoire $l \in \Omega_L$ en une succession de $n_L(l)$ perles, chacune d'entre elles étant associée à un sous-intervalle de $\{1, \dots, L\}$ que l'on note

$$I_j = \{u_{x_{j-1}} + 1, \dots, u_{x_j}\}, \quad \text{pour} \quad j \in \{1, \dots, n_L(l)\}, \tag{3.3.16}$$

de sorte que nous puissions partitionner $\{1, \dots, L\}$ en $\cup_{j=1}^{n_L(l)} I_j$. À ce stade, on peut définir la plus grande perle d'une trajectoire $l \in \Omega_L$ comme $I_{j_{\max}}$ avec

$$j_{\max} = \arg\max\big\{|I_j|, j \in \{1, \dots, n_L(l)\}\big\}. \tag{3.3.17}$$

Le second type de résultat trajectoriel que nous souhaitons obtenir concerne les limites d'échelle de l'extension horizontale et des enveloppes supérieure et inférieure d'une trajectoire typique d'IPDSAW. On peut en effet définir de façon naturelle l'enveloppe supérieure (cf. Fig 3.7) (respectivement inférieure) d'une trajectoire comme le processus cadlag qui lie successivement le haut (resp. le bas) de chacun des segments verticaux qui constituent la trajectoire.

Définition rigoureuse de l'extension horizontale et des enveloppes

Soit $l \in \Omega_L$ une trajectoire, on note $N_L(l)$ son extension horizontale, i.e., $N_L(l)$ est l'entier N tel que $l \in \mathcal{L}_{N,L}$. On définit également $\mathcal{E}_l^+ = (\mathcal{E}_{l,i}^+)_{i=0}^{N+1}$ et $\mathcal{E}_l^- = (\mathcal{E}_{l,i}^-)_{i=0}^{N+1}$ les enveloppes supérieure et inférieure de l par $\mathcal{E}_{l,0}^+ = \mathcal{E}_{l,0}^- = 0$,

$$\begin{aligned} \mathcal{E}_{l,i}^+ &= \max\{l_1 + \cdots + l_{i-1}, l_1 + \cdots + l_i\}, \quad i \in \{1, \dots, N\}, \\ \mathcal{E}_{l,i}^- &= \min\{l_1 + \cdots + l_{i-1}, l_1 + \cdots + l_i\}, \quad i \in \{1, \dots, N\}, \end{aligned} \tag{3.3.18}$$

et $\mathcal{E}_{l,N+1}^+ = \mathcal{E}_{l,N+1}^- = l_1 + \cdots + l_N$.

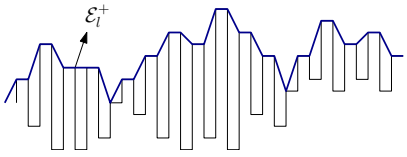

Figure 3.7: Enveloppe supérieure d'une trajectoire.

Par un changement d'échelle on définit $\widetilde{\mathcal{E}}_l^+$ et $\widetilde{\mathcal{E}}_l^-$, les versions renormalisées des deux enveloppes, i.e., les processus cadlag définis par

$$\widetilde{\mathcal{E}}_l^+(t) = \frac{1}{N+1}\,\mathcal{E}_{l,\lfloor t\,(N+1)\rfloor}^+ \quad \text{and} \quad \widetilde{\mathcal{E}}_l^-(t) = \frac{1}{N+1}\,\mathcal{E}_{l,\lfloor t\,(N+1)\rfloor}^-, \quad t \in [0,1]. \tag{3.3.19}$$

Notre objectif est donc d'obtenir une caractérisation complète de la limite d'echelle de l'IPDSAW dans chacune de ses trois phases. Ce sera chose faite en obtenant la limite en loi, lorsque $L \to \infty$, et sous la mesure polymère $P^{\mathsf{m}}_{L,\beta}$, du triplet $\big(\frac{N_l}{L^{\alpha_1}}, N_l^{\alpha_2} (\widetilde{\mathcal{E}}_l^+, \widetilde{\mathcal{E}}_l^-) \big)$, i.e.,

$$\lim_{L\to\infty} \Big(\tfrac{N_l}{L^{\alpha_1}}, N_l^{\alpha_2} (\widetilde{\mathcal{E}}_l^+, \widetilde{\mathcal{E}}_l^-) \Big)_{P^{\mathsf{m}}_{L,\beta}} \tag{3.3.20}$$

en déterminant les coefficients $\alpha_1, \alpha_2 \in [0,1]$ qui correspondent à une limite non-triviale.

Stratégie de preuve: lien avec la marche auxiliaire

Une fois encore, la représentation de notre modèle à l'aide de la marche à accroissements géométriques V sera au coeur de notre stratégie pour obtenir des résultats de limite d'échelle. On associe tout d'abord à chaque $l \in \mathcal{L}_{N,L}$ le processus cadlag $M_l = \big(M_{l,i}\big)_{i=0}^{N+1}$ qui lie successivement le milieu de chacun des segments verticaux. Ainsi, $M_{l,0} = 0$, $M_{l,N+1} = l_1 + \cdots + l_N$ et

$$M_{l,i} = l_1 + \cdots + l_{i-1} + \frac{l_i}{2}, \quad i \in \{1, \dots, N\}. \tag{3.3.21}$$

Le lien avec la marche auxiliaire s'opère avec la transformation T_N définie en Section 3.2.2, et qui associe à chaque $l \in \mathcal{L}_{N,L}$ une trajectoire $V_l = (T_N)^{-1}(l)$ définie par $V_{l,0} = 0$, $V_{l,i} = (-1)^{i-1} l_i$ pour tous $i \in \{1, \dots, N\}$ et par $V_{l,N+1} = 0$. En conséquence,

$$\begin{aligned} \mathcal{E}^+_{l,i} &= M_{l,i} + \frac{|V_{l,i}|}{2}, \quad i \in \{0, \dots, N+1\}, \\ \mathcal{E}^-_{l,i} &= M_{l,i} - \frac{|V_{l,i}|}{2}, \quad i \in \{0, \dots, N+1\}, \end{aligned} \tag{3.3.22}$$

et la droite des milieux $(M_{l,i})_{i=0}^{N+1}$ peut également être réécrite à l'aide des incréments $(v_i)_{i=1}^{N+1}$ de V_l sous la forme

$$M_{l,i} = \sum_{j=1}^{i} (-1)^{j+1} \frac{v_j}{2}, \quad i \in \{1, \dots, N\}. \tag{3.3.23}$$

En reprenant la définition de $\widetilde{\mathcal{E}}_l^+$ et $\widetilde{\mathcal{E}}_l^-$ dans (3.3.19), on définit $\widetilde{M_l}$ et $\widetilde{V_l}$ les versions renormalisées et cadlag des processus M_l and V_l, de sorte que (3.3.22) devienne

$$\widetilde{\mathcal{E}}_l^+ = \widetilde{M_l} + \frac{|\widetilde{V_l}|}{2} \quad \text{et} \quad \widetilde{\mathcal{E}}_l^- = \widetilde{M_l} - \frac{|\widetilde{V_l}|}{2}. \tag{3.3.24}$$

Ainsi, grâce à (3.3.24), la limite en (3.3.20), sera déduite directement de

$$\lim_{L\to\infty} \Big(\tfrac{N_l}{L^{\alpha_1}}, N_l^{\eta_1} \widetilde{M_l}, N_l^{\eta_2} \widetilde{V_l} \Big)_{P^{\mathsf{m}}_{L,\beta}} \tag{3.3.25}$$

avec des coefficients (η_1, η_2) correspondant à une limite non triviale.

3.3.3 Phase effondrée

Unicité de la perle macroscopique et extension horizontale

Le premier résultat trajectoriel que nous avons obtenu concerne la répartition des perles le long d'une trajectoire typique effondrée. Nous avons donc prouvé dans [27] qu'une telle trajectoire ne contient qu'une seule perle macroscopique et que le nombre de monomères en dehors de cette perle ne croît pas plus vite que $\log(L)^4$ (avec L la taille du polymère).

Theorem 3.3.5 (Unicité de la perle)**.** *Pour* $\mathsf{m} \in \{\mathsf{u}, \mathsf{nu}\}$ *et* $\beta > \beta_c^{\mathsf{m}}$*, il existe* $c > 0$ *tel que*

$$\lim_{L\to\infty} P^{\mathsf{m}}_{L,\beta}\big(|I_{j_{max}}| \geq L - c\,(\log L)^4\big) = 1. \tag{3.3.26}$$

Remark 3.3.6. *La subdivision d'une trajectoire en perles ne peut être associée à un processus de renouvellement comme c'est le cas, par exemple, pour le modèle du pinning homogène pour lequel chaque trajectoire peut être partitionnée en une succession d'excursions en dehors de l'origine (cf. [38], Chapitre 2). Cette impossibilité s'explique par une dépendance de type Markovienne entre les perles. Ainsi, après une perle de taille* 1*, c'est à dire constituée d'un seul pas horizontal, le premier segment vertical de la perle suivante peut être positif ou négatif tandis que son orientation est imposée lorsque la taille de la perle précédente est strictement plus grande que* 1*. Cependant, si l'on omet cette dépendance Markovienne entre deux perles consécutives, les estimations précises dont nous disposons concernant la fonction de partition restreinte à une perle (cf. [28] Proposition 4.2), nous permettent de lier le "processus des perles"* $(u_{x_j})_{j=0}^{n_L(l)}$ *sous* $P^{\mathsf{m}}_{L,\beta}$ *à un processus de renouvellement défectif à queue sous-exponentielle* $\tau = (\tau_i)_{i\geq 0}$ *conditionné par* $L \in \tau$*. Ce processus est caractérisé par une loi des inter-arrivées* $K : \overline{\mathbb{N}} \to [0,1]$ *qui satisfait* $K(\infty) > 0$ *et* $K(n) = L(n)e^{-c\sqrt{L}}$ *où* $L : \mathbb{N} \to \mathbb{N}$ *est une fonction à variation lente. Une fois conditionné par* $\{L \in \tau\}$*, il a été prouvé (cf. [38], Appendice A.5 pour le cas d'une loi* K *à décroissance polynomiale et plus récemment dans [82] où le cas sous-exponentiel est traité explicitement) que le nombre de renouvellements est borné et qu'il y a un unique renouvellement de taille macroscopique (cf. e.g. [6] pour une théorie général sur la théorie du renouvellement).*

En réalité, pour prouver le Théorème 3.3.5, nous prouvons simultanément que l'extension horizontale caractéristique d'une trajectoire de la phase effondrée est de l'ordre de $\sqrt{L}$ et nous identifions précisément le préfacteur. C'est l'objet du Théorème 3.3.7 en dessous.

Theorem 3.3.7 (Extension horizontale)**.** *Pour* $\mathsf{m} \in \{\mathsf{u}, \mathsf{nu}\}$ *et* $\beta > \beta_c^{\mathsf{m}}$ *il existe* $a_{\mathsf{m}}(\beta) > 0$ *tel que pour tout* $\varepsilon > 0$

$$\lim_{L\to\infty} P^{\mathsf{m}}_{L,\beta}\left(\left|\frac{N_L}{\sqrt{L}} - a_{\mathsf{m}}(\beta)\right| > \varepsilon\right) = 0. \tag{3.3.27}$$

Remark 3.3.8. *La limite $a_{\mathsf{m}}(\beta)$ est l'unique maximiseur de la fonction $a \mapsto \widetilde{G}_{\mathsf{m}}(a)$ sur $(0,\infty)$ où*

$$\widetilde{G}_{\mathsf{m}}(a) := a \log \Gamma^{\mathsf{m}}(\beta) - \tfrac{1}{a}\, \widetilde{h}_0\big(\tfrac{1}{a^2}, 0\big) + a L_\Lambda\big(\widetilde{H}\big(\tfrac{1}{a^2}, 0\big)\big). \tag{3.3.28}$$

Pour $\beta > \beta_c^{\mathsf{m}}$, la fonction $a \mapsto \widetilde{G}_{\mathsf{m}}(a)$ est $\mathcal{C}^\infty$, strictement concave et négative. Ainsi, $a_{\mathsf{m}}(\beta)$ est l'unique zéro de sa dérivée sur $(0,\infty)$. On rappelle que $\Gamma_\beta^{\mathsf{m}}$ est défini en (3.3.3) *tandis que L_Λ et $\widetilde{H}$ sont définies par*

$$\begin{aligned} L(h) &:= \log \mathbf{E}_\beta[e^{h v_1}], \quad h \in (-\tfrac{\beta}{2}, \tfrac{\beta}{2}) \\ L_\Lambda(H) &:= \int_0^1 L(x h_0 + h_1) dx, \quad H \in \mathcal{D} \end{aligned} \tag{3.3.29}$$

où $\mathcal{D} := \big\{H = (h_0, h_1) \colon \{h_0, h_0 + h_1\} \subset (-\frac{\beta}{2}, \frac{\beta}{2})\big\}$ et $\widetilde{H} : \mathbb{R}^2 \mapsto \mathcal{D}$ est l'inverse de $\nabla L_\Lambda(H)$ qui est un $\mathcal{C}^1$ difféomorphisme de $\mathcal{D}$ dans $\mathbb{R}^2$. Soit $z \in \mathbb{R}^2$, les deux coordonnées de $\widetilde{H}(z)$ sont notées respectivement $\widetilde{h}_0(z)$ et $\widetilde{h}_1(z)$.

Convergence des enveloppes vers une forme de Wulff

Le théorème 3.3.7 nous indique que les configurations qui dominent la fonction de partition dans (3.2.1) ont une extension horizontale de l'ordre de $\sqrt{L}$, négligeable devant leur taille totale L. Cependant, la contrainte sur l'aire que doivent satisfaire ces configurations, i.e., $A_N(V) = L - N$ les éloigne de leur comportement typique $A_N(V) \sim N^{3/2}$ puisque de fait elle satisfont une condition du type $A_N(V) \sim N^2$. Ceci implique que les configurations dominantes appartiennent à l'événement de grande déviation $\{A_N(V) \geq (1/a_{\mathsf{m}}(\beta))^2 N^2\}$. La fonction de taux du principe de grande déviation de Mogulski admet un unique minimum $\gamma^*_{\beta,\mathsf{m}}$ dans cet événement qui correspond à une forme de Wulff déterministe dont nous donnons une expression dans le Théorème 3.3.9 ci-dessous. C'est à partir de cette forme de Wulff que nous identifions, dans le Théorème 3.3.9, les limites d'échelles des enveloppes supérieure et inférieure d'une trajectoire typique.

Theorem 3.3.9. *Pour $\mathsf{m} \in \{\mathsf{u}, \mathsf{nu}\}$, $\beta > \beta_c^{\mathsf{m}}$ et $\varepsilon > 0$,*

$$\begin{aligned} \lim_{L\to\infty} P^{\mathsf{m}}_{L,\beta}\Big(\big\| \widetilde{\mathcal{E}}_l^+ - \frac{\gamma^*_{\beta,\mathsf{m}}}{2} \big\|_\infty > \varepsilon \Big) = 0, \\ \lim_{L\to\infty} P^{\mathsf{m}}_{L,\beta}\Big(\big\| \widetilde{\mathcal{E}}_l^- + \frac{\gamma^*_{\beta,\mathsf{m}}}{2} \big\|_\infty > \varepsilon \Big) = 0, \end{aligned} \tag{3.3.30}$$

où

$$\gamma^*_{\beta,\mathsf{m}}(s) = \int_0^s L'\big[(\tfrac{1}{2} - x)\, \widetilde{h}_0\big(\tfrac{1}{a_{\mathsf{m}}(\beta)^2}, 0\big)\big] dx, \quad s \in [0,1]. \tag{3.3.31}$$

On remarque que les Théorèmes 3.3.7 et 3.3.9 donnent la limite en probabilité de (3.3.20) avec les coefficients $\alpha_1 = 1/2$ et $\alpha_2 = 0$.

Remark 3.3.10. *Les formes de Wulff furent introduites en [83] et apparaissent dans de nombreux modèles de mécanique statistique pour décrire la forme limite d'interfaces séparant des phases pures après une renormalisation ad-hoc. Elles sont obtenues en minimisant l'intégrale de la tension de surface le long de contours continus qui satisfont des contraintes géométriques particulières. Le modèle d'Ising en dimension* 2 *et en régime de transition de phase en donne un exemple célèbre. En considérant une grande boîte carré de taille* N *avec des conditions aux bords* $-$ *et* $T < T_c$ *et en conditionnant la magnétisation totale dans la boîte à dépasser sa moyenne* $(-m^*N^2)$ *d'un facteur* $a_N \sim N^{4/3+\delta}$*, il a été prouvé dans [31] à basse température et ensuite dans [56], [57] et dans [58] jusqu'à* T_c *que cet écart à la magnétisation typique est dû à une unique île de* $+$ *dont la frontière, une fois renormalisée par* $1/\sqrt{a_N}$*, converge vers une forme de Wulff.*

Oscillation des enveloppes autour de la forme de Wulff

Dans la phase effondrée ($\beta > \beta_c^{\mathsf{m}}$), les deux processus $\widetilde{F}_l^+ := \widetilde{\mathcal{E}}_l^+ - \frac{\gamma_\beta^*}{2}$ et $\widetilde{F}_l^- := \widetilde{\mathcal{E}}_l^- + \frac{\gamma_\beta^*}{2}$ correspondent, respectivement, aux fluctuations des enveloppes supérieures et inférieures autour de leur courbe limite. Ainsi, nous avons

$$\begin{aligned} \widetilde{F}_l^+(t) &= \widetilde{M}_l(t) + \tfrac{|\widetilde{V}_l(t)|-\gamma_\beta^*(t)}{2}, \quad t \in [0,1], \\ \widetilde{F}_l^-(t) &= \widetilde{M}_l(t) - \tfrac{|l\widetilde{V}_l(t)|-\gamma_\beta^*(t)}{2}, \quad t \in [0,1]. \end{aligned} \tag{3.3.32}$$

Une conjecture raisonable nous dit que les processus $\sqrt{N_l}\,\widetilde{F}_l^+$ et $\sqrt{N_l}\,\widetilde{F}_l^-$ (sous $P_{L,\beta}^{\mathsf{m}}$) devraient satisfaire un théorème central limite (TCL) lorsque $L \to \infty$.

Nous ne parvenons pas pour l'instant à obtenir les limites respectives de ces deux processus sous $P_{L,\beta}^{\mathsf{m}}$. En revanche, nous prouvons un TCL en considérant, pour un L donné, un ensemble élargi de trajectoires $\widetilde{\Omega}_L = \cup_{L' \in K_L} \Omega_{L'}$, avec $K_L = \{L-(\log L)^5, L+(\log L)^5\}$ et en définissant, sur $\widetilde{\Omega}_L$, une mesure auxiliaire $\widetilde{P}_{L,\beta}^{\mathsf{m}}$ comme mélange des mesures $(P_{L',\beta}^{\mathsf{m}})_{L' \in K_L}$, i.e.,

$$\widetilde{P}_{L,\beta}^{\mathsf{m}}(l) = \sum_{L' \in K_L} \frac{\widetilde{Z}_{L',\beta}}{\sum_{L' \in K_L} \widetilde{Z}_{L',\beta}} P_{L',\beta}^{\mathsf{m}}(l)\, 1_{\{l \in \Omega_{L'}\}}, \quad \text{pour } l \in \widetilde{\Omega}_L, \tag{3.3.33}$$

avec $\widetilde{Z}_{L',\beta} = (e^\beta/2)^{-L'} Z_{L',\beta}$ pour $L' \in K_L$.

Il nous reste à définir le processus limite. Pour ce faire, on rappelle les définitions de (3.3.29), on considère $H = (h_0, h_1) \in \mathcal{D}$ et on définit $(\xi_H(t), 0 \le t \le 1)$ un processus Gaussien centré de covariance

$$E(\xi_H(s)\xi_H(t)) = \int_0^{s\wedge t} L''((1-x)h_0 + h_1)\, dx\,.$$

On peut constuire ξ_H à l'aide d'un mouvement brownien W en considérant l'intégrale de Wiener

$$\xi_H(t) := \int_0^t \sqrt{L''((1-x)h_0 + h_1)}\, dW_x\,.$$

Soit $\bar{t} = (t_1, \dots, t_{r_1})$ avec $0 < t_1 < \cdots < t_{r_1} < 1$, on appelle $g_{H,\bar{t}}(\bar{x})$, $\bar{x} \in \mathbb{R}^{r_1}$, la densité du vecteur Gaussien $\xi_H(\bar{t}) = (\xi_H(t_1), \dots, \xi_H(t_{r_1}))$ et on note $f_{H,\bar{t}}(z_0, z_1, \bar{x})$ la densité du vecteur Gaussien $(\int_0^1 \xi_H(s)\, ds, \xi_H(1), \xi_H(t_1), \dots, \xi_H(t_{r_1}))$. Enfin, on pose

$$f^c_{H,\bar{t}}(\bar{y}) = \frac{f_{H,\bar{t}}(0,0,\bar{y})}{\int f_{H,\bar{t}}(0,0,\bar{x})\, d\bar{x}}$$

la densité de $\xi_H(\bar{t})$ conditionnellement à $\int_0^1 \xi_H(s)\, ds = 0 = \xi_H(1)$. On définit alors $(\xi^c_H(t))_{t\in[0,1]}$ un processus indépendant de ξ_H de même loi que ξ_H conditionnellement à $\xi_H(1) = \int_0^1 \xi_H(s)\, ds = 0$.

Theorem 3.3.11. *Pour $\beta > \beta_c^{\mathsf{m}}$, on pose $H = \widetilde{H}(1/a_{\mathsf{m}}(\beta)^2, 0)$ et on a la convergence en loi*

$$\lim_{L\to\infty} \sqrt{N_l}\big(\widetilde{M}_l(s), |\widetilde{V}_l(s)| - \gamma^*_\beta(s)\big)_{s\in[0,1]} =_{\widetilde{P}^{\mathsf{m}}_{L,\beta}} (\xi_H(s), \xi^c_H(s))_{s\in[0,1]}. \tag{3.3.34}$$

Dès lors, les équations (3.3.32) et le Théorème 3.3.11 nous donnent les fluctuations des deux enveloppes autour de leur forme de Wulff limite respective.

3.3.4 La phase étendue

La phase étendue se caractérise par un paramètre $\Gamma^{\mathsf{m}}(\beta)$ strictement supérieur à 1. Ce paramètre favorise dans la fonction de partition (3.2.1), les configurations à grande extension horizontale. On peut alors conjecturer que le nombre de perles apparaissant le long d'une trajectoire typique soit du même ordre que la taille totale de la trajectoire. Pour appuyer cette conjecture, nous notons simplement que, puisque 2 pas horizontaux consécutifs marquent nécessairement la fin d'une perle, le fait que la fraction de pas horizontaux soit du même ordre que la taille totale de la trajectoire devrait correspondre à une fraction strictement positive de paires de pas horizontaux consécutifs, et donc à un nombre de perle du même ordre que la taille totale de la trajectoire.

Les résultats que nous décrivons à présent sont issus de [28] et ils rendent rigoureuse l'heuristique précédente. Tout d'abord, la taille de la plus grande perle d'une trajectoire typique de taille totale L ne dépasse pas $\log L$.

Lemma 3.3.12. *Pour tous $\beta < \beta_c$, il existe un $c > 0$ tel que*

$$\lim_{L\to\infty} P^{\mathsf{m}}_{L,\beta}\big(|I_{j_{max}}| \geq c \log L\big) = 0. \tag{3.3.35}$$

Une conséquence immédiate du Lemme 3.3.12 est que la taille du plus grand segment vertical d'une trajectoire typique ne dépasse pas $\log L$. Ceci implique de façon évidente que, pour tout $\alpha \in [0,1)$, la limite en loi, quand $L \to \infty$ et sous $P^{\mathsf{m}}_{L,\beta}$, du processus $(N_l)^\alpha |\widetilde{V}_l|$ est la fonction nulle, i.e.,

$$\lim_{L\to\infty} (N_l)^\alpha |\widetilde{V}_l| = 0_{[0,1]}. \tag{3.3.36}$$

Nous identifions également l'extension horizontale typique d'une trajectoire, pour laquelle nous donnons une loi des grands nombres.

Theorem 3.3.13. *Pour $\beta < \beta_c^{\mathsf{m}}$, il existe $a_{\mathsf{m}}(\beta) > 0$ tel que pour tout $\varepsilon > 0$,*

$$\lim_{L\to\infty} P_{L,\beta}^{\mathsf{m}}\Big(\Big|\frac{N_l}{L} - a_{\mathsf{m}}(\beta)\Big| \geq \varepsilon\Big) = 0. \tag{3.3.37}$$

Il reste alors, pour obtenir une description complète de la limite d'échelle dans la phase étendue, à identifier la limite en loi de la droite des milieux (il s'agit de la deuxième coordonnée dans (3.3.39)). C'est l'objet du théorème 3.3.14 suivant.

Theorem 3.3.14. *Pour $\beta < \beta_c^{\mathsf{m}}$, il existe $\sigma_\beta^{\mathsf{m}} > 0$ tel que ,*

$$\lim_{L\to\infty} (N_l)^{1/2}\widetilde{M}_l =_{P_{L,\beta}^{\mathsf{m}}} (\sigma_\beta^{\mathsf{m}} B_s)_{s\in[0,1]}. \tag{3.3.38}$$

où $(B_s)_{s\in[0,1]}$, un mouvement Brownien standard unidimensionel.

On peut donc exhiber la limite d'échelle complète (sous la forme suggérée en (3.3.20)) de l'IPDSAW dans sa phase étendue, en utilisant les Théorèmes 3.3.13 et 3.3.14 ainsi que (3.3.24) et (3.3.36). On obtient

$$\lim_{L\to\infty} \Big(\tfrac{N_l}{L}, N_l^{1/2}\,(\widetilde{\mathcal{E}}_l^{+}, \widetilde{\mathcal{E}}_l^{-}) \Big) =_{P_{L,\beta}^{\mathsf{m}}} \big(a_{\mathsf{m}}(\beta), \sigma_\beta^{\mathsf{m}}(B_s, B_s)_{s\in[0,1]}\big), \tag{3.3.39}$$

et on constate que les enveloppes supérieure et inférieure convergent vers le même processus Brownien, ce qui est une conséquence directe du fait que les segments verticaux d'une trajectoire typique sont bornés par $\log L$ (cf Lemme 3.3.35)

Dans [28], nous donnons une formule pour la vitesse d'extension horizontale $a_{\mathsf{m}}(\beta)$ et pour la variance du processus limite $\sigma_\beta^{\mathsf{m}}$. De ces formules, il est facile de déduire que ces quantités sont continues en β. En revanche, nous ne parvenons pas à prouver, à ce stade, qu'elles sont monotones. Nous conjecturons notamment que $\beta \to a_{\mathsf{m}}(\beta)$ est décroissante sur $(0, \beta_c^{\mathsf{m}}]$.

3.4 Perspectives

There are several short-term goals about which we are working currently. Concerning the critical case $\beta = \beta_c$, we want to determine the scaling limit of the horizontal extension of the path. In this regime, we do not expect the properly rescaled horizontal extension to converge towards a constant. We indeed believe that there exists a positive and non-constant random variable X such that $N_L/L^{2/3}$ (under $P_{L,\beta_c}^{\mathsf{m}}$) converges in law towards X. Very recently, we managed to derive such limit so that the next target is to identify the scaling limit of the whole path and to obtain the counterpart of Theorems 3.3.11 and 3.3.14 at $\beta = \beta_c$.

Concerning the collapsed phase, we would like to prove the counterpart of Theorem 3.3.11 with $P^{\mathsf{m}}_{L,\beta}$ instead of $\widetilde{P}^{\mathsf{m}}_{L,\beta}$. This requires however to obtain a local limit theorem for the arithmetic area $(\sum_{i=1}^{N} V_i)$ and for the geometric area $(\sum_{i=1}^{N} |V_i|)$ taking large values (of order qN^2 with $q > 0$) *simultaneously*. Such an estimate is out of reach for the moment but we keep working on it.

The long-term goals are also numerous. A first natural extension would be to consider a version of the model for which the strength of the interaction between two neighboring monomers is not constant but rather depends on the chemical characteristics of each monomer. This allows us to take into account both a copolymer (a polymer made of different types of monomers) and/or an inhomogeneous solvent. Studying the influence of a disorder on the phase transition of an exactly solvable homogeneous model is a challenging issue, settled recently for the model of a polymer pinned by a linear interface with, in particular, the identification of the regime of disorder relevance (we refer to Section 4.4.1 for a discussion about it). The IPDSAW also falls into the class of exactly solvable models, with the particularity that the free energy inside the collapsed phase is not constant, which makes some of the techniques that were used for the pinning inefficient. A very challenging issue could be to identify and investigate the regime of disorder relevance for the IPDSAW and show whether the random disorder smoothes the phase transition or not.

Another long-term objective is to develop a physically more realistic version of a polymer in a "poor" solvent. One step in this direction is to build a non-directed model of an interacting self-avoiding walk (ISAW). However, working with the 2-dimensional self-avoiding walk (SAW) directly is very hard, due to the level of complexity of the SAW itself (its connective constant is not even known for the moment). One option is to consider a self-interacting version of the prudent walk, i.e., a non-directed walk although more tractable than the SAW itself (see e.g. [7] for the scaling limit of the prudent walk).

In dimension 3, a directed version of the homogeneous model could be studied. We could e.g. consider the IPDSAW with a path π taking steps in $\{e_1, \pm e_2, \pm e_3\}$, where (e_1, e_2, e_3) is the canonical basis of $\mathbb{R}^3$. For such a model, even the existence of a collapse transition is not rigorously proven.

Chapter 4

Random walk in a potential

4.1 Introduction

Many models in statistical mechanics can be viewed as particular cases of a partially directed random walk in a potential. This is the case for instance of two models that generated a lot of emulation among mathematicians in the last 10 years, i.e., the polymer pinned at a linear interface and the directed polymer in random environment (also referred to as directed polymer in bulk disorder). This chapter is dedicated to the papers [18], [24], [25], [72] and [73] that are all concerned with models which may also be expressed as a partially directed random walk in a potential. We will try to present the results that have been obtained in those papers and to draw a comparison between the features of theses models whenever it is appropriate.

In Sections 4.1.1-4.1.2 below, we provide a general framework for a partially directed random walk in a potential and we display three examples of models that fall into this framework. In section 4.1.3 we classify into 4 categories the relevant questions that are addressed by mathematicians when studying such models. In Section 4.2, we study the discrete parabolic Anderson model (DPAM) and present the results of path localization that we obtained on the DPAM with heavy tailed potential. In section 4.3, we focus on the $1+1$ dimensional simple random walk in a dynamical multi-interface medium and we present the infinite volume limit that we obtained in both the pinning and the depinning cases. Finally in Section 4.4 we consider a model for a copolymer randomly pinned along a linear layer separating two solvents and we present our results concerning the weak coupling limit of the model.

4.1.1 A general setting

Consider a partially directed random walk in dimension $1+d$ ($d \in \mathbb{N}$). The random walk is denoted by $S := (i, S_i)_{i=0}^{\infty}$ such that $S_0 = 0$ and $(S_{i+1} - S_i)_{i=0}^{\infty}$ is an i.i.d. sequence of

bounded random vectors in $\mathbb{Z}^d$.

The potential in which the random walk is embedded can take different forms. Depending on the physical object that one is intending to model, this potential can be deterministic or random, time dependent or not, etc... In an attempt to account for most of these models we introduce below a general setting. Let $\boldsymbol{\xi} := (\xi^N)_{N\in\mathbb{N}}$ be a sequence of fields on $\mathbb{N}\times\mathbb{Z}^d$ taking real values, i.e.,

$$\xi^N := \left(\xi^N_{i,x}\right)_{i\in\mathbb{N},\, x\in\mathbb{Z}^d} \in \mathbb{R}^{\mathbb{N}\times\mathbb{Z}^d}. \tag{4.1.1}$$

The N dependence of ξ in (4.1.1) allows us to model a time-dependent potential, which will be important in section 4.3 to describe a dynamical multi-interface medium. In most models though, the N dependence of ξ will be dropped and ξ will either be deterministic or be the random realization of a probability law $\mathbb{P}$ on $\mathbb{R}^{\mathbb{N}\times\mathbb{Z}^d}$ equipped with its usual product sigma-algebra $(\mathrm{Bor}\,\mathbb{R})^{\otimes(\mathbb{N}\times\mathbb{Z}^d)}$. Note that, when the potential is not time dependent, it is simply denoted by ξ and does not appear in dark anymore.

In size $N\in\mathbb{N}$, we associate an Hamiltonian with each random walk trajectory S by adding up all the potential values sitting on those sites that have been visited by the trajectory up to time N, i.e.,

$$H^{\boldsymbol{\xi}}_{N,\beta}(S) = \beta\sum_{i=1}^{N}\xi^N_{i,S_i}. \tag{4.1.2}$$

We can therefore define the polymer measure in size N for a given disorder $\boldsymbol{\xi}$ by perturbing the a priori law P on S, i.e.,

$$\frac{\mathrm{d}\,\mathbf{P}^{\boldsymbol{\xi}}_{N,\beta}}{\mathrm{d}\,\mathrm{P}}(S) = \frac{e^{H^{\xi^N}_{N,\beta}(S)}}{Z^{\xi^N}_{N,\beta}}, \tag{4.1.3}$$

where $Z^{\xi^N}_{N,\beta} = \mathbf{E}\Big[\exp\Big(H^{\xi^N}_{N,\beta}(S)\Big)\Big]$ is the normalizing factor also referred to as partition function of the system.

Let us now present the three models that will be discussed in this chapter. Each of them appears as a particular case of the general setting displayed in (4.1.1–4.1.3) and will be further investigated in Sections (4.2–4.4) below.

4.1.2 Three particular cases

The discrete parabolic Anderson model (DPAM). The DPAM is a particular case of our general setting in (4.1.1–4.1.3). The coupling parameter β is taken equal to 1, there is no restriction on the dimension $d\in\mathbb{N}$ and the potential ξ is not time dependent and remains constant on each line $\mathbb{N}\times\{x\}$ for $x\in\mathbb{Z}^d$, i.e.,

$$\xi_{i,x} = \xi_x, \quad (i,x)\in\mathbb{N}\times\mathbb{Z}^d.$$

We will focus on $(\xi_x)_{x\in\mathbb{Z}^d}$ being an i.i.d. field of *heavy tailed* positive random variables and we recall that we are dealing with a *quenched disordered model*, that is we are interested in the properties of the law $\mathbf{P}_N^\xi$ for $\mathbb{P}$-typical but *fixed* realizations of the potential ξ.

The relationship between this model and the famous parabolic Anderson model comes from the Feynman Kac formula which provides the solution of the parabolic Anderson equation in terms of the partition function of a continuous time random walk in a potential. We will give more details and references in Section 4.2 below, but let us mention already that, with a heavy tailed potential, the discrete and continuous versions of the PAM display some quite different features that are worth being analyzed in details.

It is also enlightening to observe that the DPAM can be viewed as a variation of the famous directed polymer in bulk disorder (see [23], [29] or [49] for a review). The latter model indeed falls into the scope of the general setting in (4.1.1–4.1.3). It is defined with a $(1+d)$-dimensional simple random walk taking steps in $\{(1,y)\colon y\in\mathbb{Z}^d, ||y||=1\}$ with probability $\frac{1}{2d}$ each and a random potential $(\xi_{i,x})_{i\in\mathbb{N},\,x\in\mathbb{Z}^d}$ that is an i.i.d. field of random variables. The directed polymer with heavy tailed bulk disorder has been considered in [1] and it is interesting to compare its features with those of the DPAM.

Random Pinning at a linear interface. This model can also be defined as a particular case of the general setting in (4.1.1–4.1.3). In section 4.4, we will focus on the one dimensional case ($d=1$) although the model can be defined in arbitrary dimension. The coupling parameter β is taken non negative. The potential is not time dependent and is given by

$$\xi_{i,x} = \begin{cases} (1+s\,\omega_i) & \text{if } x=0,\\ -\frac{h}{\beta} & \text{if } x<0,\\ 0 & \text{otherwise,}\end{cases} \tag{4.1.4}$$

where $(\omega_i)_{i\in\mathbb{N}}$ is an i.i.d. sequence of random variables and $h,s\in[0,\infty)$. By letting $h\to\infty$, we recover the $(1+1)$-dimensional *random wetting model* which consists of a random walk that can not enter the lower half-plane (hard wall) and is random pinned at the x-axis. Note that, as for the discrete PAM above, the disorder ω is quenched, i.e., sampled from $\mathbb{P}$ but fixed.

Both the random pinning and wetting models can be viewed as random perturbations of their homogeneous counterparts for which $s=0$. An historic of the literature dedicated to the homogeneous pinning and wetting models is available in [38, Section 1.10] and in [49, Chapter 7].

Finally, let us mention that one of the model considered in Section 4.4 consists of a random copolymer pinned at a layer separating two solvents. The random repartition of the monomers along the polymer can not be modeled with a potential attached to the sites of $\mathbb{N}\times\mathbb{Z}^d$. For this reason this model can not be rigorously expressed as a particular case of our general setting although the energetic rewards that are picked by the path inside

the attractive layer of width $2U$ around the x-axis correspond to a potential

$$\xi_{i,x} = \begin{cases} \gamma_i^x & \text{if } x \in \{-U, \dots, U\}, \\ 0 & \text{otherwise,} \end{cases} \tag{4.1.5}$$

where $(\gamma_i^x)_{i\in\mathbb{N},x\in\{-U,\dots,U\}}$ is an i.i.d. field of random variables.

Pinning/depinning in a dynamical multi-interface layer. The model is defined with our general setting in (4.1.1–4.1.3). We consider a simple random walk in dimension $1+1$, i.e., S takes steps $(1,1)$ and $(1,-1)$ with probability $\frac{1}{2}$ each. We impose no restriction on the coupling parameter $\beta \in \mathbb{R}$. The potential is time-dependent and is defined for $N \in \mathbb{N}$ as

$$\xi_{i,x}^N = \begin{cases} 1 & \text{if } x \in T_N\,\mathbb{Z}, \\ 0 & \text{otherwise,} \end{cases} \tag{4.1.6}$$

where $(T_N)_{N\in\mathbb{N}}$ is a non-decreasing sequence in $\mathbb{N}$. In Section 4.3, we will see that, for symmetry reasons, each result obtained with the multi-interface medium can be reexpressed as a result for a model of a random walk in a slit with attractive/repulsive walls. The latter model is again a particular case of the general setting in (4.1.1–4.1.3) but with the following potential

$$\xi_{i,x}^N = \begin{cases} 1 & \text{if } x \in \{0, T_N\}, \\ 0 & \text{if } 0 < x < T_N, \\ -\infty & \text{otherwise.} \end{cases} \tag{4.1.7}$$

The random walk in a slit with attractive/repulsive walls has been studied intensively by physicists (see [16], [65] and [71]) because it models for instance the steric/depletion stabilization phenomenon which are used to maintain the stability of a colloid by adding some ad hoc polymers in the solution.

4.1.3 Most relevant issues

When studying such models, there is a large variety of issues that are interesting from the mathematical point of view and meaningful from the physical point of view, in the sense that they allow for a deeper understanding of the phenomenon under investigation. Without been exhaustive one can classify these issues into 4 main categories, that we display below.

1) **Free energy**: the first object to be considered when working on such models is its limiting free energy, i.e.,

$$f^{\boldsymbol{\xi}}(\beta) = \lim_{N\to\infty} \frac{1}{N} \log Z_{N,\beta}^{\xi^{\mathbf{N}}}. \tag{4.1.8}$$

Note that, the existence and the finiteness of such a limit are not guaranteed a priori, especially when the potential is time-dependent or random. In the latter case, the question of the sample dependence of the free energy also raises naturally.

The free energy turns out to be a good tool to identify the *phase transitions* that the model may undergo. These transitions are indeed associated with a non analyticity of the free energy at some critical point β_c that needs to be computed or at least estimated as precisely as possible. The asymptotic of the free energy at β_c also provides key informations such as the order of the phase transition which characterizes the smoothness of this transition. Such issues will be closely considered in Section 4.4.

Generally speaking about discrete models in Satistical Mechanics, it is often interesting to identify the asymptotic of their free energy when the coupling parameters vanish. It sometimes allow to identify a limiting continuous model that is universal in the sense that it does not depend much on the fine details of the model. We will investigate this issue in Sections 4.3 and 4.4 with the copolymer randomly pinned at a selective interface.

2) Influence of a disorder: with some particular choices of deterministic potentials in (4.1.1), the model in (4.1.3) falls into the class of those exactly solvable models in Statistical Mechanics. This means, for such models, that their analytical investigation can be pushed quite far, by providing for instance an explicit expression of their free energy and of their critical point β_c, as well as a precise asymptotic of $f(\beta)$ close to β_c. These models are natural candidates to study the effect of a random perturbation of the Hamiltonian on their phase transition. Understanding how some features of a phase transition can be modified by the introduction of some small random perturbations in the interactions is a long standing and difficult issue that has been settled recently for pinning models (see [39] and [81]). In Section 4.4, we will also present a contribution in this direction.

3) Infinite volume limit: it is interesting to characterize the speed of displacement of S in the $\mathbb{Z}^d$ hyperplane. To be more specific, one has to identify $\alpha \in [0,1)$ such that the limit in law of $\frac{S_N}{N^\alpha}$ (under $\mathbf{P}^{\boldsymbol{\xi}}_{N,\beta}$) as $N \to \infty$ exists and is non trivial. Section 4.3 will be partially dedicated to the presentation of such results for the multi-interface pinning/depinning model.

In some cases, the investigation can be pushed further to obtain the *scaling limit* of the whole path. In this case, we consider the time-space rescaled process $\widetilde{S}_N$ defined as

$$\widetilde{S}_N(t) = \frac{1}{N^\alpha} S_{\lfloor t\, N \rfloor}, \quad t \in [0,1]. \tag{4.1.9}$$

The goal, then, is to identify the limiting object of $\widetilde{S}_N$ (under $\mathbf{P}^{\boldsymbol{\xi}}_{N,\beta}$) as $N \to \infty$. This object may be a deterministic curve that has to be computed or a random continuous process on $[0,1]$ whose law has to be displayed. Such questions have been answered for different models as for instance the periodic copolymer with adsorption in [22].

4) Localization of the path: one can sometimes identify the smallest set of points $\mathcal{R}_{N,\xi} \in \mathbb{Z}^d$ such that the law of S_N under $\mathbf{P}^{\boldsymbol{\xi}}_{N,\beta}$ concentrates on $\mathcal{R}_{N,\xi}$, i.e.,

$$\lim_{N\to\infty} \mathbf{P}^{\boldsymbol{\xi}}_{N,\beta}(S_N \in \mathcal{R}_{N,\xi}) = 1. \tag{4.1.10}$$

We will prove such results in Section 4.2 for the discrete PAM with $\mathcal{R}_{N,\xi}$ restricted to a unique point that can be computed explicitly.

In some cases, one can go further and prove localization of the whole path and not only of its right extremity S_N. Such results can be obtained by identifying a set of points $\mathcal{D}_{N,\xi}$ such that, under $\mathbf{P}^{\boldsymbol{\xi}}_{N,\beta}$, the excursions of the random walk away from $\mathcal{D}_{N,\xi}$ are exponentially tight. Inside its localized phase, any pinning or wetting model satisfies such property with $\mathcal{D}_{N,\xi} = \{0\}$. In Section 4.3, and with $\beta > 0$, we will prove a localization result of that type for the multiple interface pinning model with $\mathcal{D}_{N,\xi} = T_N\,\mathbb{Z}$.

4.2 The discrete parabolic Anderson model

We present in this Section the results obtained in [18] about the discrete PAM introduced in Section 4.1 above. Let us first be a little bit more specific about the definition of the model. Since the potential ξ is constant on each line $\mathbb{N}\times\{x\}$ for $x \in \mathbb{Z}^d$, we can safely omit the first coordinate of the random walk in the general setting (4.1.1–4.1.3). We will focus on $S = (S_k)_{k=0}^{\infty}$ being a (lazy) nearest-neighbor random walk on $\mathbb{Z}^d$, started at zero and such that the variables $\{S_{k+1} - S_k\}_{k\geq 0}$ are i.i.d. with $\mathrm{P}(S_1 = y) = 0$ if $|y| > 1$. We also assume the following irreducibility conditions:

$$\mathrm{P}(S_1 = 0) =: \kappa > 0 \qquad \text{and} \qquad \mathrm{P}(S_1 = y) > 0 \quad \forall y \in \mathbb{Z}^d \text{ with } |y| = 1\,. \tag{4.2.1}$$

The usual assumption $\mathrm{E}(S_1) = 0$ is not necessary and we could actually deal with random walks with finite range, i.e., for which there exists $R > 0$ such that $\mathrm{P}(S_1 = y) = 0$ if $|y| > R$, but we stick for simplicity to the case $R = 1$.

As mentioned in Section 4.1, the potential $\xi = \{\xi(x)\}_{x\in\mathbb{Z}^d}$ is an i.i.d. field of random variables that are Pareto distributed, that is

$$\mathbb{P}(\xi(0) \in \mathrm{d}x) = \frac{\alpha}{x^{1+\alpha}}\, 1_{[1,\infty)}(x)\,\mathrm{d}x\,, \tag{4.2.2}$$

for some $\alpha \in (0,\infty)$. Although the precise assumption (4.2.2) on the law of ξ could be relaxed to a certain extent, we prefer to keep it for the sake of simplicity.

4.2.1 Endpoint distribution

Intuitively, under the perturbed law $\mathbf{P}^{\xi}_{N}$, the random walk has the tendency to target those sites or groups of sites where the potential is very large. For this reason, it is useful

to introduce the endpoint law and to identify the smallest set of points in $\mathcal{B}_N := \{x \in \mathbb{Z}^d : |x| \leq N\}$ on which the endpoint of the path concentrates. Thus, given $N \in \mathbb{N}$ and a $\mathbb{P}$-typical realization of the variables $\xi = \{\xi(y)\}_{y\in\mathbb{Z}^d}$, we let

$$p_{N,\xi}(x) := \mathbf{P}_N^{\xi}(S_N = x) = \frac{u_{N,\xi}(x)}{Z_N^{\xi}}, \tag{4.2.3}$$

where the *constrained partition function* $u_{N,\xi}(x)$ is defined for $x \in \mathbb{Z}^d$ by

$$u_{N,\xi}(x) := \mathrm{E}\left[\exp\left(\sum_{i=1}^{N}\xi(S_i)\right)1_{\{S_N=x\}}\right], \tag{4.2.4}$$

so that $Z_N^{\xi} = \sum_{x\in\mathbb{Z}^d} u_{N,\xi}(x)$.

Remark 4.2.1. An alternative interpretation in terms of population growth. Our model can also be used to describe the spatial distribution of a population evolving in time. At time zero, the population consists of one individual located at the site $x = 0 \in \mathbb{Z}^d$. In each time step, every individual in the population performs one step of the random walk S, independently of all other individuals, jumping from its current site x to a site y (possibly $y = x$) and then splitting into a number of individuals (always at site y) distributed like a $\mathrm{Po}(e^{\xi(y)})$, where $\mathrm{Po}(\lambda)$ denotes the Poisson distribution of parameter $\lambda > 0$. The expected number of individuals at site $x \in \mathbb{Z}^d$ at time $N \in \mathbb{N}$ is then given by $u_{N,\xi}(x)$, as one checks easily.

4.2.2 Link with the continuous parabolic Anderson model

The closest relative of our model is obtained by considering the continuous-time analogue $\hat{u}_{t,\xi}(x)$ of (4.2.4), defined for $t \in [0,\infty)$ and $x \in \mathbb{Z}^d$ by

$$\hat{u}_{t,\xi}(x) := \mathrm{E}\left[\exp\left(\int_0^t \xi(\hat{S}_u)\,\mathrm{d}u\right)1_{\{\hat{S}_t=x\}}\right], \tag{4.2.5}$$

where $(\{\hat{S}_u\}_{u\in[0,\infty)}, \mathrm{P})$ denotes the continuous-time, simple symmetric random walk on $\mathbb{Z}^d$. One can check that the function $\hat{u}_{t,\xi}(x)$ is the solution of the following Cauchy problem:

$$\begin{cases} \frac{\partial}{\partial t}\hat{u}_{t,\xi}(x) = \Delta\hat{u}_{t,\xi}(x) + \xi(x)\,\hat{u}_{t,\xi}(x) \\ \hat{u}_{0,\xi}(x) = 1_0(x) \end{cases} \qquad \text{for } (t,x) \in (0,\infty)\times\mathbb{Z}^d,$$

known in the literature as the *parabolic Anderson problem* and introduced by P. Anderson in 1958 in the context of entrapment of electrons in crystals with impurities. Another possible interpretation is the investigation of the kinetics for a chemical reaction in the presence of a catalyst. We refer to [36, 37, 47] and references therein for deeper physical motivations behind this problem and for a survey of the main results.

The case of a potential ξ that is i.i.d. of Pareto law (like in (4.2.2)) with parameter $\alpha > d$ has been investigated in [63]. The asymptotic properties of $\hat{u}_{t,\xi}(\cdot)$ as $t \to \infty$ have been derived and it turns out that a very strong form of localization takes place, that is for large t, the function $\hat{u}_{t,\xi}(\cdot)$ is essentially concentrated at two points almost surely and at a single point in probability. More precisely, for all $t > 0$ and $\xi \in \mathbb{R}^{Z^d}$, one can exhibit $\hat{z}^{(1)}_{t,\xi}, \hat{z}^{(2)}_{t,\xi} \in \mathbb{Z}^d$, such that

$$\lim_{t\to\infty} \frac{\hat{u}_{t,\xi}(\hat{z}^{(1)}_{t,\xi}) + \hat{u}_{t,\xi}(\hat{z}^{(2)}_{t,\xi})}{\sum_{x\in\mathbb{Z}^d} \hat{u}_{t,\xi}(x)} = 1\,, \qquad \mathbb{P}\text{-almost surely}\,, \tag{4.2.6}$$

$$\lim_{t\to\infty} \frac{\hat{u}_{t,\xi}(\hat{z}^{(1)}_{t,\xi})}{\sum_{x\in\mathbb{Z}^d} \hat{u}_{t,\xi}(x)} = 1\,, \qquad \text{in } \mathbb{P}\text{-probability}\,, \tag{4.2.7}$$

cf. [63, Theorems 1.1 and 1.2]. The points $\hat{z}^{(1)}_{t,\xi}, \hat{z}^{(2)}_{t,\xi}$ are typically at superballistic distance $(t/\log t)^{1+q}$ with $q = d/(\alpha - d) > 0$, cf. [63, Remark 6]. We point out that localization at one point like in (4.2.7) cannot hold $\mathbb{P}$-almost surely, that is, the contribution of $\hat{z}^{(2)}_{t,\xi}$ cannot be removed from (4.2.6): this is due to the fact that $\hat{u}_{t,\xi}(x)$ is a continuous function of t for every fixed $x \in \mathbb{Z}^d$, as explained in [63, Remark 1].

4.2.3 The main results

Generally speaking, models built over discrete-time or continuous-time simple random walks are not expected to be very different. This is however clearly not true for the PAM with a heavy tailed potential, simply because the localization points $\hat{z}^{(1)}_{t,\xi}, \hat{z}^{(2)}_{t,\xi}$ of the continuous-time model grow at a superballistic speed, a feature that is clearly impossible for the discrete-time model, for which $u_{N,\xi}(x) \equiv 0$ for $|x| > N$. For this reason, we decided to have a closer look in [18] at the asymptotic localization of the endpoint of the path for the discrete model. This is the object of Theorems and Propositions (4.3.3–4.2.5) below, in which we prove that, for $\mathbb{P}$-a.e. ξ, the localization occurs asymptotically at a unique site $\mathrm{w}_{N,\xi}$ (Theorem 4.3.3) and that, for $\mathbb{P}$-a.e. ξ, this unique localization site $\mathrm{w}_{N,\xi}$ belongs to a two-points set $\{z^{(1)}_{N,\xi}, z^{(2)}_{N,\xi}\}$ that can be computed explicitly (Theorem 4.2.3). When simply requiring a convergence in probability instead of a $\mathbb{P}$ almost sure convergence, the two points set can be restricted to the unique site $z^{(1)}_{N,\xi}$ (Theorem 4.2.3), although, at least in dimension one, the probability that $\mathrm{w}_{N,\xi} = z^{(2)}_{N,\xi}$ for infinitely many $N \in \mathbb{N}$ is equal to 1 (Proposition 4.2.5).

Later on, we will state some localization results for the whole path. We will identify a very narrowed set of trajectories $\mathcal{C}_{N,\xi}$ that, $\mathbb{P}(\mathrm{d}\xi)$-almost surely, concentrates asymptotically the whole mass of $\mathbf{P}^{\xi}_N$ (Theorem 4.2.6) and we will even prove that in dimension 1 the subset $C_{N,\xi}$ can be restricted to a unique explicit trajectory.

Another important point about our work in [18] is that the technics of proof that have been used are much simpler and more direct than the technics used in [63] for the continuous-time model. The proof of two-sites localization given in [63] indeed exploits tools from potential theory and spectral analysis. Such tools can be applied also in the discrete-time setting, but they turn out to be unnecessary. Our proof is indeed based on shorter and simpler geometric arguments. For instance, we exploit the fact that before reaching a site $x \in \mathbb{Z}^d$ a discrete-time random walk path must visit a least $|x| - 1$ different sites ($\neq x$) and spend at each of them a least one time unit. Of course, this is no longer true for continuous-time random walks.

Endpoint asymptotic localization

Let us settle some notations before stating the results from [18]. We recall that $\mathcal{B}_N := \{x \in \mathbb{Z}^d : |x| \leq N\}$. It is not difficult to check that the values $\{p_{N,\xi}(x)\}_{x\in\mathcal{B}_N}$ are all distinct, for $\mathbb{P}$-a.e. ξ and for all $N \in \mathbb{N}$, because the potential distribution is continuous, cf. (4.2.2). Therefore we can safely set

$$\mathrm{w}_{N,\xi} := \arg\max\big\{p_{N,\xi}(x) : \ x \in \mathcal{B}_N\big\}\,, \tag{4.2.8}$$

which, $\mathbb{P}$-almost surely, is defined uniquely and represents the point at which $p_{N,\xi}(\cdot)$ attains its maximum. We can now state our first main result.

Theorem 4.2.2 (One-site localization)**.** *We have*

$$\lim_{N\to\infty} p_{N,\xi}(\mathrm{w}_{N,\xi}) \,=\, \lim_{N\to\infty} \frac{u_{N,\xi}(\mathrm{w}_{N,\xi})}{\sum_{x\in\mathbb{Z}^d} u_{N,\xi}(x)} \,=\, 1\,, \qquad \mathbb{P}(\mathrm{d}\xi)\text{-}\textit{almost surely}\,. \tag{4.2.9}$$

Furthermore, as $N \to \infty$ we have the following convergence in distribution:

$$\frac{\mathrm{w}_{N,\xi}}{N} \implies \mathrm{w}\,, \qquad \textit{where} \qquad \mathbb{P}(\mathrm{w} \in \mathrm{d}x) \,=\, c_\alpha\,(1-|x|)^\alpha\,1_{\{|x|\leq 1\}}\,\mathrm{d}x\,, \tag{4.2.10}$$

and $c_\alpha := (\int_{|y|\leq 1}(1-|y|)^\alpha \mathrm{d}y)^{-1}$.

Recalling the definition (4.2.3) of $p_{N,\xi}(x)$, Theorem 4.3.3 shows that S_N under $\mathbf{P}_{N,\xi}$ is localized at the ballistic point $\mathrm{w}_{N,\xi} \approx \mathrm{w}\cdot N$.

Next we look more closely at the localization site $\mathrm{w}_{N,\xi}$. We introduce two points $z^{(1)}_{N,\xi}, z^{(2)}_{N,\xi} \in \mathbb{Z}^d$, defined explicitly in terms of the potential ξ, through

$$\begin{aligned} z^{(1)}_{N,\xi} &:= \arg\max\Big\{\Big(1-\tfrac{|x|}{N+1}\Big)\,\xi(x) \ : \ x \in \mathcal{B}_N\Big\}\,,\\ z^{(2)}_{N,\xi} &:= \arg\max\Big\{\Big(1-\tfrac{|x|}{N+1}\Big)\,\xi(x) \ : \ x \in \mathcal{B}_N \setminus \big\{z^{(1)}_{N,\xi}\big\}\Big\}\,. \end{aligned} \tag{4.2.11}$$

Again, the values of $\{(1-\frac{|x|}{N+1})\xi(x)\}_{x\in\mathcal{B}_N}$ are $\mathbb{P}$-a.s. distinct, by the continuity of the potential distribution, therefore $z^{(1)}_{N,\xi}$ and $z^{(2)}_{N,\xi}$ are $\mathbb{P}$-a.s. single points in $\mathcal{B}_N$.

Note that the prefactor $(1 - \frac{|x|}{N+1})$ in front of $\xi(x)$ in the definition (4.2.11) can easily be understood. A site $x \in \mathcal{B}_N$ can indeed not be visited more than $N+1-|x|$ times by an N-step trajectory and therefore, the contribution of $\xi(x)$ to the Hamiltonian of any N-step trajectory S is bounded above by $(N+1-|x|)\xi(x)$. Thus, a site x associated with a large potential ξ_x but located close to the boundary of $\mathcal{B}_N$ sees its attractivity drastically lowered, which justifies the introduction of an effective potential given by $\{(1 - \frac{|x|}{N+1})\xi(x)\}_{x\in\mathcal{B}_N}$.

We can now give the discrete-time analogues of (4.2.6) and (4.2.7).

Theorem 4.2.3 (Two-sites localization)**.** *The following relations hold:*

$$\lim_{N\to\infty} \Big(p_{N,\xi}\big(z^{(1)}_{N,\xi}\big) + p_{N,\xi}\big(z^{(2)}_{N,\xi}\big) \Big) \,=\, 1 \qquad \mathbb{P}(\mathrm{d}\xi)\text{-}\textit{almost surely}\,, \tag{4.2.12}$$

$$\lim_{N\to\infty} p_{N,\xi}\big(z^{(1)}_{N,\xi}\big) \,=\, 1 \qquad \textit{in } \mathbb{P}(\mathrm{d}\xi)\text{-}\textit{probability}\,. \tag{4.2.13}$$

Putting together Theorems 4.2.2 and 4.2.3, we obtain the following information on $\mathrm{w}_{N,\xi}$.

Corollary 4.2.4. *For $\mathbb{P}$-a.e. ξ, we have $\mathrm{w}_{N,\xi} \in \{z^{(1)}_{N,\xi}, z^{(2)}_{N,\xi}\}$ for large N. Furthermore,*

$$\lim_{N\to\infty} \mathbb{P}\left(\mathrm{w}_{N,\xi} = z^{(1)}_{N,\xi}\right) \,=\, 1\,. \tag{4.2.14}$$

In Proposition 4.2.5 below, we stress that the convergence in (4.2.13) does not occur $\mathbb{P}(\mathrm{d}\xi)$-almost surely in dimension $d = 1$, i.e., $\mathrm{w}_{N,\xi}$ is not equal to $z^{(1)}_N$ for all N large enough. We strongly believe that the latter remains true for $d > 1$.

Proposition 4.2.5. *In dimension $d = 1$, we have*

$$\mathbb{P}\left(\mathrm{w}_{N,\xi} = z^{(2)}_{N,\xi} \textit{ for infinitely many } N\right) \,=\, 1\,. \tag{4.2.15}$$

Further path properties

Theorem 4.3.3 states that $\mathbb{P}(\mathrm{d}\xi)$-a.s. the probability measure $\mathbf{P}^{\xi}_N$ concentrates on the subset gathering those random walk trajectories S such that $S_N = \mathrm{w}_{N,\xi}$. It turns out that this subset can be radically narrowed. In fact, we can introduce a restricted subset $\mathcal{C}_{N,\xi}$ of random walk trajectories, defined as follows:

- the trajectories in $\mathcal{C}_{N,\xi}$ must reach the site $\mathrm{w}_{N,\xi}$ for the first time before time N, following an injective path, and then must remain at $\mathrm{w}_{N,\xi}$ until time N;
- the length of the injective path until $\mathrm{w}_{N,\xi}$ differs from $|\mathrm{w}_{N,\xi}|$ (which is the minimal one) at most for a small error term $h_N := (\log\log N)^{2/\alpha}\, N^{1-1/\alpha}$ if $\alpha > 1$ and $h_N := (\log N)^{1+2/\alpha}$ if $\alpha \le 1$ (note that in any case $h_N = o(N)$);
- all the sites x visited by the random walk before reaching $\mathrm{w}_{N,\xi}$ must have an associated field $\xi(x)$ that is strictly smaller than $\xi(\mathrm{w}_{N,\xi})$.

More formally, denoting by $\tau_x = \tau_x(S) := \inf\{n \geq 0 \colon S_n = x\}$ the first passage time at $x \in \mathbb{Z}^d$ of a random walk trajectory S, we set

$$\begin{aligned} \mathcal{C}_{N,\xi} := \Big\{ S \in \Omega_S \colon\ & S_i \neq S_j \ \forall i < j \leq \tau_{\mathrm{w}_{N,\xi}}\,,\ S_i = \mathrm{w}_{N,\xi} \ \forall i \in \{\tau_{\mathrm{w}_{N,\xi}}, \dots, N\}\,, \\ & \xi(S_i) < \xi(\mathrm{w}_{N,\xi}) \ \forall i < \tau_{w_{N,\xi}}\,,\ \tau_{\mathrm{w}_{N,\xi}} \leq |\mathrm{w}_{N,\xi}| + h_N \Big\}\,. \end{aligned} \tag{4.2.16}$$

We then have the following result.

Theorem 4.2.6. *For $\mathbb{P}$-a.e. ξ, we have*

$$\lim_{N\to\infty} \mathbf{P}_{N,\xi}(\mathcal{C}_{N,\xi}) = 1. \tag{4.2.17}$$

Remark 4.2.7. It is worth stressing that in dimension $d = 1$ the set $\mathcal{C}_{N,\xi}$ reduces to *a single N-steps trajectory*. In fact, we have $\mathcal{C}_{N,\xi} = \mathcal{S}^{(N,\mathrm{w}_{N,\xi})}$, where we denote by $\mathcal{S}^{(N,x)}$, for $x \in \mathcal{B}_N$, the set of those trajectories S such that

$$S_i := \begin{cases} i \cdot \mathrm{sign}(x) & \text{for } 0 \leq i \leq |x| \\ x & \text{for } |x| \leq i \leq N \end{cases}.$$

As stated in Corollary 4.2.4, for large N the site $\mathrm{w}_{N,\xi}$ is either $z^{(1)}_{N,\xi}$ or $z^{(2)}_{N,\xi}$. Note that $z^{(1)}_{N,\xi}$ and $z^{(2)}_{N,\xi}$ are easily determined, by (4.2.11). In order to decide whether $\mathrm{w}_{N,\xi} = z^{(1)}_{N,\xi}$ or $\mathrm{w}_{N,\xi} = z^{(2)}_{N,\xi}$, by Theorem 4.2.6 it is sufficient to compare the explicit contributions of just two trajectories, i.e., $\mathbf{P}_{N,\xi}(\mathcal{S}^{(N,z^{(1)}_{N,\xi})})$ and $\mathbf{P}_{N,\xi}(\mathcal{S}^{(N,z^{(2)}_{N,\xi})})$. More precisely, setting $\kappa(i) := \mathrm{P}(S_1 = i)$ for $i \in \{\pm 1, 0\}$ (so that $\kappa = \kappa(0)$, cf. (4.2.1)) and

$$b_{N,\xi}(x) := e^{\sum_{i=1}^{|x|-1} \xi(i\,\mathrm{sign}(x)) + (N+1-|x|)\xi(x)} \kappa(\mathrm{sign}(x))^{|x|} \kappa(0)^{N-|x|}\,,$$

we have $w_{N,\xi} = z^{(1)}_{N,\xi}$ if $b_{N,\xi}(z^{(1)}_{N,\xi}) > b_{N,\xi}(z^{(2)}_{N,\xi})$ and $w_{N,\xi} = z^{(2)}_{N,\xi}$ otherwise. Therefore, in dimension $d = 1$, we have a very explicit characterization of the localization point $\mathrm{w}_{N,\xi}$.

Remark 4.2.8. As mentioned in section 4.1.2, our model is somewhat close in spirit to the much studied *directed polymer in random environment*, in which the rewards $\xi(i, x)$ depend also on $i \in \mathbb{N}$ (and are usually chosen to be jointly i.i.d.). In our model, the rewards are constant in the "deterministic direction" $(1, 0)$, a feature which makes the environment much more attractive from a localization viewpoint because a site x with a large reward $\xi(x)$ yields a favorable straight corridor $\{0, \dots, N\} \times \{x\}$ for the polymer $\{(i, S_i)\}_{0\leq i\leq N}$. This can be illustrated by comparing the "localization power" of the energetically optimal trajectory (the one that maximizes $\sum_{i=1}^N \xi(S_i)$) for the discrete PAM with the "localization power" of its counterpart (the one that maximizes $\sum_{i=1}^N \xi(i, S_i)$) for the directed polymer with bulk disorder. It is indeed proven in [1] for the directed polymer model with a "very heavy tailed" random environment (Pareto distributed with $\alpha < 2$) that, in any dimension,

and for any $\delta > 0$, the polymer of size N remains, with probability $1 - e^{-c_\delta N}$ ($c_\delta > 0$), in a cylinder of width δN around the optimal trajectory. For the discrete PAM, in turn, the polymer stay with a probability that converges to 1 at a distance smaller than $h(N)$ (recall the definition above (4.2.16)) from the optimal trajectory and in dimension 1 is even equal to this optimal trajectory.

4.3 Polymer pinning/depinning in a multi-interface medium

As mentioned in Section 4.1.1, the present Section is dedicated to a model for a (1+1)-dimensional simple random walk interacting with infinitely many horizontal interfaces. The coupling constant will be denoted by $\delta \in \mathbb{R}$ (instead of β in the general setting) so that our notations match with those in the two papers [24] and [25] that are concerned with this model.

Pick $T \in \mathbb{N}$ that gives the distance between two consecutive interfaces and the interaction between the random walk and the medium is described by the following Hamiltonian:

$$H_{N,\delta}^T(S) \;:=\; \delta \sum_{i=1}^N 1_{\{S_i \in T\mathbb{Z}\}} \;=\; \delta \sum_{k\in\mathbb{Z}} \sum_{i=1}^N 1_{\{S_i = k\,T\}}, \tag{4.3.1}$$

where $N \in \mathbb{N}$ is the size of the polymer and $\delta \in \mathbb{R}$ is the intensity of the energetic reward (if $\delta > 0$) or penalty (if $\delta < 0$) that the polymer receives when touching the interfaces (see Figure 4.1). More precisely, the model is defined by the following probability law $\mathbf{P}_{N,\delta}^T$ on $\mathbb{R}^{\mathbb{N}\cup\{0\}}$:

$$\frac{\mathrm{d}\mathbf{P}_{N,\delta}^T}{\mathrm{d}\mathbf{P}}(S) \;:=\; \frac{\exp\big(H_{N,\delta}^T(S)\big)}{Z_{N,\delta}^T}, \tag{4.3.2}$$

where $Z_{N,\delta}^T = \mathbf{E}\big(\exp(H_{N,\delta}^T(S))\big)$ is the *partition function*. Note finally that, by picking $T = \infty$, the model defined by (4.3.1) and (4.3.2) is nothing but the simple random walk pinned at a unique linear line $\mathbb{N} \times \{0\}$, which is well studied now (cf. [38, Chapter 2]) and displays a phase transition at $\delta = 0$.

We are interested in media that are evoluting in time, meaning that the distance T between two consecutive interfaces grows with the system size N. Thus, we let $\mathbf{T} := (T_N)_{N\in\mathbb{N}}$ be a non decreasing sequence and we assume, for simplicity, that $T_N \in 2\mathbb{N}$ for all $N \in \mathbb{N}$. As a consequence, the sequence T_N converges towards either $T_\infty = \infty$ or $T_\infty \in 2\mathbb{N}$ and in this latter case $T_N = T_\infty$ for N large enough.

In Section 4.3.1 below we will investigate the limiting free energy of the system and see whether the growth speed of sequence $\mathbf{T}$ has an influence on the phase transition of the system or not. In Section 4.3.2 we will focus on the vertical growth speed of the right extremity of the path (S_N) depending on the coupling parameter δ and on the growth speed of $\mathbf{T}$.

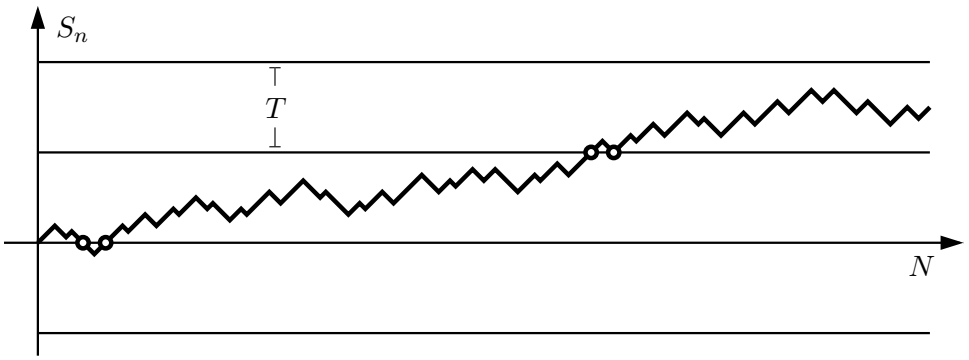

Figure 4.1: An example of a path $\{S_n\}_{0\le n\le N}$ under the polymer measure $\mathbf{P}^T_{N,\delta}$, for $N = 158$ and $T = 16$. The circles indicate the points where the polymer touches the interfaces, that are penalized by $\delta < 0$ each.

4.3.1 Analysis of the free energy

The standard way of studying the effect of the interaction (4.3.1) for large N is to look at the *free energy* of the model, defined as the limit

$$\phi(\delta, \boldsymbol{T}) \;:=\; \lim_{N\to\infty} \phi_N(\delta, \boldsymbol{T})\,, \qquad \text{where} \qquad \phi_N(\delta, \boldsymbol{T}) \;:=\; \frac{1}{N}\log Z^{T_N}_{N,\delta}\,. \tag{4.3.3}$$

The importance of the free energy can be illustrated by the fact that, as soon as $\phi(\delta, \boldsymbol{T})$ is differentiable, its first derivative with respect to δ gives the asymptotic contact fraction between the polymer and the interfaces, i.e., $\frac{\partial}{\partial\delta}\phi(\delta, \boldsymbol{T}) \;=\; \lim_{N\to\infty} \mathbf{E}^{T_N}_{N,\delta}\Big(\frac{\sum_{i=1}^N 1_{\{S_i\in T_N\mathbb{Z}\}}}{N}\Big)$. Intuitively and by analogy with what is known for the single interface model, if a phase transition occurs, it should be between a phase where the asymptotic proportion of time spent by the polymer on the interfaces is strictly positive and another one where it is 0.

It turns out that $\phi(\delta, \mathbf{T})$ can be computed explicitly for all choices of δ and $\mathbf{T}$. This is addressed by Theorem 4.3.1 below, after introducing for $T \in 2\mathbb{N}\cup\{+\infty\}$ the random variable τ^T_1 defined by

$$\tau^T_1 \;:=\; \inf\big\{n > 0 :\; S_n \in \{-T, 0, +T\}\big\}\,, \tag{4.3.4}$$

and after denoting by $Q_T(\lambda)$ its Laplace transform under the simple random walk law $\mathbf{P}$:

$$Q_T(\lambda) \;:=\; \mathbf{E}\big(e^{-\lambda\tau^T_1}\big) \;=\; \sum_{n=1}^{\infty} e^{-\lambda n}\,\mathbf{P}\big(\tau^T_1 = n\big)\,. \tag{4.3.5}$$

Theorem 4.3.1. ([24], Theorem 1). *Denoting by $T_\infty = \lim_{N\to\infty} T_N$, the free energy $\phi(\delta, \boldsymbol{T}) = \phi(\delta, T_\infty)$ depends only on δ and T_∞ and is given by*

$$\phi(\delta, T_\infty) \;=\; \begin{cases} \big(Q_{T_\infty}\big)^{-1}(e^{-\delta}) & \text{if } T_\infty < +\infty \\ \big(Q_\infty\big)^{-1}(e^{-\delta}\wedge 1) & \text{if } T_\infty = +\infty\,. \end{cases} \tag{4.3.6}$$

It follows that for $T_\infty < +\infty$ the function $\delta \mapsto \phi(\delta, \boldsymbol{T})$ is analytic on the whole real line, while for $T_\infty = +\infty$ it is not analytic only at $\delta = 0$.

Let us explain in a few words how Theorem 4.3.1 is proven. First of all, we recall from [24, Section 2.2] that

- for $T < \infty$, there exists a $\lambda_0^T < 0$ such that Q_T is finite on (λ_0^T, ∞) only and is an analytic one to one correspondence between (λ_0^T, ∞) and $(0, \infty)$.
- Q_∞ is finite on $[0, \infty)$ only and is an (analytic on $(0, \infty)$) one to one correspondence between $[0, \infty)$ and $(0, 1]$.

A straightforward consequence is that for $\delta < 0$ and $T_\infty = \infty$ we have $(Q_\infty)^{-1}(e^{-\delta} \wedge 1) = 0$ and therefore it suffices to check that the limiting entropy per step carried by the trajectories in $\{(S_i)_{i=0}^N \colon 1 \le S_i \le T_N - 1 \ \forall i \in \{1, N\}\}$ is null to complete the proof of the theorem.

For the other cases, i.e., ($\delta > 0$) or ($\delta < 0$ and $T_\infty < \infty$), we admit for simplicity (but this is not hard to prove) that the limiting free energy in (4.3.3) remains the same if we restrict the partition function to those trajectories with an endpoint S_N that lies in $T_N\mathbb{Z}$. Therefore, we only consider $N \in 2\mathbb{N}$ (since $T_N \in 2\mathbb{N}$ and S_N and N have the same parity) and we denote by $Z_{N,\delta}^{T_N,c}$ the restricted partition function. At this stage, we decompose the path into excursions away from the set $T_N\mathbb{Z}$ which allows us to rewrite the partition function $Z_{N,\delta}^{T_N,c}$ with the help of an underlying renewal process on $\mathbb{N}$ whose inter-arrivals follow the law (recall (4.3.4) and (4.3.5))

$$\mathcal{P}_{\delta,T_N}(n) = e^{\delta}\, \mathbf{P}\big(\tau_1^{T_N} = n\big) e^{-\lambda_{\delta,T_N} n},$$

where $\lambda_{\delta,T_N} = (Q_{T_N})^{-1}(e^{-\delta})$ exists in $\mathbb{R}$ by the properties of Q_T mentioned above. The partition function becomes

$$Z_{N,\delta}^{T_N,c} = e^{\lambda_{\delta,T_N}} \mathcal{P}_{\delta,T_N}(N \in \tau), \tag{4.3.7}$$

and it remains to observe that $\lim_{N\to\infty} \lambda_{\delta,T_N} = Q_{T_\infty}(e^{-\delta})$, which is clearly the case when $T_\infty < \infty$ and is proven in [24, Lemma 4] for $\delta > 0$ and $T_\infty = \infty$. Completing the proof requires to prove that the exponential growth rate of $\mathcal{P}_{\delta,T_N}(N \in \tau)$ is null, and this is a straightforward application of the renewal theorem when $T_\infty < \infty$ while a uniform version of this theorem is needed for $\delta > 0$ and $T_\infty = \infty$.

A straightforward consequence of Theorem 4.3.1 is that there is a phase transition in our model only when $T_\infty = +\infty$, in which case $\phi(\delta, \infty)$ is not analytic at $\delta = 0$. This fact is well-known, because $\phi(\delta, \infty)$ is nothing but the free energy of the classical homogeneous pinning model $\mathbf{P}_{N,\delta}^{\infty}$, cf. [38]. One consequence of Theorem 4.3.1 is that any $\boldsymbol{T}$ such that $T_\infty = \infty$ yields *the same free energy* $\phi(\delta, \boldsymbol{T}) = \phi(\delta, \infty)$ as the classical homogeneous

pinning model. However we are going to see that the actual path behavior of $\mathbf{P}_{N,\delta}^{T_N}$ as $N \to \infty$ depends strongly on the speed at which $T_N \to \infty$, a phenomenon which is not caught by the free energy.

4.3.2 Scaling limit of the path

The scaling limit of S_N in the depinning case turns out to be harder to obtain than its counterpart in the pinning case. For this reason we will treat separately the case $\delta > 0$ and $\delta < 0$. However, the following heuristic consideration holds true in both cases. As long as $(T_N)_{N\in\mathbb{N}}$ does not grow to fast, that is $T_N \ll g(N)$ where $(g(N))_{N\in\mathbb{N}}$ is a threshold speed to be determined, the number of jumps $h_N(S)$ made by a path S (under $\mathbf{P}_{N,\delta}^{T_N}$) between neighboring interfaces up to time N should typically diverge with N and therefore the number of different interfaces visited by S before time N should diverge as well. Moreover, we can denote by $(Y_i)_{i=0}^{h_N(S)}$ the simple random walk on $\mathbb{Z}$ which increases (respectively decreases) by one unit every time S jumps to the neighboring interface above (resp. below) the one it visited before. We can then safely write $S_N = Y_{h_N} T_N + O(T_N)$. The fact that, the process of jumps between neighboring interfaces may be viewed as an auxiliary renewal process let us hope that, at least as long as $T_N \ll g(N)$, $h_N(S)$ satisfies a weak law of large number, that is we can identify a deterministic increasing sequence $(v(N))_{N\in\mathbb{N}}$ such that $\lim_{N\to\infty} \mathbf{P}_{N,\delta}^{T_N}(|\frac{h_N(S)}{v(N)} - 1| \geq \varepsilon) = 0$ for all $\varepsilon > 0$. But at this stage, we can safely apply the standard central limit theorem to $(Y_i)_{i=0}^{h_N(S)}$ and obtain that

$$\lim_{N\to\infty} \frac{S_N}{T_N\sqrt{v_N}} =_{P_{N,\delta}^{T_N}} \mathcal{N}(0,1).$$

When, $T_N \gg g(N)$, in turn, the polymer should typically not manage to reach any interface except the one at the origin.

At this stage, it appears clearly that the key objects to be determined are the two sequences $(g_N)_{N\in\mathbb{N}}$ and $(v_N)_{N\in\mathbb{N}}$ which both will be related to the typical time $R(\delta, T_N)$ needed by the polymer to hop from an interface to one of its neighbors under $\mathbf{P}_{N,\delta}^{T_N}$.

The pinning case

We focus on the case $\delta > 0$. As mentioned previously, the characteristic time required to reach a neighboring interface $R(\delta, T_N)$ is of crucial importance to determine $(g_N)_{N\in\mathbb{N}}$ and $(v_N)_{N\in\mathbb{N}}$. We obtain in [24] that $R(\delta, T)$ grows exponentially with T as $e^{c_\delta T}$ where $c_\delta := \frac{\delta}{2} + \log\sqrt{2 - e^{-\delta}}$ which yields $g(N) = \frac{\log N}{c_\delta}$ and $v(N) \approx N e^{-c_\delta T_N}$. With Theorem 4.3.2 below, we make these heuristics rigorous.

Theorem 4.3.2. *Let $\delta > 0$ and $\boldsymbol{T} = (T_N)_{N\in\mathbb{N}}$ such that $T_N \to \infty$ as $N \to \infty$.*

(i) If $T_N - \frac{\log N}{c_\delta} \to -\infty$ *as* $N \to \infty$*, then under* $\mathbf{P}_{N,\delta}^{T_N}$ *as* $N \to \infty$

$$\frac{S_N}{C_\delta \left(e^{-\frac{c_\delta}{2} T_N}\, T_N\right) \sqrt{N}} \implies \mathcal{N}(0,1)\,, \tag{4.3.8}$$

where $C_\delta := (1 - e^{-\delta})\sqrt{\frac{2e^\delta}{2-e^{-\delta}}}$ *is an explicit positive constant.*

(ii) If there exists $\zeta \in \mathbb{R}$ *such that* $T_{N'} - \frac{\log N'}{c_\delta} \to \zeta$ *along a sub-sequence* N'*, then under* $\mathbf{P}_{N',\delta}^{T_{N'}}$ *as* $N' \to \infty$

$$\frac{S_{N'}}{T_{N'}} \implies S_\Gamma\,, \tag{4.3.9}$$

where Γ *is a random variable independent of the* $\{S_i\}_{i\geq 0}$ *and with a Poisson law of parameter* $t_{\delta,\zeta} := 2e^\delta \frac{(1-e^{-\delta})^2}{2-e^{-\delta}} \cdot e^{-c_\delta \zeta}$.

(iii) If $T_N - \frac{\log N}{c_\delta} \to +\infty$ *as* $N \to \infty$*, then the family of laws of* $\{S_N\}_{N\in\mathbb{N}}$ *under* $\mathbf{P}_{N,\delta}^{T_N}$ *is tight, i.e.,*

$$\lim_{L\to\infty} \sup_{N\in\mathbb{N}} \mathbf{P}_{N,\delta}^{T_N}\big(|S_N| > L\big) \;=\; 0\,. \tag{4.3.10}$$

Let us make a few comment about the statements of the Theorem.

- The statement in case (i) holds true also when $T_N \equiv T < \infty$ for all $N \in \mathbb{N}$. This situation is not included in Theorem 4.3.2 for notational convenience, but a straightforward adaptation of our proof shows that in this case $S_N/(\mathcal{C}_T\sqrt{N}) \Longrightarrow \mathcal{N}(0,1)$ for a suitable $\mathcal{C}_T$ satisfying $\mathcal{C}_T \sim C_\delta\, e^{-\frac{c_\delta}{2}T}\, T$ as $T \to \infty$, thus matching perfectly with (4.3.11). Still in case (i), we note that, independently of $(T_N)_N$ (such that $\Delta_N \to -\infty$), the limit law of S_N, properly rescaled, is always the standard Normal distribution. However the scaling constants $\left(e^{-\frac{c_\delta}{2}T_N}\, T_N\right)\sqrt{N}$ do depend on the sequence $(T_N)_N$ and in particular they are *sub-diffusive* as soon as $T_N \to \infty$. Also notice that, by varying T_N from $O(1)$ to the critical case $\frac{\log(N)}{c_\delta} + O(1)$, the scaling constants decrease smoothly from $\sqrt{N}$ to $\log N$.

- Concerning point (ii), the reason for considering subsequences satisfying $T_{N'} - \frac{\log N'}{c_\delta} \to \zeta$ with $\zeta \in \mathbb{R}$ is because T_N takes integer values and therefore the full sequence $T_N - \frac{\log N}{c_\delta}$ cannot have a finite limit. In general, equation (4.3.9) implies that S_N/T_N is tight when the full sequence $|T_N - \frac{\log N}{c_\delta}|$ is bounded. In case (ii), we consider the case in which T_N grows exactly at the critical speed $\frac{\log(N)}{c_\delta}$ at which the polymer visits a finite number of different interfaces and therefore the scaling behavior of S_N is the same as T_N, i.e., $S_N \approx \log N$. The explicit form S_Γ of the scaling distribution has the following interpretation: the number Γ of different interfaces visited by the polymer is distributed according to a Poisson law and, conditionally on Γ, the polymer just performs Γ steps of a simple symmetric random walk on the interfaces.

- In case (iii), then the only interface visited by the polymer is the x-axis. The other interfaces are indeed too distant from the origin to be convenient for the polymer to visit them. Therefore, the model $\mathbf{P}_{N,\delta}^{T_N}$ becomes essentially the same as the classical homogeneous pinning model $\mathbf{P}_{N,\delta}^{\infty}$, where only the interface located at $S = 0$ is present. Since $\delta > 0$, we are in the localized regime for $\mathbf{P}_{N,\delta}^{\infty}$ and it is well-known that $S_N = O(1)$.

The depinning case

We focus on the case $\delta < 0$. We obtain in [25] that $R(\delta, T)$, i.e., the hopping time between neighboring interfaces for $T < \infty$, grows as T^3 when $T \to \infty$. Thus, $g(N) = N^{1/3}$ and $v(N) \approx N/T_N^3$. We state rigorously the scaling limits of S_N in the different growth regime of $\mathbf{T}$ in Theorem 4.3.3 below.

Note that, for the ease of notation and for $(a_N)_{N\in\mathbb{N}}$ a non-decreasing sequence of positive numbers, we will write $S_N \asymp a_N$ if $(S_N/a_N)_{N\in\mathbb{N}}$ is tight and if there exists $\eta > 0$ and $\rho > 0$ such that $\mathbf{P}_{N,\delta}^{T_N}(|\frac{S_N}{a_N}| \geq \eta) > \rho$ for N large enough.

Theorem 4.3.3. *Let $\delta < 0$ and $\{T_N\}_{N\in\mathbb{N}} \in (2\mathbb{N})^{\mathbb{N}}$ be such that $T_N \to \infty$ as $N \to \infty$.*

(i) If $T_N \ll N^{1/3}$, then $S_N \asymp \sqrt{N/T_N}$. More precisely, there exist two constants $0 < c_1 < c_2 < \infty$ such that for all $a, b \in \mathbb{R}$ with $a < b$ we have for N large enough

$$c_1\, P\big[a < Z \leq b\big] \;\leq\; \mathbf{P}_{N,\delta}^{T_N}\left(a < \frac{S_N}{C_\delta \sqrt{\frac{N}{T_N}}} \leq b\right) \;\leq\; c_2\, P\big[a < Z \leq b\big]\,, \qquad (4.3.11)$$

where $C_\delta := \pi/\sqrt{e^{-\delta} - 1}$ is an explicit positive constant and $Z \sim \mathcal{N}(0,1)$.

(ii) If $T_N \sim (const.)N^{1/3}$, then $S_N \asymp T_N$. More precisely, for every $\varepsilon > 0$ small enough there exist constants $M, \eta > 0$ such that $\forall N \in \mathbb{N}$

$$\mathbf{P}_{N,\delta}^{T_N}\big(|S_N| \leq M\, T_N\big) \;\geq\; 1 - \varepsilon\,, \qquad \mathbf{P}_{N,\delta}^{T_N}\big(|S_N| \geq \eta\, T_N\big) \;\geq\; 1 - \varepsilon\,. \qquad (4.3.12)$$

(iii) If $N^{1/3} \ll T_N \leq (const.)\sqrt{N}$, then $S_N \asymp T_N$. More precisely, for every $\varepsilon > 0$ small enough there exist constants $L, \eta > 0$ such that $\forall N \in \mathbb{N}$

$$\mathbf{P}_{N,\delta}^{T_N}\big(0 < |S_n| < T_N\,,\ \forall n \in \{L, \dots, N\}\big) \;\geq\; 1 - \varepsilon\,, \qquad \mathbf{P}_{N,\delta}^{T_N}\big(|S_N| \geq \eta\, T_N\big) \;\geq\; 1 - \varepsilon\,. \qquad (4.3.13)$$

(iv) If $T_N \gg \sqrt{N}$, then $S_N \asymp \sqrt{N}$. More precisely, for every $\varepsilon > 0$ small enough there exist constants $L, M, \eta > 0$ such that $\forall N \in \mathbb{N}$

$$\mathbf{P}_{N,\delta}^{T_N}\big(0 < |S_n| < M\sqrt{N}\,,\ \forall n \in \{L, \dots, N\}\big) \;\geq\; 1-\varepsilon\,, \qquad \mathbf{P}_{N,\delta}^{T_N}\big(|S_N| \geq \eta\sqrt{N}\big) \;\geq\; 1-\varepsilon\,. \qquad (4.3.14)$$

We can give an alternative and somehow more intuitive way of presenting the scaling results from Theorem 4.3.3. To that aim we consider the concrete example $T_N \sim (const.)N^a$: in this case we have

$$S_N \asymp \begin{cases} N^{(1-a)/2} & \text{if } 0 \le a \le \frac{1}{3} \\ N^a & \text{if } \frac{1}{3} \le a \le \frac{1}{2} \\ N^{1/2} & \text{if } a \ge \frac{1}{2} \end{cases} . \tag{4.3.15}$$

Thus, we surprisingly observe that, as the growth speed of T_N increases, in a first time (until $a = \frac{1}{3}$) the scaling of S_N decreases, reaching a minimum $N^{1/3}$, after which it increases to reattain the initial value $N^{1/2}$, for $a \ge \frac{1}{2}$. As a consequence, we can tell that the asymptotic behavior of our model displays two transitions, at $T_N \approx \sqrt{N}$ and at $T_N \approx N^{1/3}$. While the first one is somewhat natural, in view of the diffusive behavior of the simple random walk, the transition happening at $T_N \approx N^{1/3}$ is certainly more surprising and somehow unexpected.

Let us make some further comments on Theorem 4.3.3.

- In case (i), that is when $T_N \ll N^{1/3}$, equation (4.3.11) implies that the sequence $\{S_N/(C_\delta\sqrt{N/T_N})\}_N$ is *tight*, and the limit law of any converging subsequence must be absolutely continuous with respect to the Lebesgue measure on $\mathbb{R}$, with density bounded from above and from below by a multiple of the standard normal density.

  In the restricted regime $T_N \ll N^{1/6}$, we can actually strengthen equation (4.3.11) to a full convergence in distribution: $S_N/(C_\delta\sqrt{N/T_N}) \Longrightarrow \mathcal{N}(0,1)$ and we conjecture that this convergence holds up to $T_N \ll N^{1/3}$ but we are not able to prove it so far.

- The case when $T_N \to T \in \mathbb{R}$ as $N \to \infty$ has not been included in Theorem 4.3.3 for the sake of simplicity. However a straightforward adaptation of our proof shows that in this case equation (4.3.11) still holds true, with C_δ replaced by a different (T-dependent) constant $\widehat{C}_\delta(T)$ which converges to C_δ as $T \to \infty$.

- We stress that in regimes (iii) and (iv) the polymer really touches the interface at zero a finite number of times, after which it does not touch any other interface.

4.3.3 A link with a polymer in a slit

It turns out that our model is closely related to a model which has received quite some attention in the recent physical literature, the so-called *polymer confined between two walls and interacting with them* [16, 65, 71] (also known as polymer in a slit). For simplicity, we consider a constrained version of our model, that is $\mathbf{P}^{T,c}_{N,\delta}$ which is nothing but the free

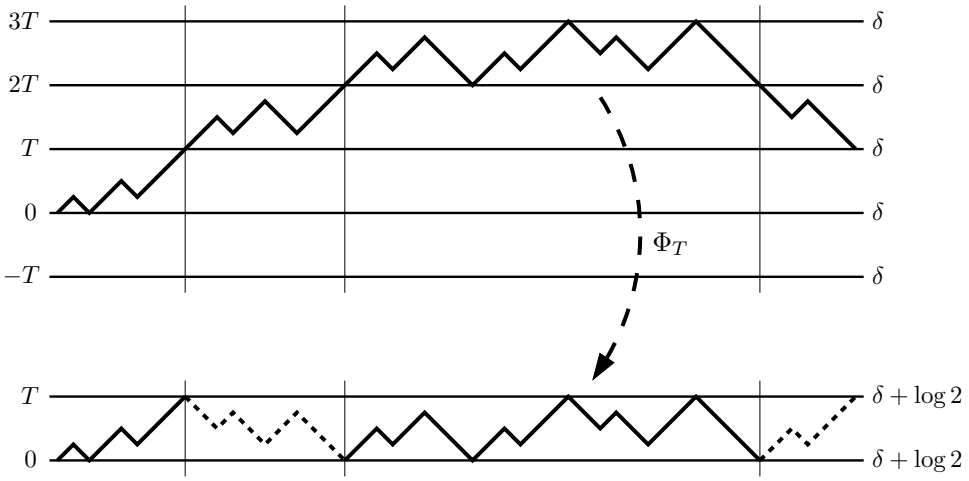

Figure 4.2: A polymer trajectory in a multi-interface medium transformed, after reflection on the interfaces 0 and T, in a trajectory of polymer in a slit. The dotted lines correspond to the parts of trajectory that appear upside-down after the reflection.

model conditioned by $S_N \in T\mathbb{Z}$, i.e., $\mathbf{P}^T_{N,\delta}(\cdot|S_N \in T\mathbb{Z})$ such that

$$\frac{\mathrm{d}\mathbf{P}^{T,c}_{N,\delta}}{\mathrm{d}\mathbf{P}}(S) = \frac{e^{\delta \sum_{i=1}^N 1_{\{S_i \in T\mathbb{Z}\}}}}{Z^{T,\,c}_{N,\delta}}\, 1_{\{S_N \in T\mathbb{Z}\}}. \tag{4.3.16}$$

The model for a polymer in a slit can be described as follows: given $N, T \in 2\mathbb{N}$, take the first N steps of the simple random walk constrained not to exit the interval $[0, T]$ and to end at one of the wall ($S_N \in \{0, T\}$) and give each trajectory a reward/penalty $\gamma \in \mathbb{R}$ each time it touches 0 or T. We are thus considering the probability measure $Q^T_{N,\gamma}$ defined by

$$\frac{\mathrm{d}\mathbf{Q}^T_{N,\gamma}}{\mathrm{d}\mathbf{P}}(S) = \frac{e^{\gamma \mathcal{N}_{N,T}(S)}}{Z^{T,\,\mathrm{slit}}_{N,\gamma}}\, 1_{\{\mathcal{V}_{N,T}\}}(S), \tag{4.3.17}$$

where $\mathcal{N}_{N,T}(S)$ is the number of times the path has touched the walls before time N, where $\mathbf{P}$ remains the law of the simple random walk and where

$$\mathcal{V}_{N,T} = \{S\colon S_i \in [0, T],\ \forall i \le N \text{ and } S_N \in \{0, T\}\}.$$

Consider now the simple random walk *reflected* on both walls 0 and T up to time N, which may be defined as $\{\Phi_{N,T}(S_n)\}_{n\ge 0}$, where $(\{S_n\}_{n\ge 0}, \mathbf{P})$ is the ordinary simple random walk (see Figure 4.2 for a graphical description). The law of $\{\Phi_{N,T}(S_n)\}_{n\ge 0}$ is simply denoted by $\Phi_{N,T}(\mathbf{P})$ and satisfies

$$\frac{\mathrm{d}\Phi_{N,T}(\mathbf{P})}{\mathrm{d}\mathbf{P}}(S) = 2^{\mathcal{N}_{N,T}(S)}\, 1_{\{\mathcal{V}_{N,T}\}}(S).$$

If we consider the reflection under $\Phi_{N,T}$ of our model, that is the process $\{\Phi_{N,T}(S_n)\}_{0\le n\le N}$ under $\mathbf{P}^{T,c}_{N,\delta}$, whose law will be denoted by $\Phi_{N,T}(\mathbf{P}^{T,c}_{N,\delta})$, then it comes

$$\frac{\mathrm{d}\Phi_T(\mathbf{P}^{T,c}_{N,\delta})}{\mathrm{d}\mathbf{P}}(S) = \frac{e^{(\delta+\log 2)\mathcal{N}_{N,T}(S)}}{Z^{T,\,c}_{N,\delta}}\, 1_{\{\mathcal{V}_{N,T}\}}(S). \tag{4.3.18}$$

At this stage, a look at equations (4.3.17) and (4.3.18) points out the link with our model: we have the basic identities $Q^T_{N,\delta+\log 2} = \Phi_{N,T}(\mathbf{P}^{T,c}_{N,\delta})$ and $Z^{T,\,c}_{N,\delta} = Z^{T,\,\mathrm{slit}}_{N,\delta+\log 2}$ for all $\delta \in \mathbb{R}$ and $T, N \in 2\mathbb{N}$. In words, the polymer confined between two attractive walls is just the reflection of our model through $\Phi_{N,T}$, up to a shift of the pinning intensity by $\log 2$. This allows a direct translation of all our results in this new framework.

Let us now use the analogy between the polymer in a slit and the multi-interface depinning model to improve what was done by physicists about one particular issue concerning the polymer in a slit. An important question for physicists indeed consists in computing the pressure that is applied by the polymer on the walls, i.e.,

$$\mathrm{Press}(N,\gamma,T) = \frac{1}{N}\log\frac{Z^{T+1,\mathrm{slit}}_{N,\gamma}}{Z^{T,\mathrm{slit}}_{N,\gamma}} \tag{4.3.19}$$

such that the polymer pushes the walls away from each other when $\mathrm{Press}(N,\delta,T) > 0$ and pulls them to each other when $\mathrm{Press}(N,\gamma,T) < 0$. This question is particularly interesting when $T = T_N$ is allowed to vary with N because it interpolates between the two extreme cases when one of the two quantities T and N tends to ∞ before the other. Obtaining a sharp estimate on $\mathrm{Press}(N,\gamma,T)$ requires a good asymptotic expansion of $Z^{T,\mathrm{slit}}_{N,\gamma}$ when $T, N \to \infty$ and this was considered in [71], where the authors obtained

$$Z^{T,\mathrm{slit}}_{N,\gamma} \;\approx\; \frac{(const.)}{N^{3/2}}\, f_{\mathrm{phase}}\left(\frac{\sqrt{N}}{T}\right), \tag{4.3.20}$$

where the function $f_{\mathrm{phase}}(x)$ is such that

$$f_{\mathrm{phase}}(x) \;\to\; 1 \;\text{ as }\; x \to 0\,, \qquad f_{\mathrm{phase}}(x) \;\approx\; x^3\, e^{-\pi^2 x^2/2} \;\text{ as }\; x \to \infty\,. \tag{4.3.21}$$

When $\gamma < \log 2$, the correspondence $\delta = \gamma - \log 2$ described above, allows us to use the asymptotic expansion of $Z^{T,c}_{N,\delta}$ with $\delta < 0$ to improve (4.3.20–4.3.21). When $T = T_N \to \infty$ we can indeed use the expression of the partition function with an underlying renewal process stated in (4.3.7) and an asymptotic expansion of the free energy $\phi(\delta, T_N)$ (see [25, Appendix A]) to obtain that, as $N, T \to \infty$,

$$Z^{T,c}_{N,\delta} \;=\; \frac{O(1)}{N^{3/2}}\, \max\left\{1, \left(\frac{\sqrt{N}}{T}\right)^3\right\} \exp\left(-\frac{\pi^2}{2}\frac{N}{T^2} + \frac{2\pi^2}{e^{-\delta}-1}\frac{N}{T^3} + o\left(\frac{N}{T^3}\right)\right).$$

which allows us to improve (4.3.20) into

$$Z_{N,\gamma}^{T,\mathrm{slit}} \;\approx\; \frac{(const.)}{N^{3/2}}\, f_{\mathrm{phase}}\left(\frac{\sqrt{N}}{T}\right) g\left(\frac{N^{1/3}}{T}\right), \qquad \text{where} \;\; g(x) \;\approx\; e^{\frac{2\pi^2}{e^{-\delta}-1}x} \;\; \text{as } x \to \infty$$

We have therefore obtained a refinement of equations (4.3.20–4.3.21). This is linked to the fact that we have gone beyond the first order in the asymptotic expansion of the free energy $\phi(\delta, T_N)$, making an additional term of the order N/T_N^3 appear. We stress that this new term gives a non-negligible (in fact, exponentially diverging!) contribution as soon as $T_N \ll N^{1/3}$. This corresponds to the fact that, by Theorem 4.3.3, the trajectories that touch the walls a number of times of the order N/T_N^3 are actually dominating the partition function when $T_N \ll N^{1/3}$.

4.4 Pinning and copolymer

In this section, I will briefly recall the results obtained in [72] and [73] during my PhD. The results in both papers have subsequently been strongly improved, even sometimes until complete settlement.

4.4.1 Influence of a disorder on the localization transition of a pinning model

In [73], we consider the random pinning of a $(1+1)$-dimensional simple random walk $S = (S_i)_{i\in\mathbb{N}}$ at a single linear interface. As mentioned in Section 4.1.1, defining the Hamiltonian of a given trajectory requires two positive coupling parameters $s \geq 0$ and $u \geq 0$ so that

$$H_{N,s,u}^{\omega}(S) = \sum_{i=1}^{N} (-u + s\,\omega_i)\, 1_{\{S_i=0\}}, \tag{4.4.1}$$

where $(\omega_i)_{i\in\mathbb{N}}$ is an i.i.d. sequence of centered and normalized random variables with finite exponential moments. The homogeneous model (that is $s = 0$) displays a phase transition at $u = 0$ between a delocalized phase $u \geq 0$ and a localized phase $u < 0$. An important issue at the time was to determine as precisely as possible the critical value $u_c(s)$ of the non-homogeneous model ($s \neq 0$). An annealed upper bound on the quenched free energy yields

$$u_c(\log \mathbf{E}(e^{s\omega_1})) := u_c^{\mathrm{ann}}(s) \geq u_c(s). \tag{4.4.2}$$

The object of [73] consisted in providing a lower bound on $u_c(s)$ by perturbing the law of each excursion of S away from the origin depending on the local disorder ω seen upon the excursion. With such techniques we could prove the following Theorem.

Theorem 4.4.1. *If $Var(w_1) \in (0, \infty)$, then there exist $c_3, c_4 > 0$ such that, for every $s \leq c_3$,*

$$u_c(s) \geq c_4 s^2.$$

Note that, when $Var(w_1) = 1$, the lower bound of $u_c(s)$ in Theorem 4.4.1 has the same scale (i.e., cs^2 as $s \to 0$) as the one of the annealed upper bound which satisfies $u_c^{\mathrm{ann}}(s) = (1 + o(1))s^2/2$ when $s \to 0$. This result followed a first lower bound in [2] established with a model for the pinning of irreducible Markov chain trajectories on $\mathbb{N}$ and which, once applied to our case, gives $u_c(s) > u_c(0)$ as soon as $s > 0$.

In the following 10 years, these results have been strongly improved. First, a more general framework has been introduced that accounts for all models of a random walk pinned at a linear interface (independently of the dimension), but also for Poland Scheraga model for DNA denaturation, wetting transition of Ising 2D interface (see [39, Section 2.5] or [81, Section 1.1]. This new setting is referred to as "pinning of a renewal process by a defect line" and is built as follows. Consider a renewal process $\tau = (\tau_0, \tau_1, \dots)$ on $\mathbb{N}$ such that $\tau_0 = 0$ and $(\tau_{i+1} - \tau_i)_{i=0}^{\infty}$ is an i.i.d. sequence of random variables in $\mathbb{N}$ whose law $K : \overline{\mathbb{N}} \to [0, 1]$ may be defective (in which case $K(\infty) > 0$) and satisfies the assumption

$$K(n) = \frac{L(n)}{n^{1+\alpha}}, \tag{4.4.3}$$

where L is a function slowly varying at ∞. The model is built by perturbing the law $\mathbf{P}_\tau$ of the renewal process with the Gibbs exponential factor

$$H_{N,s,u}^{\omega}(\tau) = \sum_{n \in \tau \cap (0,N]} (-u + s\,\omega_n), \tag{4.4.4}$$

where ω is defined as in (4.4.1) above. We note easily that our model in (4.4.1) of a simple random walk pinned at a linear interface clearly enters this new framework with a kernel K that corresponds to the law of the length of an excursion of the random walk off the origin.

At this stage, a quenched free energy can be computed that turns out to be self-averaging in ω and therefore only depends on the kernel choice K and of the law of ω_1. A phase transition occurs between a localized phase, where the free energy is strictly positive and a delocalized phase where it is 0. Thus, some general results of localization transition can be stated. Although, these results are based on the kernel K and on the law of ω_1 only, they remain valid for any model entering this general framework.

In this spirit, the issue of disorder relevance has been investigated in depth from a mathematical point of view. We recall that, when considering a weakly disordered pinning model (s small), the disorder is said to be *relevant* if $u_c(s) < u_c^{\mathrm{ann}}(s)$ whereas it is said to be *irrelevant* if $u_c(s) = u_c^{\mathrm{ann}}(s)$. The Harris criterion did forecast that relevance happens

for $\alpha > \frac{1}{2}$ whereas irrelevance occurs for $\alpha < \frac{1}{2}$ so that the case $\alpha = \frac{1}{2}$ (corresponding to the 1-dimensional simple random walk) remains marginal.

The relevance/irrelevance issue was mathematically settled recently in a succession of contributions where it has been shown that $\alpha < 1/2$ indeed corresponds to an irrelevant regime (see [3], [5], [45] and [80]) while $\alpha > 1/2$ corresponds to a relevant regime (see [4] and [30]). The marginal case strongly depends on the fine asymptotic of $L(k)$ as $k \to \infty$. It is indeed proven in [40] that, at $\alpha = 1/2$ and for L constant asymptotically, the disorder remains relevant. With a non asymptotically constant function L in turn, the quantity $T(L) := \sum_{k\in\mathbb{N}} \frac{1}{k} \frac{1}{L(k)^2}$ discriminates between disorder irrelevance when $T(L) < \infty$ and disorder relevance when $T(L) = \infty$ (see [3], [41], [80]).

4.4.2 Weak coupling limit of a copolymer pinned at a selective layer between two immiscible solvents

The paper [72] is dedicated to a model for a copolymer randomly pinned at a selective layer of finite width between two solvents. This paper generalizes the results and the approach developed in [12] to derive the weak coupling limit of the same model but without the pinning term.

Some discrete models in statistical mechanics can be shown to converge towards an associated continuous model when their coupling parameters tend to zero simultaneously and at appropriate speeds. Of course, the type of convergence has to be specified but in this chapter, we will focus on the convergence of the free energies. Two important features of such convergence are their universality and the informations they provide concerning the discrete model at small coupling parameters. To be more specific about the former feature, one indeed expect that the limiting continuous model does not depend on the fine properties of the discrete model but rather depends on some more fundamental characteristic e.g. the variance of the random walk increments, the exponential moments of the disorder variables etc... Concerning the latter feature, we note that some quantities related to the continuous model can be computed explicitly (with some technics from stochastic calculus) whereas their discrete counterpart can not. By using the discrete-to-continuous convergence, these exactly computable continuous quantities provide the behavior of their discrete counterparts when the coupling is weak (see for instance the slope of the critical curve at the origin for the copolymer model below).

The discrete model

The copolymer is made of a random concatenation of monomers that are either hydrophilic or hydrophobic and interacts with a medium made of two solvents (oil in the upper-half plane and water in the lower-half plane) and of a thin layer of impurities that are trapped

around the selective interface. For the discrete model, the allowed configurations for the copolymer are given by the trajectories of a $(1+1)$-dimensional simple random walk S. The composition of the copolymer is encoded by an i.i.d. sequence $w = (w_i)_{i\geq 1}$ of bounded and symmetric random variables so that the hydrophilic (resp. hydrophobic) monomers are associated with the positive (resp. negative) elements of w. The layer of impurities is modeled by an i.i.d. sequence of random vectors $\gamma = ((\gamma_i^{-U}, \dots, \gamma_i^U))_{i\geq 1}$ such $U \in \mathbb{N}_0$ and the variables $\gamma_1^{-U}, \dots, \gamma_1^U$ are independent and can have different laws. Finally, w and γ are independent and defined under the probability law $\mathbb{P}$.

At this stage, in size N, and with the coupling parameters $\lambda, h \in \mathbb{R}^+$ and $\beta \in \mathbb{R}$ we can associate with each given trajectory S an Hamiltonian that takes into account the microscopic interactions between the copolymer and the medium, i.e.,

$$H^{w,\gamma}_{N,\beta,\lambda,h}(S) = \lambda \sum_{i=1}^{N} (w_i + h)\Lambda_i + \beta \sum_{j=-U}^{U} \sum_{i=1}^{N} \gamma_i^j \; 1_{\{S_i = j\}}, \tag{4.4.5}$$

where $\Lambda_i = \text{sign}(S_i)$ when $S_i \neq 0$ and $\Lambda_i = \Lambda_{i-1}$ otherwise. Note, on the one hand, that the copolymer is rewarded energetically for each monomer it puts in its favorite solvent and is penalized otherwise and, on the other hand, that the copolymer picks some random values of the potential when it enters the layer of impurities. The limiting free energy per step can therefore be defined as

$$\Phi(\beta, \lambda, h) = \lim_{N\to\infty} \mathbb{E}\Big[\tfrac{1}{N} \log E\big[e^{H^{w,\gamma}_{N,\beta,\lambda,h}(S)}\big]\Big]. \tag{4.4.6}$$

A phase transition occurs between a localized phase $\mathcal{L}$ characterized by $\Phi > \lambda h$ and inside which the contact fraction between the copolymer and the oil-water interface is strictly positive and a delocalized phase for which $\Phi = \lambda h$ and for which the number of excursions performed by the copolymer off the linear interface is $o(N)$. At $\beta \in \mathbb{R}$ fixed, the two phases $\mathcal{L}$ and $\mathcal{D}$ are separated in the (λ, h)-phase diagramm by a critical curve $\lambda \mapsto h_c^\beta(\lambda)$.

The continuous model

For the continuous counterpart of the discrete model, the configurations of the polymer are given by the trajectories of 1-dimensional Brownian motion $(s, B_s)_{s\in[0,\infty)}$. The coupling constants remain $\lambda, h \geq 0$ and $\beta \in \mathbb{R}$ and the Hamiltonian associated with every trajectory B is

$$\widetilde{H}^{R,t}_{\beta,\lambda,h}(B) = \lambda \int_0^t \Lambda(s)(dR_s + h ds) + \beta L_t^0, \tag{4.4.7}$$

where L_t^0 is the local time spent at 0 by B up to time t and where $\Lambda_s = \text{sign}(B_s)$. We denote by $\widetilde{\mathbb{P}}$ the law of $R = (R_s)_{s\geq 0}$, which is a standard Brownian motion, independent of B such that dR_s plays the role of w_i.

A limiting free energy can be computed in the continuous case as well, i.e.,

$$\widetilde{\Phi}(\beta,\lambda,h)=\lim_{t\to\infty}\widetilde{\mathbb{E}}\Big[\tfrac{1}{t}\log\widetilde{E}\big[e^{\widetilde{H}^{R,t}_{\beta,\lambda,h}(B)}\big]\Big] \tag{4.4.8}$$

and, similarly to what is observed for the discrete model, a phase transition occurs between a localized phase ($\widetilde{\Phi}>\lambda h$) and a delocalized phase ($\widetilde{\Phi}=\lambda h$). At β fixed, an important feature of this model is that the critical curve is linear with slope k_c^β.

Main results

In [72], we apply a coarse-graining procedure that was initially displayed in [12] for the copolymer model without the pinning term. When the coupling parameters $(a\beta, a\lambda, ah)$ vanish ($a\to 0$), we first divide the system into large blocks of size $1/a^2$. Then, on each such block, some invariance principles can be applied as $a\to 0$ to replace the random walk trajectories by Brownian paths and the discrete disorder w by the Brownian increments of R. This technic allowed us to prove the following Theorem.

Theorem 4.4.2. *Let $\beta\in\mathbb{R}$, $\lambda>0$, $h\geq 0$, and $\Sigma=\sum_{j=-U}^{U}\mathbb{E}(\gamma_1^j)$. Then*

$$\lim_{a\to 0}\ \frac{1}{a^2}\ \Phi(a\beta,a\lambda,ah)=\widetilde{\Phi}(\beta\Sigma,\lambda,h) \tag{4.4.9}$$

and

$$\lim_{\delta\to 0}\frac{h_c^{\delta\beta}(\delta)}{\delta}=k_c^{\beta\Sigma}. \tag{4.4.10}$$

The weak coupling limits in both [12] and [72] have been generalized in [20] to what Caravenna and Giacomin defined as the α-copolymer model. Based on the observation that, when $K=0$ in (4.4.5), the partition function can be expressed as the expectation of a function of only the lengths and signs of the excursions of S off the origin, it becomes natural to define a generalized version of the model with an underlying renewal process $\tau=(\tau_i)_{i\in\mathbb{N}}$ on $\mathbb{N}$ and an independent sequence of random signs $(\varepsilon_i)_{i\in\mathbb{N}}$ that are i.i.d. and take values -1 and 1 with probability $1/2$ each. In this framework, for $i\in\mathbb{N}$, the random variable $\tau_{i+1}-\tau_i$ (resp. ε_i) accounts for the length (resp. the sign) of the i-th excursion of S off the origin. The model can therefore be defined by simply specifying the law K of the renewal. Then, the copolymer is of type $\alpha\in(0,1)$ as soon as K satisfies (4.4.3).

For $\alpha\in(0,1)$, they define a continuous version of the α-copolymer, which is build exactly like the continuous model in (4.4.7) except that the Brownian motion B is replaced by a Walsh process of index α (which for $\alpha=1/2$ is the Brownian motion). Finally, they provide an extension of Theorem 4.4.2 to the α-copolymer when $\alpha\in(0,1)$.

4.5 Perspectives

A short term goal related to the model of a polymer in a multi-interface medium could be to let the energetic reward δ depend on the system size N as well. In the pinning case for instance, for a given $(T_N)_{N\in\mathbb{N}}$ and for $(\delta_N)_{N\in\mathbb{N}}$ a sequence of positive numbers that vanish as $N \to \infty$, it would be interesting to check whether the criterion from Theorem 4.3.2 still holds true. In other words, does $T_N - \frac{\log N}{c_{\delta_N}} \to \infty$ still implies that the number of different interfaces visited by the polymer up to time N typically diverges as $N \to \infty$? Such questions are relevant in the depinning case as well. Generally speaking, can we formulate the counterparts of Theorems 4.3.2 and 4.3.3 with δ vanishing as $N \to \infty$.

One could also consider a model where the reward picked by the polymer when touching the interface kL_N ($k \in \mathbb{Z}$) becomes k dependent. For instance, $\boldsymbol{\delta} := (\delta_k)_{k\in\mathbb{N}}$ is an i.i.d. sequence of Bernoulli trials taking values ± 1 with probability $1/2$ each, and a natural question would be, for a quenched disorder $\boldsymbol{\delta}$, to derive the scaling limit of S_N (the right extremity of the polymer).

A long-term project which also involves a polymer in a multi-interface medium and falls into the general framework of a random walk in a potential could be described as follows. For a system of size N, instead of considering infinitely many equispaced linear interfaces, the environment consists of k_N independent copies of S. In other words, the polymer of size N is pinned at k_N random walk trajectories. Of course k_N can be constant, i.e., $k_N \equiv k \in \mathbb{N}$, and this model can be viewed as an extension of the homogeneous pinning of a polymer by a random walk trajectory (see [8], [9] and [10]). Note that this model is, via the Feynman Kac formula, also closely related to the Parabollic Anderson Model with k catalysts moving as random walks. Among the issues raised by this multiple pinning random walk, we will focus on

- in dimension $1 + d$, identify the critical growth rate of k_N above which the limiting free energy becomes strictly larger than the one with only one random interface (i.e., with $k_N \equiv 1$),
- in dimension $1+d$, for the annealed version of the model and with $k_N \equiv k \in \mathbb{N}$, prove that the diffusion constant of S_N decreases with k and identify the speed at with this constant decays.

Bibliography

[1] A. Auffinger and O. Louidor, *Directed polymers in random environment with heavy tails*, Comm. Pure Appl. Math. **64** (2010) 183–204.

[2] K. Alexander and V. Sidoravicius, *Pinning of polymers and interfaces by random potential*, Ann. Appl. Probab. **16** (2006) 639-669.

[3] K. Alexander, *The effect of disorder on polymer depinning transitions*, Comm. Math. Phys. **279** (2008) 117-146.

[4] K. Alexander and N. Zygouras, *Quenched and annealed critical points in polymer pinning models*, Comm. Math. Phys. **291** (2009) 659-689.

[5] K. Alexander and N. Zygouras, *Equality of critical points for polymer depinning transition with loop exponent one*, Ann. Appl. Probab. **20** (2010) 356-366.

[6] S. Asmussen, *Applied probability and queues* (2nd ed.), Applications of Mathematics **51**, Springer, New York, 2003.

[7] V. Beffara, S. Friedli and Y. Velenik, *Scaling limit of the prudent walk*, Electron. Commun. Probab. **15** (2010) 44-58.

[8] Q. Berger, F.L. Toninelli, *On the critical point of the Random Walk Pinning Model in dimension $d = 3$*, Electron. Journal Probab. **15** (2010) 654-683.

[9] M. Birkner and R. Sun, *Annealed vs quenched critical points for a random walk pinning model*, Ann. Instit. H. Poincaré (B) Probab. Stat. **46** (2010) 414-441.

[10] M. Birkner and R. Sun, *Disorder relevance for the random walk pinning model in dimension 3*, Ann. Instit. H. Poincaré **47** (2011) 259-293.

[11] T. Bodineau and G. Giacomin, *On the localization transition of random copolymers near selective interfaces*, J. Stat. Phys. **117** (2004) 801-818.

[12] E. Bolthausen and F. den Hollander, *Localization for a polymer near an interface*, Ann. Probab. **25** (1997) 1334-1366.

[13] R. Brak, P. Dyke, J. Lee, A. L. Owczarek, T. Prellberg, A. Rechnitzer and S. G. Whittington, *A self-interacting partially directed walk subject to a force*, J. Phys. A: Math. Theor. **42** (2009) 085001.

[14] R. Brak, A. J. Guttman and S. G. Whittington, *A scaling theory of the collapse transition in geometric cluster models of polymers and vesicles*, J. Phys. A: Math. Gen. **26** (1993) 4565-4579.

[15] R. Brak, A. J. Guttman and S. G. Whittington, *A collapse transition in a directed walk model*, J. Phys. A: Math. Gen. **25** (1992) 2437-2446.

[16] R. Brak, A.L. Owczarek, A. Rechnitzer and S.G. Whittington, *A directed walk model of a long chain polymer in a slit with attractive walls*, J. Phys. A: Math. Gen. **38** (2005) 4309-4325.

[17] F. Caravenna, *Random walk models and probabilistic techniques for inhomogeneous polymer chains*, Ph.D. Thesis, 2005, University of Milano-Bicocca, Italy, and University of Paris 7, France.

[18] F. Caravenna, P. Carmona and N. Pétrélis, *The discrete time parabolic Anderson model with heavy tailed potential*, Ann. Instit. H. Poincaré (B) Probab. Stat. **48** (2012) 1049-1080.

[19] F. Caravenna and G. Giacomin, *On constrained annealed bounds for pinning and wetting models*, Elect. Comm. Probab. **10** (2005) 179-189.

[20] F. Caravenna and G. Giacomin, *The weak coupling limit of disordered copolymer models*, Ann. Probab. **38** (2010) 2322-2378.

[21] F. Caravenna, G. Giacomin and M. Gubinelli, *A numerical approach to copolymer at selective interfaces*, J. Stat. Phys. **122** (2006) 799-832.

[22] F. Caravenna, G. Giacomin and L. Zambotti, *A renewal theory approach to periodic copolymers with adsorption*, Ann. Appl. Probab. **17** (2007) 1362-1398.

[23] F. Caravenna, F. den Hollander and N. Pétrélis, *Lectures on Random Polymers*. In *Probability and Statistical Physics in Two and more Dimensions*, Clay Mathematics Proceedings **15** (2012) 319-393.

[24] F. Caravenna and N. Pétrélis, *A polymer in a multi-interface medium*, Ann. Appl. Probab. **19** (2009) 1803-1839.

[25] F. Caravenna and N. Pétrélis, *Depinning of a polymer in a multi-interface medium*, Elec. J. Probab. **14** (2009) 2038-2067.

[26] P. Carmona and Y. Hu, *On the partition function of a directed polymer in a Gaussian random environment*, Probab. Theory Rel. Fields **124** (2002) 431-457.

[27] P. Carmona, G. B. Nguyen and N. Pétrélis, *Interacting partially self-avoiding walk, from phase transition to the geometry of the collapsed phase*, preprint arXiv:1306.4887 [math PR].

[28] P. Carmona and N. Pétrélis, *Scaling limits of the interacting partially directed self-avoiding walk*, in preparation.

[29] F. Comets, T. Shiga, and N. Yoshida, *Probabilistic analysis of directed polymers in a random environment: a review.* In *Stochastic analysis on large scale interacting systems*, Adv. Stud. Pure Math. **39** (2004) 115–142, Math. Soc. Japan, Tokyo.

[30] B. Derrida, G. Giacomin, H. Lacoin and F. Toninelli, *Fractional moment bounds and disorder relevance for pinning models*, Comm. Math. Phys **287** (2009) 867-887.

[31] R. Dobrushin, R. Kotecky and S. Schlosman, *Wulff construction: a global shape from local interaction*, Translations of mathematical Monographs **104**, AMS, Providence, RI, 1992.

[32] R. Durrett, *Probability: theory and examples* (3rd ed.), Duxbury Press, Belmont (2005).

[33] G. Forgacs, J.M. Luck, Th.M. Nieuwenhuizen and H. Orland, *Exact critical behaviour of two-dimensional wetting problems with quenched disorder*, J. Stat. Phys. **51** (1988) 29-56.

[34] S. Fujishige, K. Kubota and I. Ando, *Phase transition of aqueous solutions of poly(N-isopropylacrylamide) and poly(N-isopropylmethacrylamide)*, J. Phys. Chem. **93** (1989) 3311-3313.

[35] T. Garel, D.A. Huse, S. Leibler and H. Orland, *Localization transition of random chains at interfaces*, Europhys. Lett. **8** (1989) 9-13.

[36] J. Gärtner and W. König, *The parabolic Anderson model.* In *Interacting Stochastic Systems* (2005) 153-179, Springer, Berlin.

[37] J. Gärtner and S.A. Molchanov, *Parabolic problems for the Anderson model. I. Intermittency and related topics*, Comm. Math. Phys. **132** (1990) 613-655.

[38] G. Giacomin, *Random polymer models*, Imperial College Press (2007), World Scientific, London.

[39] G. Giacomin, *Disorder and critical phenomena through basic probability models*, École d'Été de Probabilités de Saint-Flour XL-2010, Lecture Notes in Mathematics **2025**, Springer, Berlin, 2011.

[40] G. Giacomin, H. Lacoin and F. L. Toninelli, *Marginal relevance of disorder for pinning models*, Commun. Pure Appl. Math. **63** (2010) 233-265.

[41] G. Giacomin, H. Lacoin and F. L. Toninelli, *Disorder relevance at marginality and critical point shift*, Ann. Inst. H. Poicarré (B) Probab. Stat. **47** (2011) 148-175.

[42] G. Giacomin and F. Toninelli, *Estimates on path delocalization for copolymers at selective interfaces*, Probab. Theory Rel. Fields **133** (2005) 464-482.

[43] G. Giacomin and F. L. Toninelli, *Smoothing effect of quenched disorder on polymer depinning transitions*, Comm. Math. Phys. **266** (2006) 1-16.

[44] G. Giacomin and F.L. Toninelli, *The localized phase of disordered copolymers with adsorption*, Alea **1** (2006) 149-180.

[45] G. Giacomin and F.L. Toninelli, *On the irrelevant disorder regime of pinning models*, Ann. Probab. **37** (2009) 1841-1873.

[46] R. van der Hofstad and A. Klenke, *Self-attractive random polymer*, Ann. Appl. Probab. **11** (2001) 1079–1115.

[47] R. van der Hofstad, W. König and P. Mörters, *The universality classes in the parabolic Anderson model*, Comm. Math. Phys. **267** (2006) 307-353.

[48] R. van de Hofstad, F. den Hollander and W. König, *Weak interaction limits for one dimensional random polymers*, Probab. Theory Rel. Fields **125** (2003) 483-521.

[49] F. den Hollander, *Random Polymers*, École d'Été de probabilités de Saint Flour XXXVII-2007, Lecture Notes in Mathematics **1976**, Springer, Berlin, 2009.

[50] F. den Hollander and N. Pétrélis, *On the localized phase of a copolymer in an emulsion: supercritical percolation regime*, Commun. Math. Phys. **285** (2009) 825-871.

[51] F. den Hollander and N. Pétrélis, *On the localized phase of a copolymer in an emulsion: subcritical percolation regime*, J. Stat. Phys. **134** (2009) 209-241.

[52] F. den Hollander and N. Pétrélis, *A mathematical model for a copolymer in an emulsion*, J. Math. Chem. **48** (2010) 83-94.

[53] F. den Hollander and N. Pétrélis, *Phase diagram of a copolymer in an emulsion*, preprint arXiv:1309.1635 [math.PR].

[54] F. den Hollander and S.G. Whittington, *Localization transition for a copolymer in an emulsion*, Theor. Prob. Appl. **51** (2006) 193-240.

[55] O. Hryniv and Y. Velenik, *Universality of critical behaviour in a class of recurrent random walks*, Probab. Theory Rel. Fields **130** (2004) 222-258.

[56] D. Ioffe, *Large deviations for the 2d Ising model: a lower bound without cluster expansion*, J. Stat. Phys. **74** (1994) 411-432.

[57] D. Ioffe, *Exact large deviation bounds up to T_c for the Ising model in 2 dimensions*, Probab. Theory Rel. Fields **102** (1995) 313-330.

[58] D. Ioffe and R Schonmann, *Dobrushin-Kotecky-Shlosman theorem up to the critical temperature*, Comm. Math. Phys. **199** (1998) 117-167.

[59] P. Jaiswal, G. Aggarwal, S.L. Harikumar and A. Kaur, *Bioavailability enhancement of poorly soluble drugs by smeeds: a review*, Journal of Drug Delivery and Therapeutics **3** (2013) 98-109.

[60] S. Janson, *Brownian excursion area, Wright's constants in graph enumeration, and other Brownian areas*, Probability Surveys **3** (2007) 80-145.

[61] M. Kac, *On the average of a certain Wiener functional and a related limit theorem in calculus of probability*, Trans. Amer. Math. Soc. **59** (1946) 401-414.

[62] H. Kallabis and M. Lassig, *Strongly inhomogeneous surface growth on polymers*, Phys. Rev. Lett. **75** (1995) 1578-1581.

[63] W. König, H. Lacoin, P. Mörters and N. Sidorova, *A two cities theorem for the parabolic Anderson model*, Ann. Probab. **37** (2009) 347-392.

[64] H. Lacoin, *New bounds for the free energy of directed polymers in dimension $1+1$ and $1+2$*, Comm. Math. Phys. **294** (2010) 471-503.

[65] R. Martin, E. Orlandini, A. L. Owczarek, A. Rechnitzer and S. Whittington, *Exact enumeration and Monte Carlo results for self-avoiding walks in a slab*, J. Phys. A: Math. Gen. **40** (2007) 7509-7521.

[66] G. B. Nguyen, *Marche aléatoire auto-évitante en auto-interaction*, Ph.D. Thesis, 2013, University of Nantes, France.

[67] G. B. Nguyen and N. Pétrélis, *A variational formula for the free energy of the partially directed polymer collapse*, J. Stat. Phys. **151** (2013) 1099-1120.

[68] E. Orlandini, M.C. Tesi and S.G. Whittington, *Adsorption of a directed polymer subject to an elongation force*, J. Phys. A: Math. Gen. **37** (2004) 1535-1543.

[69] A. L. Owczarek and T. Prellberg, *Exact solution of semi-flexible and super-flexible interacting partially directed walks*, J. Stat. Mech.: Theor. Exp. (2007) P11010.

[70] A. L. Owczarek, T. Prellberg and R. Brak, The tricritical behavior of self-interacting partially directed walks. J. Stat. Phys. 72 (1993) 737-772.

[71] A. L. Owczarek, T. Prellberg and A. Rechnitzer, *Finite-size scaling functions for directed polymers confined between attracting walls*, J. Phys. A: Math. Theor. **41** (2008) 1-16.

[72] N. Pétrélis, *Copolymer at selective interfaces and pinning potentials: Weak coupling limits*, Ann. Inst. H. Poincaré (B) Probab. Stat. **45** (2009) 175-200.

[73] N. Pétrélis, *Polymer pinning at an interface*, Stoch. Proc. Appl. **116** (2006) 1600-1621.

[74] D. Schmaljohann, *Thermo- and pH-responsive polymers in drug delivery*, Advanced Drug Delivery Reviews **58** (2006) 1655-1670.

[75] S.F. Sun, C.C. Chou and R.A. Nash, *Viscosity study of the collapsed state of polystyrene*, J. Chem. Phys. **93** (1990) 7508-7509.

[76] A. I. Sakhanenko, *On unimprovable estimates of the rate of convergence in invariance principle*, Colloq. Math. Soc. János Bolyai 32 Nonparametric Statistical Inference, Budapest, Hungary (1980) 779-783.

[77] H. S. Samanta and D. Thirumalai, *Exact solution of the Zwanzig-Lauritzen model of polymer crystallization under tension*, J. Chem. Phys. **138** (2013) 104901.

[78] K. Svoboda and S.M. Block, *Biological applications of optica forces*, Annu. Rev. Biophys. Biomol. Struct. **23** (1994) 247-285.

[79] T.F. Tadros, A. Vandamme, B. Levecke, K. Booten, C.V. Stevens, *Stabilization of emulsions using polymeric surfactant based on inulin*, Adv. Colloid and Interface Science **108-109** (2004) 207-226.

[80] F. Toninelli, *A replica-coupling approach to disordered pinning models*, Comm. Math. Phys. **280** (2008) 389-401.

[81] F. Toninelli, *Polymères en milieu aléatoire: Localisation, Phénomènes critiques et Critère de Harris*, Habilitation à Diriger des Recherches en Mathématiques, 2010, Ecole Normale Supérieure de Lyon, France.

[82] N.Torri, *Pinning model with heavy tailed disorder*, in preparation.

[83] G. Wulff, *Zur frage der geschwindigkeit des wachstums und der auflosung der krystallflagen*, Z. Kryst. Mineral. **38** (1901) 449.

[84] R. Zwanzig and J. I. Lauritzen, *Exact calculation of the partition function for a model of two dimensional polymer crystallization by chain folding*, J. Chem. Phys. **48** (1968).